Hydrogenation Chemistry of 1,3-bis (2,4,6-trimethylphenyl) Imidazolium Carboxylate

by

Onyinyechukwu Flora Oburu

Submitted in Partial Fulfillment of the Requirements

For the Degree of

Master of Science

In the

Chemistry Program

YOUNGSTOWN STATE UNIVERSITY

December 2023

Hydrogenation Chemistry of Bis-Mesityl Imidazolium Carboxylate

Onyinyechukwu Flora Oburu

I hereby release this thesis to the public. I understand that this thesis will be made available from the OhioLINK ETD Center and the Maag Library Circulation Desk for public access. I also authorize the University or other individuals to make copies of this thesis as needed for scholarly research.

Signature:

_____

Onyinyechukwu Oburu, Student Date

Approvals:

_____

Dr. Clovis A. Linkous, Thesis Advisor Date

_____

Dr. Joe Simeonsson, Committee Member Date

_____

Dr. John Jackson, Committee Member Date

_____

Dr. Salvatore A. Sanders, Dean of Graduate Studies Date

Abstract

Global climate change is a major crisis with no solution in sight due to the continual production of greenhouse gases (GHGs). Carbon dioxide (CO_2) is a major GHG whose atmospheric concentration has been rising constantly from increased human activities that lead to its formation. Developing new applications for CO_2 is a viable means for reducing its atmospheric concentration and consequently controlling global climate change. N-heterocyclic carbenes (NHCs) are known to form molecular adducts when exposed to CO_2, in this work, the adduct 1,3-bis(2,4,6-trimethylphenyl) imidazolium carboxylate (IMes-CO_2), where Mes = 2,4,6-trimethylphenyl or mesityl, was prepared by reacting CO_2 with the corresponding carbene (IMes), which was prepared by deprotonation of the imidazolium chloride (IMes-Cl) salt at the C2 position with potassium hexamethyldisilazide (KHMDS). Synthesis of IMes-CO_2 was confirmed via nuclear magnetic resonance and infrared spectroscopy, thermogravimetric analysis and mass spectrometry. The chemical nature of IMes-CO_2 was studied via attempted catalytic hydrogenation reactions at varying reaction conditions. The analytical results obtained showed that IMes-CO_2 was generally unreactive at room temperature and 30 atm of H_2 pressure for up to 3 days. Moreover, the solvated adduct would slowly dissociate unless a background pressure of CO_2 was supplied. In Pd/C-catalyzed hydrogenation reactions, the C2-CO_2 bond of IMes-CO_2 is broken and the C2 is rehydrogenated, regenerating the imidazolium, as observed in the reappearance of the H2 peak position above 10 ppm in the ^{1}H-NMR spectrum. However, no further reduction occurred, as the H1 peak corresponding to the C=C double bond of the imidazole ring remained at 7.74 ppm, along with the aromatic H4 peak at 7.09 ppm and the IMes methyl peaks at 2.37 ppm and 2.18 ppm. Likewise, spectroscopic signatures for CO_2 reduction products (formate, oxalate, methanol, etc.) were not observed. Nevertheless, the mesityl imidazolyl carbene demonstrated reversible uptake of CO_2 at ambient pressure and temperature, which could find application in a CO_2 adsorption cycle.

Keywords: carbon dioxide; synthesis; N-Heterocyclic compound; hydrogenation; catalysis

Acknowledgements

My heartfelt gratitude to God Almighty, for all his blessings and favors on me throughout the pursuit of my master's degree.

I specially thank my amazing research advisor Dr. Clovis Linkous for the opportunity to be a member of his research team, and his unwavering support and continuous guidance meted to me at every step of my research journey. I extend my gratitude to Dr. John Jackson for his commitment as a member of my committee and for providing comments and suggestions on my NMR analysis. I also thank Dr. Joe Simeonsson for being a dedicated member of my committee and for his continuous encouragement.

I thank all the YSU Chemistry Department faculty and staff for the assistantship and opportunity to complete my master's program. I sincerely thank Mr. Ray Hoff for his assistance with the analytical instruments.

Special thanks to my Husband and Family for their love, support, and confidence in me to pursue and complete my degree.

Dedication

To Nneoma,
My daughter, my world

Table of Contents

List of Figures

List of Equations

List of Tables

List of Abbreviations

Abbreviation	Meaning
CO_2	Carbon dioxide
GHE	Greenhouse Effect
GHG	Greenhouse Gas
CH_4	Methane
NO	Nitric oxide
O_3	Ozone
H_2O	Water
$C_6H_{12}O_6$	Glucose
O_2	Oxygen
H_2	Hydrogen
CO	Carbon monoxide
RWGS:	Reverse water gas shift
CH_3OH:	Methanol
NHC:	N-Heterocyclic Carbene /Compound
IMes-Cl	1,3-bis (2,4,6-trimethyl-phenyl) imidazolium chloride
IMes-CO_2	1,3-bis (2,4,6-trimethyl-phenyl) imidazolium carboxylate
THF	Tetrahydrofuran
DMSO	Dimethyl sulfoxide
KO^tBu	Potassium tert-butoxide
NaH	Sodium hydride
Pd/C	Palladium on carbon
KHMDS	Potassium Hexamethyldisilazide
NH_3	Ammonia
NMR	Nuclear Magnetic Resonance
$CDCl_3$	Deuterated Chloroform
IR	Infrared
TGA	Thermal Gravimetric Analysis
MS	Mass Spectrometry
GC	Green Chemistry
ppm	parts per million

Chapter One

Introduction

Carbon dioxide concentration in the atmosphere has increased drastically in the past decades due to increasing worldwide fossil fuel consumption, which has profoundly impacted our environment.[1] Geographically, carbon dioxide emissions are more concentrated in developed places such as the United States, Europe, Japan, and in populous developing countries like China due to massive industrialization and energy infrastructure developments.[1] Svante Arrhenius was the first to publish a paper quantifying the effects of carbon dioxide concentration on the greenhouse effect, in which he referred to carbon dioxide as carbonic acid and predicted its long-term effect on climate at varying atmospheric levels.[2] According to him, carbonic acid, as was the conventional name during his time, was released into the atmosphere through volcanic eruptions and geological phenomena, combustion of carbonaceous meteorites, and decay of organic matter.[2] Scientifically, it has been established that the quality of life on planet Earth is greatly affected by the natural greenhouse effect (GHE) brought about by the greenhouse gases (GHGs), and it occurs at the lower layer of the atmosphere called the troposphere.[3] The GHGs have both natural and anthropogenic sources and they include water vapor, carbon dioxide (CO_2), methane (CH_4), nitrous oxides (NO), and ozone (O_3).[3] The GHE phenomenon arises when the GHGs trap the sun's radiation, as well as radiation emitting from the earth's surface, which leads to heat generation in the atmosphere as demonstrated in **Figure 1.**[3]

Ordinarily, the supposed estimated temperature of the earth's surface would be -19 ˚C, which would have made planet earth less inhabitable but thanks to GHE, the current average earth's surface temperature has risen to 14 ˚C, making the earth a comfortable place to live.[3]

The atmospheric concentrations of each greenhouse gas vary daily, seasonally, and annually, hence producing a respective individualistic greenhouse effect from the other gases.[3]

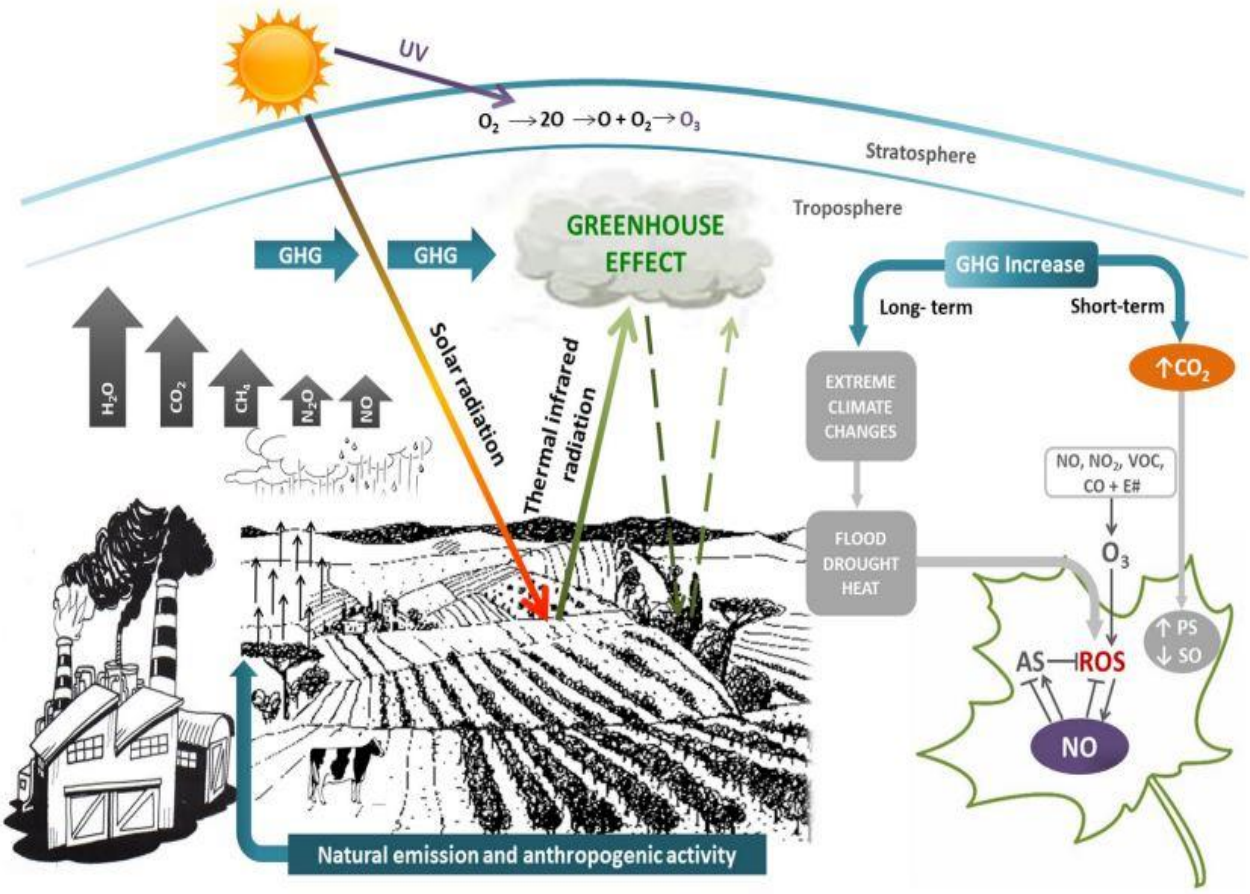

Figure 1. Greenhouse Gases with their Short-term and Long-term Effects.

[Cassia Raul et al. Front. Plant Sci. **2018**. Downloaded 15th December 2023]

Figure 1 illustrates how the greenhouse gases of both natural and anthropogenic origin contribute to the greenhouse effect. One major aspect of increased greenhouse gases is the corresponding increased atmospheric CO_2 concentration, which plays an important role in plants' photosynthesis but becomes counterproductive in the long term as it causes extreme climate conditions such as heat, droughts, and floods leading to hostile environments for both plants and animals.[3] The most naturally abundant GHG in the atmosphere is water vapor whereas carbon dioxide is the most produced GHG through human activities.[4] Natural sources of GHGs are comprised of respiration, decomposition of biological compounds, marine extracts, and ocean release to the atmosphere, while anthropogenic sources are burning of fossil fuels, deforestation, combustion, and industrial production.[4] The anthropogenic sources of carbon dioxide have been on a continuous rise and have significantly increased the atmospheric concentration of CO_2 for the past two centuries, leading to an increased global mean surface temperature.[5]

Globally, scientists have intensified efforts to develop more effective ways of reducing atmospheric carbon dioxide concentration, subsequently reducing the greenhouse effect, and ultimately mitigating its impact on the environment. Since carbon dioxide emission into the atmosphere is difficult to curtail due to the constant rise in its anthropogenic sources, finding alternative applications of the greenhouse gas, to reduce its atmospheric concentration has become of great interest to researchers.[5]

Existing Chemical Conversions of Carbon Dioxide

An alternative solution to the current global adverse climate change would be a developed efficient system of converting CO_2 into hydrocarbon fuel precursors using various renewable and clean energy sources such as the wind and the sun.[6]

Naturally, plants utilize CO_2 in the presence of sunlight and chlorophyll to produce carbohydrates through the process of photosynthesis shown in **Equation 1**.[7]

$$6\ CO_2 + 6\ H_2O \xrightleftharpoons[\text{Chlorophyll}]{\text{Sunlight}} C_6H_{12}O_6 + 6\ O_2$$

Equation 1. Photosynthesis

In photosynthesis, one molecule of glucose is produced when six molecules of carbon dioxide are reduced with six molecules of water using solar energy in the presence of chlorophyll, and six molecules of oxygen are also released.[7]

Industrially, extensive studies have been carried out on the reduction of carbon dioxide to useful products, **Figure 2** illustrates the conversion routes for carbon dioxide-derived fuels such as methanol and methane, plus other chemical intermediates.[8]

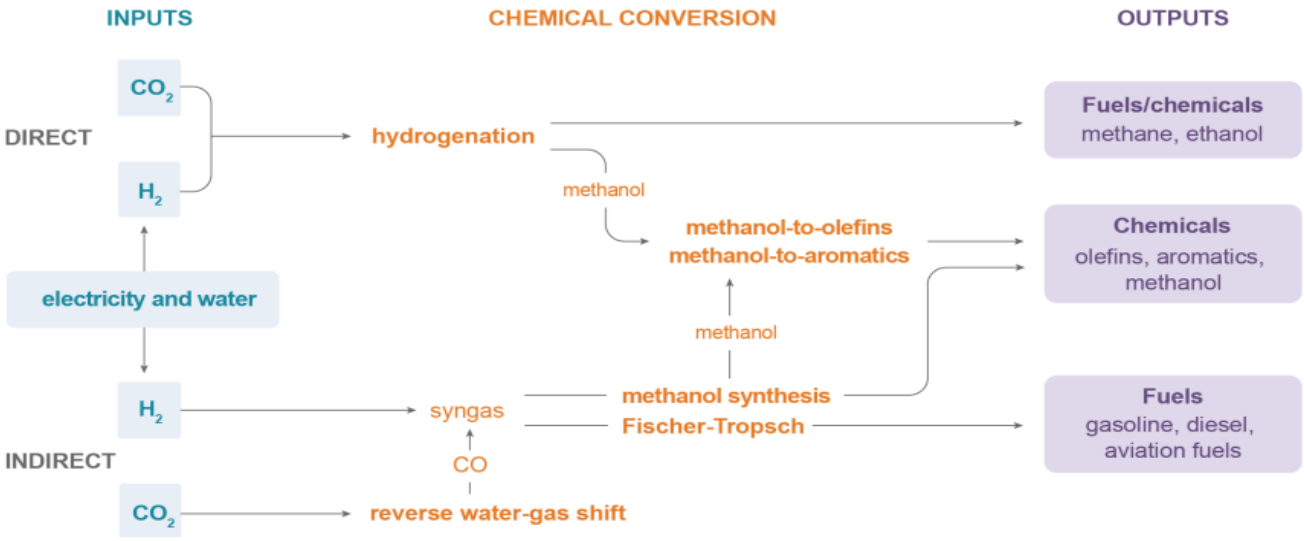

Figure 2. Conversion Pathways for CO_2-derived Fuels and Chemical Intermediates.

[Berghout, N. and McCulloch, S. **2019**. Downloaded 15th December 2023]

Some of these fuels can be produced directly or indirectly from the carbon contained in the carbon dioxide through some chemical conversion processes as shown in **Figure 2**, but at a relatively high energy cost.[8] CO_2 can be hydrogenated to CO via the reverse water gas shift (RWGS) reaction (**Equation 2)**, and the CO reacts with hydrogen gas through the syngas system leading to methanol and aviation fuel formation via methanol and Fischer-Tropsch syntheses.[8]

$$CO_2 + H_2 \longrightarrow CO + H_2O$$

Equation 2. Reverse Water Gas Shift

The electrochemical system of reducing CO_2 has become valuable in combining wind turbine or solar-generated electricity with carbon-based energy storage systems integrated with carbon capture, and utilization without distorting the controlled atmospheric CO_2 level.[6]

Electrochemically, methanol can be generated by reducing CO_2 with copper-based electrodes, but this process is limited by the associated low current, low faradaic efficiency, and high overpotentials.[9] Though hydrosilylation and hydroboration reduction of CO_2 to methanol has already been demonstrated by Guan, et al., the technology cannot be used on a larger scale yet, but the H_2 reduction of CO_2 to methanol using geothermal energy and heterogenous catalysis has gained major momentum and has already been industrialized in some countries like Iceland.[9] It is worth noting that although catalytic hydrogenation of CO_2 to methanol in **Equation 3** is an important chemical process, most of the known catalysts are used at temperatures above 220 ^oC, which adversely reduces the theoretical yield of the methanol produced and deactivates the catalyst through sintering.[9]

$$CO_2(g) + 3H_2(g) \rightleftharpoons CH_3OH(l) + H_2O(l)$$

Equation 3. Methanol Synthesis

Another major challenge facing the hydrogenation of carbon dioxide is its thermal instability, which slows down the conversion process according to Ye et al., and they demonstrated that some additives such as alcohols, amines, or amino alcohols are applied in stoichiometric or catalytic amounts in the reaction to convert CO_2 into intermediates that can be further hydrogenated to methanol.[9]

Furthermore, an important CO_2 conversion route to methane demonstrated by Randall et al., when they catalytically produced methane from CO_2 (**Equation 4)** at high temperature and pressure, in the year 1928.[10]

$$CO_2(g) + 4H_2(g) \rightleftharpoons CH_4(g) + 2H_2O(g)$$

Equation 4. Methane Synthesis

These carbon dioxide applications occur at a faster pace than Nature's photosynthesis and are usually carried out through the catalytic hydrogenation processes under high temperatures and pressure.[10]

Green Chemistry and Chemical Reactions

In recent times, organic chemistry processes such as hydrogenation reactions have been targeted towards being green chemistry (GC) to ensure their eco-friendliness, by adopting the green chemistry principles in their reaction processes.[11] Green chemistry refers to the act of developing chemical products and processes that function properly without releasing harmful materials into the environment.[12] There are twelve principles of Green Chemistry established in the year 1998 by Paul Anastas and John Warner, which serve as guidelines for chemical procedures and processes, and they include Waste Prevention, Atom utilization, Non-hazardous Synthesis, Safe Chemical Design, Controlled use of Solvents and Auxiliaries, Energy Efficiency, Renewable Feedstocks, Reduced Derivative Generation, Catalysis, Biodegradation, Real-Time Analysis to avoid Pollution and Accident Prevention.[12] According to the GC frameworks, green chemistry functions as a system of interconnected principles that aims at reducing the innate dangers

associated with chemical processes and is applicable at all stages of a chemical cycle, thereby maintaining the planet's habitability.[12]

In a review done by Shao-Tao et al, they demonstrated the general concept of a sustainable future carbon-neutral cycle based on hydrogenation processes involved in the CO_2 capture and utilization technologies and were able to compare the carbon neutral cycle involving the green principle such as green hydrogen in the hydrogenation process with the current carbon cycle as seen in the fossil-based industries.[13]

The hydrogenation reactions in this study were carried out in strict adherence to the green chemistry principles and frameworks especially catalysis, non-hazardous synthesis, safe design, controlled use of solvents, and accident prevention.

Our intent here is to deploy the IMes-CO_2 to yield methanol as the desired product, being one of the most important synthetic targets of CO_2 utilization.[14] This involves manipulating CO_2 as a raw material, particularly in the formation of a molecular complex that can act as a catalyst in the reduction of CO_2. The target bond to be broken in the reaction is the C-C bond between the imidazole ring and the CO_2 in a proposed overall **Equation (5)** for the methanol synthesis via imidazolium salt.

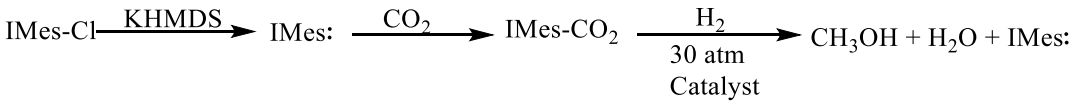

Equation 5. Proposed Synthesis and Reduction of Imes-CO_2

In addition to the environmental advantages of reducing CO_2 to methanol via hydrogenation reaction, the methanol produced has further vital economic applications such as its use as a transportation fuel[15] and for making important methyl tert-butyl ether and dimethyl ether.[16]

Chemical Catalysis

Catalysis as one of the twelve principles of green chemistry helps in maintaining a sustainable carbon-neutral society as a catalyzed reaction consumes the least amount of energy and generates the least amount of waste than the same reaction involving the stoichiometric reagents.[17]

The conversion of CO_2 to a variety of chemical products had been an uphill task owing to the associated challenges in developing the right catalysts with high reactivity and selectivity towards the specific desired products.[18] A catalytic process usually involves distinct geometric coordination, organic ligands, and metal complex cores, with the catalyst acting independently as an active site which allows for reactivity adjustment in synthesis and assessment of its detailed mechanistic and kinetic approaches.[18] Catalyst is essential in promoting the CO_2 reduction reactions through its ability to lower the activation energy barriers, increase product selectivity and increase the reaction rates.[19]

Catalysis has been an important technique in all major scientific aspects, including energy, medicine, pharmacology, and manufacturing, and has improved the quality of human lives as one major solution to fossil energy and CO_2 emission problems is the development of catalysis technologies for renewable carbon-neutral energies, chemicals, and materials.[13]

Generally, when comparing the hydrogenation processes involved in the reduction of CO_2 to formic acid and methanol respectively, the latter reaction process is thermodynamically more favored, and this is due to the formation of water associated with the reaction. [13]

Nonetheless, catalytically reducing CO_2 to methanol is a more difficult process due to its kinetics and compatibility challenges, one of which is that most of the known catalysts are used at temperatures above 220 ^oC, which restricts the theoretical yield of the methanol obtained as the reaction is exothermic in nature and reduces the catalytic activity via catalyst sintering.[13]

Homogeneous and Heterogeneous Catalysis

Chemical catalysts are classified as homogeneous catalysts when the catalyst exists in the same phase as the reactants and heterogeneous catalysts when the catalysts are not in the same phase as the reactants.[20]

Homogeneous Catalysis: A homogeneous catalytic activity depends on the solubility strength of its catalysts and is known to be highly active and selective in producing the desired products during a chemical process such as the CO_2 reduction reaction.[20,19] It is however limited by its relative instability, low current densities,[19] and recycling difficulties.[20] Nonetheless, homogeneous catalysis has shown activities in the CO_2 hydrogenation reaction to methanol under mild conditions but only in the presence of specific metal complexes such as ruthenium.[21] The first homogeneous molecular complex catalyzed hydrogenation of CO_2 to methanol was recorded in 1993 when Ken-ichi Tominaga et al performed the catalytic reaction at 240 ^oC in the presence of $Ru_3(CO)_{12}$-KI and they obtained methanol, CO, and methane through the Reverse Water -Gas Shift Reaction (RWGSR) process.[22]

In carbon dioxide hydrogenation under mild conditions, the molecular catalysts usually exhibit high performance but unlike its conversion reaction to formic acid, its conversion to methanol involves more hydrogenation steps and based on their mode of catalysis, they are three major categories:[13]

1) Monofunctional Molecular Catalysts

2) M/NH Bifunctional Molecular Catalysts

3) Aromatization-dearomatization Bifunctional Molecular Catalysts

Monofunctional Molecular Catalysts

The monofunctional molecular catalytic steps involved in the CO_2 hydrogenation process include; i) hydrogen coordination, ii) hydrogen activation, and iii) hydride transfer, occurring within the metal center as shown in **Figure 3**[23] and Shao-Tao Bai et al in their review, demonstrated that the major challenge with this class of catalyst is their deactivation and loss of their catalytic activity over a long reaction time.[13]

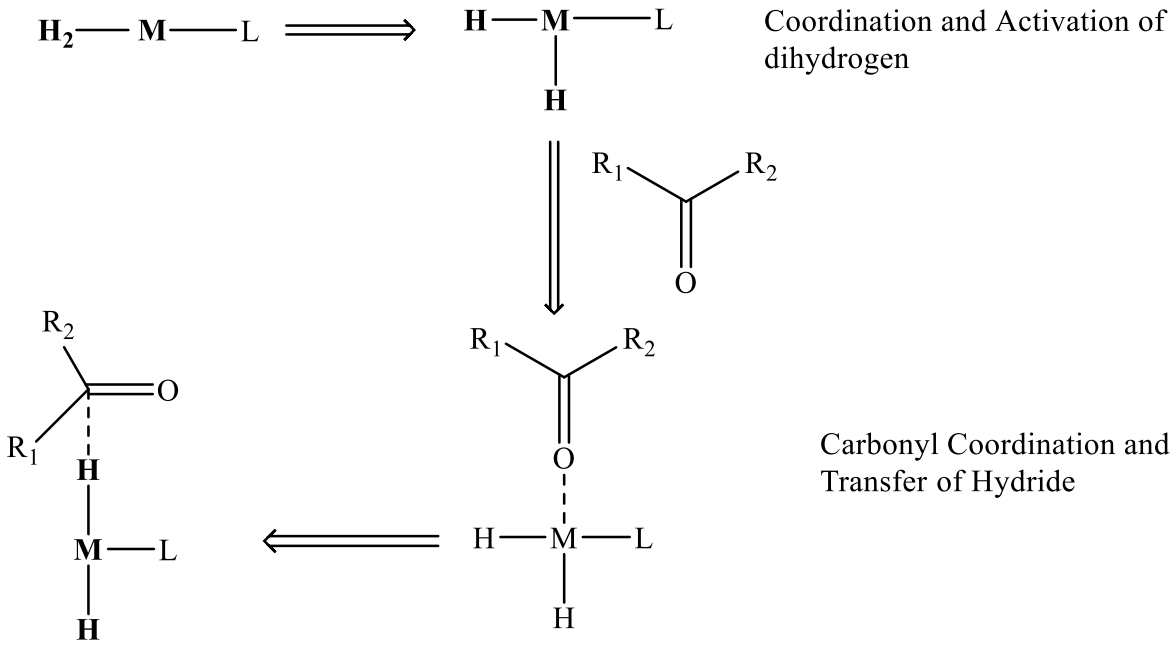

Figure 3. The Steps of Monofunctional Molecular Catalysis in Hydrogen Molecule Activation and Hydride Transfer.

Also, Eric S. Wiedner et al were able to demonstrate that a similar complex as seen in **Figure 4** is not active enough to hydrogenate CO_2 to methanol but instead is more active as a

ligand with three atoms acting as donor atoms in a coordination complex.[24] They further demonstrated that as a tridentate, there will be an increase in the electron density on the metal center, which improves the tendency of the metal-hydride formed to be transferred to the substrate, hence pushing the hydride transfer to the carbonyl group of CO_2 and subsequently resulting in the formation of methanol.[24]

M/NH Bifunctional Molecular Catalysts

The second category known as the Metal/NH bifunctional molecular catalyst was discovered in 1995 by Noyori and his co-workers when they first revealed an improved catalytic activity of Ru(II)-BINAP complex (BINAP: 2,2' -bis(diphenyl-phosphino)-1,1' -binaphthyl), in the enantioselective hydrogenation of ketones to secondary alcohol in the presence of an alkaline base, such as KOH, KO-*i*-C_3H_7, KO-*t*-C_4H_9, or ethylenediamine, as shown in **Equation 6**.[25]

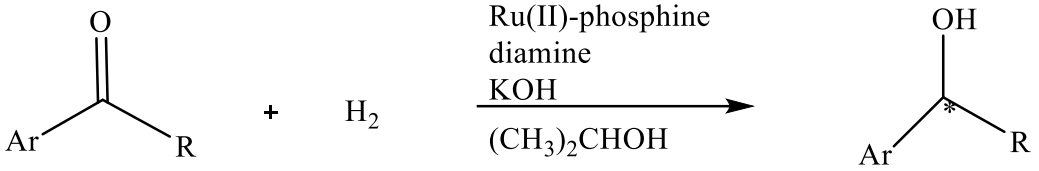

Equation 6. Catalytic activity of Ru (II)-BINAP complex

They later developed a series of phosphine-free Ru/NH bifunctional catalysts with enhanced catalytic activities than the regular monofunctional catalysts due to noticeable cooperation existing between the NH function of its ligand and Ru metal, and they were similarly used for asymmetric hydrogenation of aldehydes, ketones, carbonic and carboxylic acid derivatives.[25] This cooperation helps in the activation of the molecular dihydrogen and the proton or hydride transfer process in the M/NH bifunctional catalysis in **Figure 4,** and the N-H

functionality provides the proton for the protonolysis process, lowers the energy barrier and is regenerated at the metal-hydride via bifunctional hydrogen molecule activation.[13]

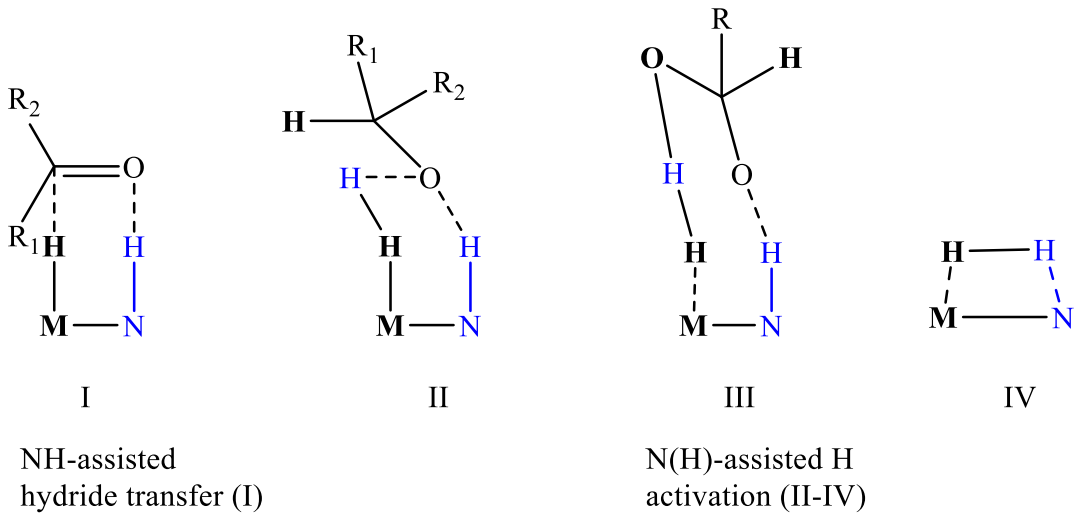

Figure 4. The Dihydrogen Activation Steps Involving the Hydride/Proton Transfer in M/NH Bifunctional Molecular Catalyst.

There are four major cycles involved in the overall mechanism of the M/NH bifunctional catalysis during the hydrogenation of CO_2 to methanol, and they include the metal catalyst/formic acid cycle, hemiaminal cycle, methanol cycle, and the formamide cycle, in the presence of an amine additive.[26] Each of the cycles plays a pivotal role in ensuring the completion of the four vital steps involved in the catalysis which are classified majorly into dihydrogen activation and the metal hydride/proton transfer to the stabilized carbonyl group with transition states allowing the occurrence of O---H----N hydrogen bonding interaction.[27] The M/NH bifunctional catalysts have been an important tool in the CO_2 capture and conversion to methanol process and their hydrogenation catalysis has been extended to other metals such as manganese and iron.[13]

Aromatization-Dearomatization Bifunctional Molecular Catalysts

Milstein and Gunanathan were the first to discover a new mode of metal-ligand cooperation that produces uncommon bond activation and catalysis as seen in the aromatization-dearomatization processes of some ligands, such as the pincer-type ligands derived from pyridine or acridine and were able to develop many vital catalytic processes such as:[28]

i) Dehydrogenation of secondary alcohols to ketones without an acceptor.

ii) Coupling of alcohols directly with amines to produce polyamides and amides

iii) Dehydrogenative coupling of alcohol to esters without an acceptor

iv) Acylation of secondary alcohols by esters with the release of dihydrogen

v) Hydrogenation of ketones to secondary alcohols under mild hydrogen pressures

These processes are efficient green synthetic processes that occur under mild conditions, with no waste production, and form useful economic products with hydrogen and water as the only byproducts.[28]

In similarity to the M/NH bifunctional catalysts, aromatization-dearomatization bifunctional molecular catalysts can absorb and give off hydrogen but the major difference is that while the former has a secondary amine in their pincer ligand, which subsequently changes to an amide during the catalytic process, the later depends on the nitrogen of an azine-based pincer ligand moving between the imine and the enamide by losing a proton from the benzylic position instead of the nitrogen position shown in **Figure 5**.[13]

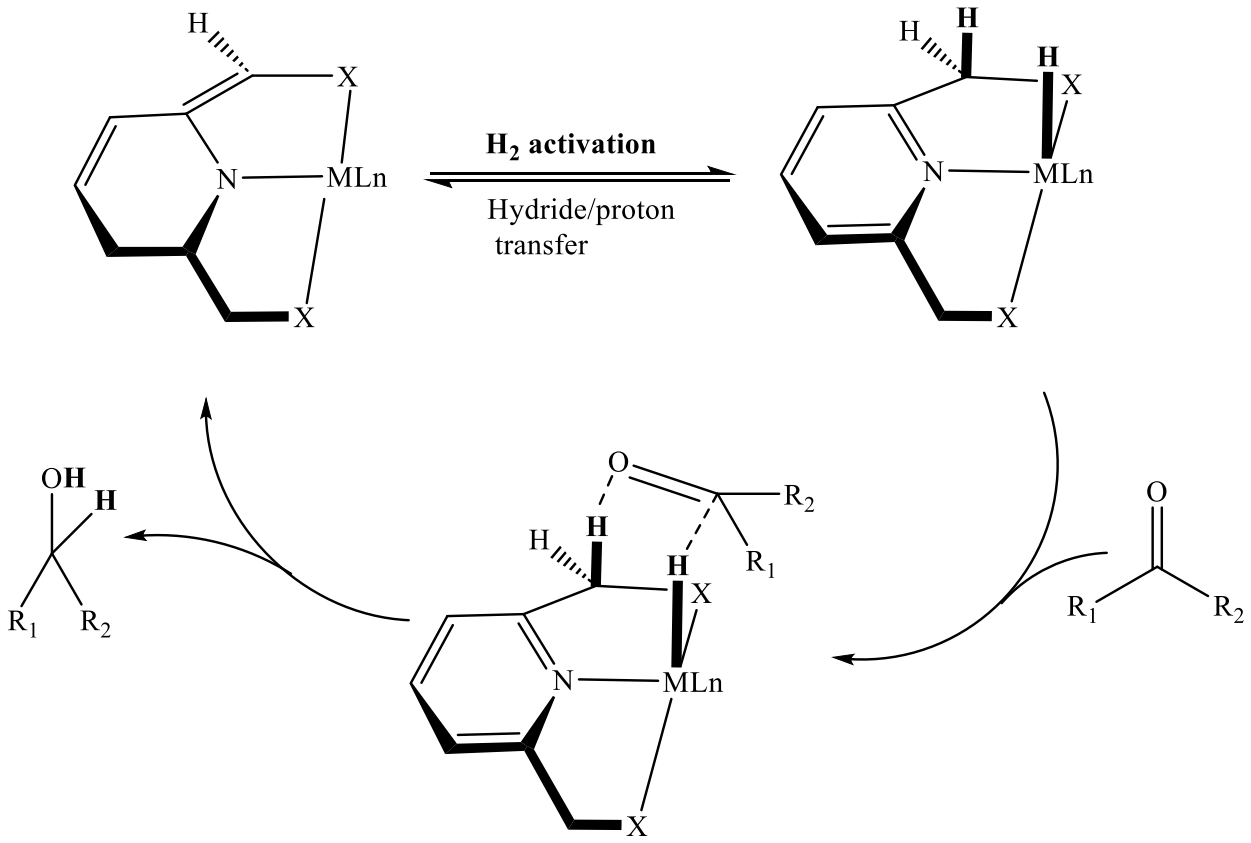

Figure 5. The General Mechanism for Hydrogen Activation and Hydride/Proton Transfer to a Carbonyl Group in Aromatization-Dearomatization Bifunctional Molecular Catalysis.

This type of catalysis is involved in the hydrogenation of many CO_2 – derived organic compounds such as carboxylic acids, carbonic acids, carbamates, carbonates, urea, polycarbonates, and formates to their respective amines and alcohols.[26]

Since CO_2 is the major source of these derivatives, their hydrogenation through this type of catalysis helps in solving some kinetic and thermodynamic challenges experienced in the direct formation of methanol from CO_2.[13]

Heterogeneous Catalysis: Heterogeneous catalysts are more stable, cost-effective,[13] easily recyclable, with higher current densities and reduced catalyst distance which permits more efficient reactions but with reduced activity and product selectivity.[20,19]

Heterogeneous catalysts have also been used extensively in the CO_2 hydrogenation to methanol at mild reaction conditions, and based on their mechanism and composition, are classified into three major categories:[13]

1) Metal/Metal and Metal/Support Bifunctional Catalysts.

2) Active-site/N or Active-site/OH Bifunctional Catalysts.

3) Cooperation of Catalyst and Additives in a Tandem Process via Crucial Intermediates.

Metal/Metal and Metal/Support Bifunctional Heterogeneous Catalysts

This class of catalysts achieves their catalytic activities by utilizing the supports provided by the surrounding metal nanoparticles (NPs) and second metal and its oxide nanoparticles, which could act as the co-catalytic sites to form the intermediates that are subsequently reduced to methanol as seen in **Figure 6**.[13]

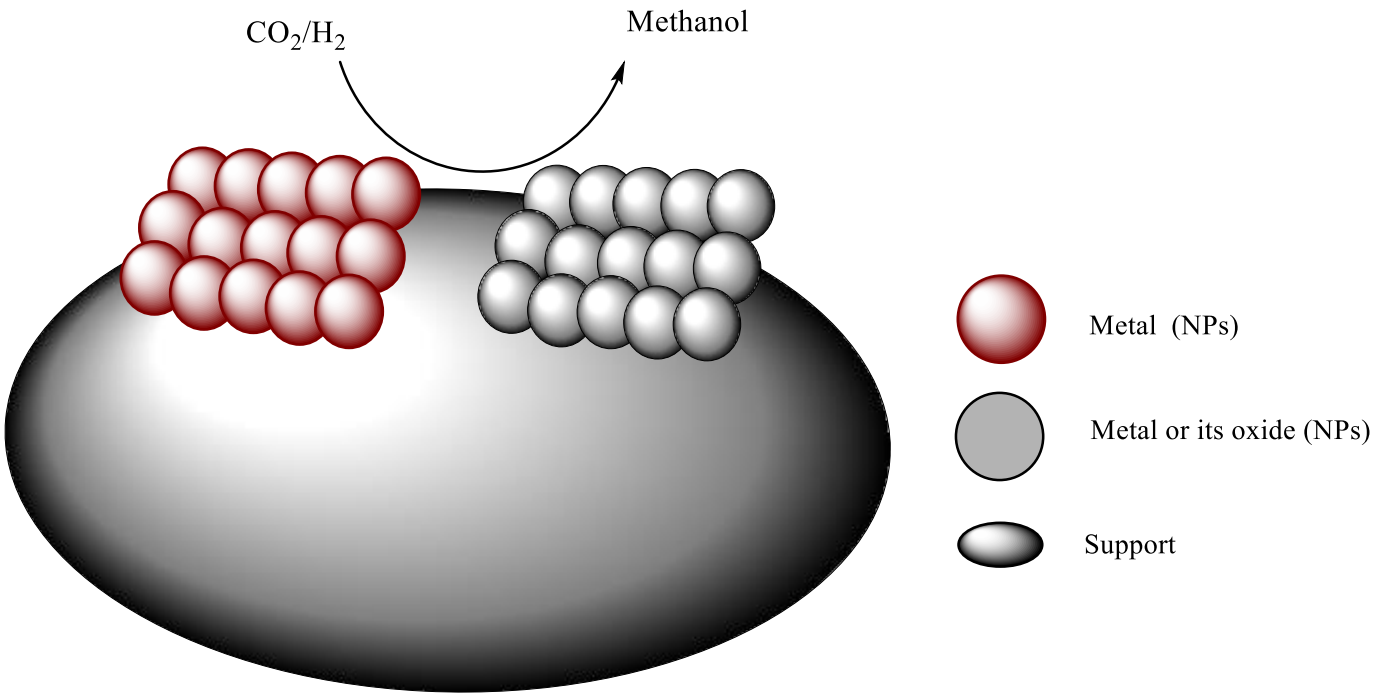

Figure 6. The General Scope of Metal/Metal and Metal/Support Bifunctional Heterogeneous Catalysis in Hydrogenation of CO_2 to Methanol.

Active-site/N or Active-site/OH Bifunctional Heterogeneous Catalysts

This approach attracted many research interests for some industrial applications, including the conversion of CO_2 to methanol, and it involves an active collaboration between the superficial OH or N-functional groups and the active metal sites leading to the activation of the dihydrogen, adsorption of the carbon dioxide, transfer of the hydride/proton, and stabilization of the intermediate formed in the process as seen in **Figure 7.**[13]

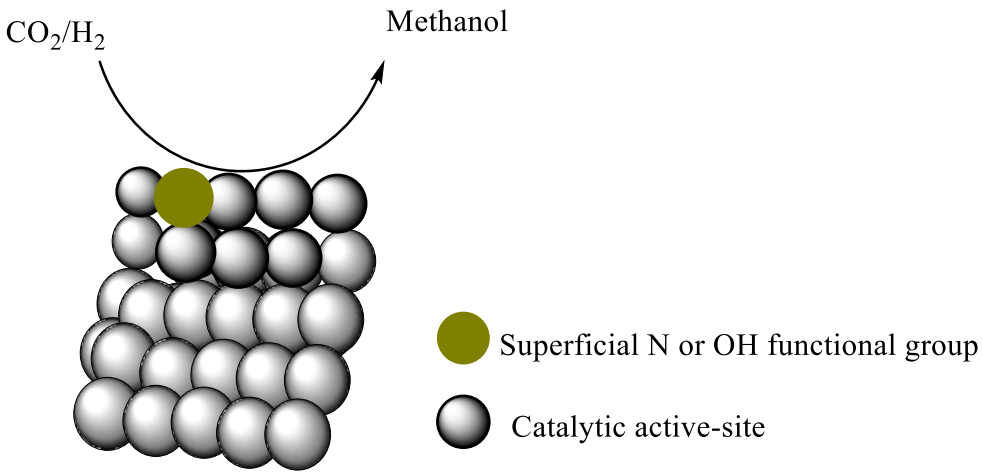

Figure 7. The General Concept of Active-site/N or Active-site/OH Bifunctional Heterogeneous Catalysis in Hydrogenation of CO_2 to Methanol.

Cooperation of Catalyst and Additives in a Tandem Process via Crucial Intermediates

This tandem catalytic system occurs either as an auto, when involving only one catalyst[29] or orthogonal, when involving two or more catalysts, depending on the number of catalysts needed for the catalytic cycles as required during the process. Additives play an important role in this type of catalysis as they cooperate with the catalysts as shown in **Figure 8** and unlike the homogeneous catalysts that usually encounter compatibility challenges, the heterogeneous catalysts can set apart their catalytic active sites on surfaces thus allowing for more efficient catalytic hydrogenation of CO_2 to methanol.[29]

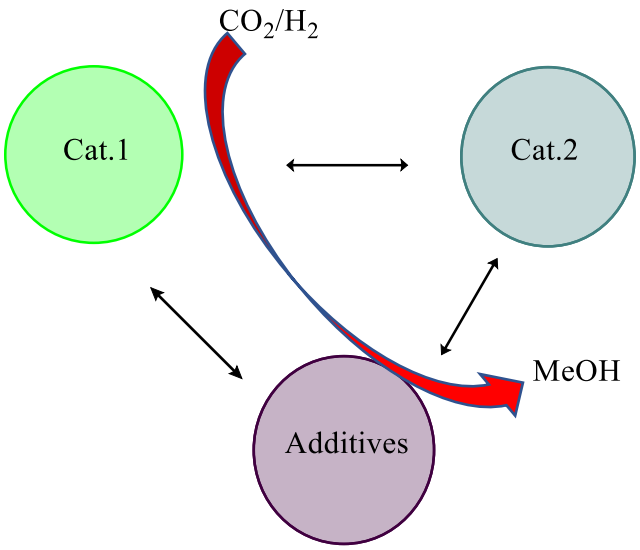

Figure 8. The General Concept in CO_2 Hydrogenation to Methanol via a Tandem Process Involving Cooperation between the Catalysts and Additives.

Though the performances of both the homogeneous and heterogeneous catalytic systems are not yet well developed enough for higher industrial applications, recent improvements have combined the concepts of both the molecular and heterogeneous control strategies as evidenced in

the molecular approaches of the metal-free catalysts, the covalent organic frameworks (COFs), the metal-organic frameworks (MOFs), N-heterocyclic compounds (NHCs), and N-substituted pyridines in reducing CO_2 to desirable materials.[19]

In addition, an ideal catalyst is one that is designed by synergizing both concepts of catalysis **Figure 9**, which makes it more selective, active, stable, and easily recyclable as has been achieved with specially designed catalysts such as nanoparticles, single atoms, and supported complexes. [20]

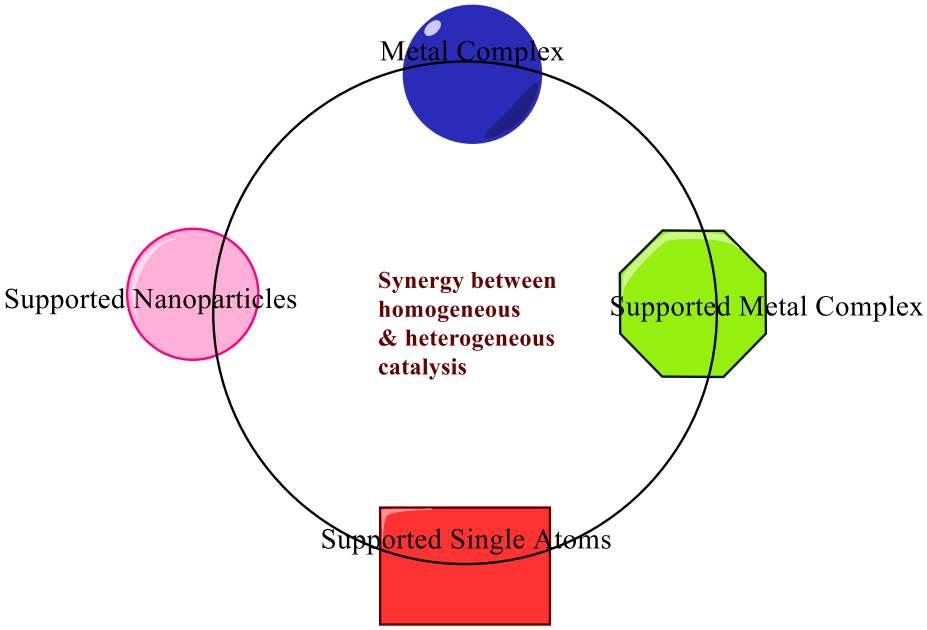

Figure 9. The Synergy between Homogeneous and Heterogeneous Catalysis

Carbon dioxide capture and storage (CCS) technology has proven to play an important role in controlling the global climate change has been recognized globally, and its demand has increased significantly.[30] Many countries have also tried to substantially reduce global CO_2 emissions via processes like CCS, but these applications have been faced with challenges such as capacity, cost, sustainability, and safety but efforts are being made to build improved and cost-efficient versions and have them readily available.[30]

Chapter Two

Carbenes and N-Heterocyclic Compounds

Carbenes are carbon compounds with two nonbonding electrons on a single atomic center, with no charge on the carbon atom which is mostly represented in an oxidation state of II but can be formulated to exist as zwitterions (ylides).[31] Carbenes are generally known as reactive species but the imidazolium carbene is known to be a stable carbene and was first isolated by Arduengo in 1991, when it was also called a persistent carbene due to its peculiar stability.[32] Arduengo et al. reported the synthesis, characterization, and structure of 1,3-di-1-adamantyl-imidazol-2-ylidene as the first crystalline carbene synthesized through the deprotonation of the 1,3-di-1-adamantylimidazolium chloride salt in THF, with dimethyl sulfoxide catalyst (cat. DMSO) or potassium tert-butoxide (cat. KO^{t}Bu) and 1 equivalent of sodium hydride, at room temperature **Figure 10.**[32]

Synthesis of Carbene

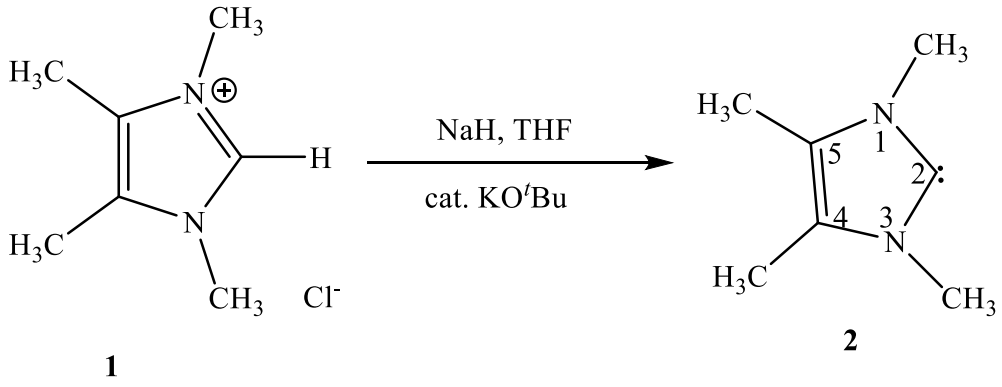

1 **2**

Figure 10. Synthesis of a Carbene

According to the authors, the kinetic and thermodynamic stability of the carbene in the absence of air and water has eased off its isolation, characterization, and efforts to study their reactive intermediates since they have become well-known reaction intermediates with vital roles in many chemical processes.[32]

Dixon and Arduengo studied the electronic structure of the nucleophilic carbene and discovered that the carbene stability is due to the steric effects and electronic features allowing the electron-rich atoms to donate electrons into the carbene p-orbital.[33]

Organic N-heterocyclic compounds are cyclic structured compounds with at least one carbon atom and one or more different non-carbon atoms in their rings.[34] So much work has been done on N-heterocyclic compounds, which are the largest division in organic chemistry when compared with those of aliphatic and carbocyclic compounds, and more studies on them remain on-going since the discovery of their enormous industrial applications.[34] Some of the most common and important heterocyclic compounds are found in secondary metabolites formed by aquatic and terrestrial living organisms, and they include imidazole, oxazole, and thiazole as shown in **Figure 11**, containing nitrogen, oxygen, and sulfur atoms respectively.[35]

Examples of Heterocyclic Compounds

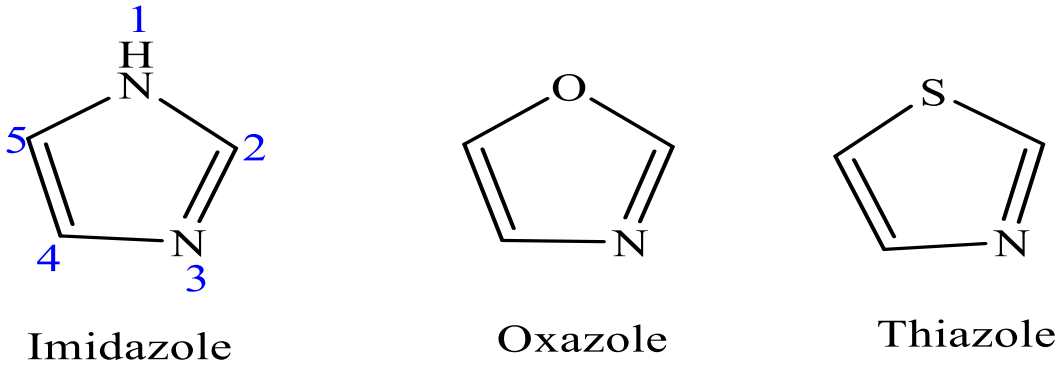

Figure 11. Examples of Heterocyclic Compounds

Similarly, there has been great progress made in the field of imidazole chemistry, a major N-heterocyclic compound and this is evidenced in the vast records of discoveries, work, literature, and materials available on imidazole and its derivatives.[35] Some of the major derivatives of imidazole such as imidazolines, imidazolidines, and benzimidazoles possess with unique physical and chemical properties s are, are prepared from oxidizing or reducing imidazole to various states **Figure 12.**[35]

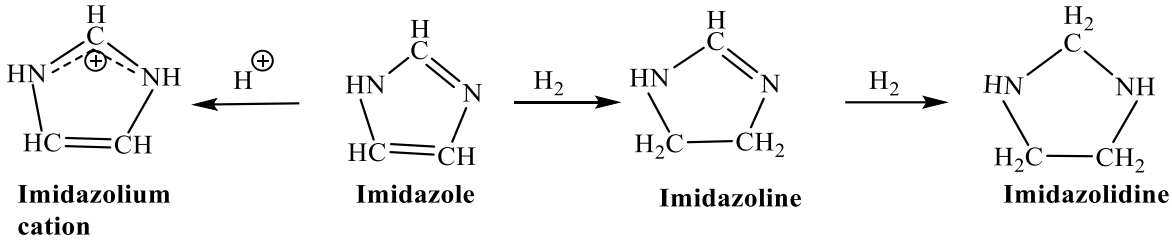

Figure 12. Imidazole and its Redox Structures

Heinrich Debus was the first to synthetically produce imidazole in 1858, by reacting a dialdehyde with formaldehyde in ammonia, as shown in **Figure 13,** and he first called the product the glyoxaline since it was produced from glyoxal, and the product is also called iminazole.[36]

Synthesis of Imidazole

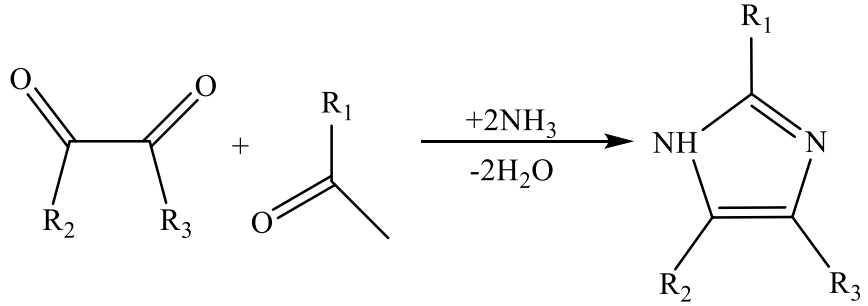

Figure 13. Synthesis of Imidazole

Imidazole is an amphoteric polar molecule, it is highly polar, water soluble and has two tautomeric forms, since the hydrogen atom can be found on any of the two nitrogen atoms, with some the resonance structures as shown in **Figure 14**.[36]

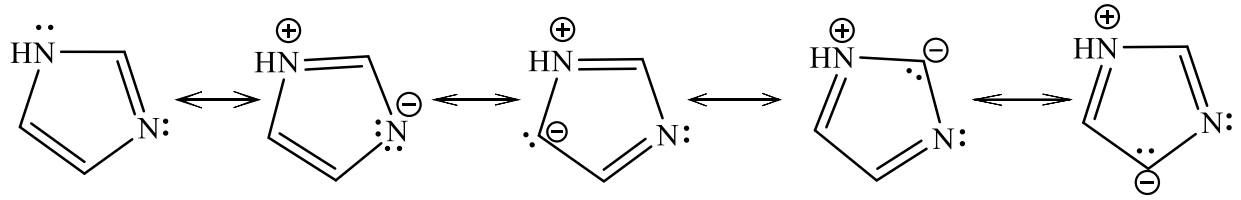

Figure 14. Resonance Structures of Imidazole

The high basicity of the imidazole ring is seen to be due to the nitrogen atoms present in the ring, which allows the resonance stabilization of the protonated species.[37] Some alkaloid plants contain imidazolium ring, and their nitrogen atoms forming the heterocyclic ring is derived from the L-histidine amino acid **Figure 15**.[37]

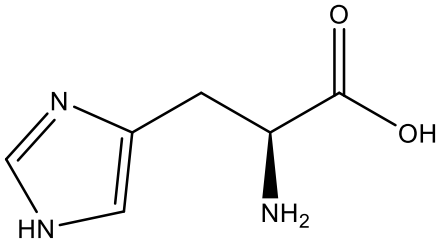

Figure 15. Structure of L-histidine, an Imidazole-containing Amino Acid.

Importance Of N-Heterocyclic Organic Compounds

(i) Bio-medicinal uses: Some organic compounds derived from heterocyclic compounds like imidazole or its derivatives are important compounds with a wide range of applications and are usually found in essential biological, hormonal, physiological, and pharmacological natural products.[38] Some scientists, like Vedanjali et al, have been able to demonstrate the importance of natural products in the production of unique drug prototypes with about 60% antiviral propensity, for the treatment of cancerous and non-cancerous diseases.[38] Natural products are secondary metabolites formed by living organisms and are useful in pharmaceuticals for the manufacturing of drugs such as anesthesia, antibiotics, procedural sedative drugs, anti-anxiety drugs, and antifungal drugs, are also essential vital constituents in the invention of fragrances.[39] The chemical structure of such a drug containing an imidazole ring is midazolam **Figure 16,** an anesthesia used for sedative effects**.**[40]

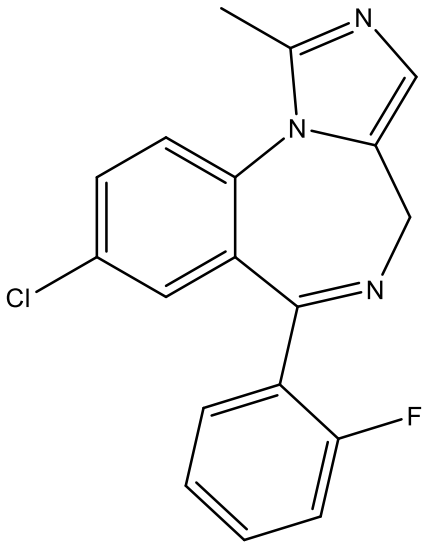

8-chloro-6-(2-fluorophenyl)-1-methyl-4H-imidazo[1,5-a][1,4]benzodiazepine

Figure 16. Structure of Midazolam, an Imidazole-containing Pharmaceutical.

(ii) Ligands for organometallic catalysts: N-heterocyclic carbene compounds (NHC) have become vital components in homogeneous catalytic reactions, where they act as ligands and form a variety of NHC complexes of palladium, platinum, rhodium, copper, ruthenium, and iridium etc., and are easily transferrable within the reaction cycle.[41] In some synthetic reactions, the NHC - complexes act as either a strong base or basic ligand by deprotonating the precursor imidazolium salt and oxidatively adding the C-H bond to it.[41] Voutchkova et al further demonstrated in their study that an NHC-complex such as imidazolium carboxylate is air-stable and can act as precursor for the synthesis of imidazolidenes.[41]

(iii) Organocatalytic nucleophiles: NHC-carboxylate and imidazolidenes both possess the ability to act as vital transient metal catalytic ligands and organocatalytic nucleophiles in a chemical synthesis.[42] N-heterocyclic carbenes exhibit more catalytic performance than the electron-rich phosphine ligands in forming metal complexes and the special class of compounds used as nucleophiles in polymerization catalytic reactions.[42] Consequently, polymerization reactions catalyzed by N-Heterocyclic carbenes can be controlled due to the NHCs' ability to form stable zwitterions in their reaction with carbon dioxide.[43]

(iv) Cyclotrimerization: Essential aromatic compounds such as triaryl isocyanurates and triallyl isocyanurate used in polymerization and post-polymerization reactions are products of the cyclotrimerization reaction.[44] N-heterocyclic compounds such as 1,3-bis-(2,6-diisopropylphenyl)-4,5-dihydroimidazol-2-ylidene plays a vital catalytic role in synthesizing isocyanurates through the cyclotrimerization of isocyanates.[44] Generally, isocyanurates are used industrially to improve in the production of nylons, co-polymer resins, polyurethanes, laminating, and coating materials.[44]

(v) Coupling of epoxides and CO_2: Due to the zwitterionic nature of the N-Heterocyclic carbene-complexes, the NHC-CO_2 had proven to be a vital organocatalyst in the formation of

cyclic carbonates through the catalytic coupling reactions of epoxides and CO_2.[45] The NHC-CO_2 can readily give off the CO_2 and transfer the NHC to the transition metal complexes under mild conditions, and when substituted can also exchange with the free CO_2 available in the solution.[45]

(vi) Capturing and delivering of carbon dioxide: Tommasi and Sorrentino have been able to demonstrate that Imidazolium carboxylates can be used to deliver carbon dioxide as seen in the carboxylation reaction of acetophenone.[46] Moreso, in organic chemistry, it has been recognized and recorded, that carbon dioxide can be captured with organic compounds such as imidazolidenes, but the reaction process and its carboxylate product are yet to become generally applicable.[46] Similarly, there have been significant discoveries made in the field of other N-heterocyclic compounds used in CO_2 capturing, but their actual applications are yet to be fully utilized.[47]

In this study, our focus is on activating CO_2 via molecular adduct formation followed by catalytic hydrogenation. Such adducts are known to form by exposing CO_2 to N-heterocyclic carbenes.

Hydrogenation Reactions

The diverse CO_2 applications are possible due to the existence of hydrogenation processes, whose chemistry plays important roles in the modification of chemical raw materials and petrochemical engineering.[48] Hydrogenation reactions are useful chemical reactions involving the use of hydrogen to remove a double bond or saturate unsaturated bonds in alkene, alkynes or polyenes in the presence of a catalyst, and a successful hydrogenation process does not occur in an inert condition but at high pressure with a substantial amount of energy supply.[48] The imidazole ring had however shown high notable resistance to being catalytically hydrogenated in the past,

apart from lophine (2,4,5-triphenyl-1H-imidazole) and amarine which are platinum catalyzed in an acetic acid medium.[48]

Chapter Three

Synthesis of Bis-Mesityl Imidazolium Carboxylate

Starting material: A commercial bottle of 1,3-bis (2,4,6-trimethyl-phenyl) imidazolium chloride salt (compound **1,** 5 g), with 95% purity was obtained from Sigma Aldrich.

Sample Preparation and Reaction Set-up

The starting material (IMes-Cl) was used directly for the synthetic reaction without further purification.

The 2 two-necked round-bottom flasks, glass corks, frit funnel, Erlenmeyer flask, two cannulas, stir bar, needle, and syringe were dried overnight in the oven.

The nitrogen and carbon dioxide gas tanks were well positioned and connected jointly via a T-tubing system which ensured that there was only one supply pipe inlet via the drying chamber into the reaction system. The drying chamber contained blue Dri-rite granules sandwiching the anhydrous calcium chloride in the middle of the chamber. This further ensured that no oxygen no water entered our reaction system, as nitrogen was bubbled first through the entire set-up for 10 minutes to chase out any water or air present before the reaction was begun.

A pipe was attached to the reaction's round-bottom flask to collect the emissions from the reaction and release them to a nearby oil bath, which also served as an indicator of the gas flow rate to the reaction system.

Table 1. Reagent details for IMes-CO_2 preparation

Name of reagent	Imidazolium Chloride	Toluene	Potassium Hexamethyldisilazide (KHMDS, 0.5 M in toluene)
CAS Number	141556-45-8	108-88-3	40949-94-8
Melting Point (°C)	280-286	-95 to -93	194-195
Boiling point (°C)	499.2	110.6	111
Molecular mass (g)	340.9	92.14	199.48
No of moles (mm)	1.47	708.16	11.47
Density (g/cm3)	1.03	0.87	0.88
Volume (ml)	0.49	75	2.6
Amount used (g)	0.5	65.25	2.29

Safety and Handling

Moisture and oxygen contamination was strictly avoided throughout the experiment and the procedure was conducted in the hood under an inert atmosphere.

KHMDS as a strong base must be properly handled. Toluene is lachrymatory and irritates the skin when exposed to it, hence must be handled carefully.

Procedure

The method used in synthesizing the 1,3-Bis(2,4,6-trimethylphenyl) imidazolium carboxylate was adopted from a literature procedure.[26] The complete synthesis was completed in two phases, the first phase **Figures 17.** and the second phase **Figures 19.**

The first phase (**Figure 19**)**:** Synthesis of 1,3-Bis(2,4,6-trimethylphenyl) imidazolium carbene **2** from 1,3-bis (2,4,6-trimethyl-phenyl) imidazolium chloride **1**.

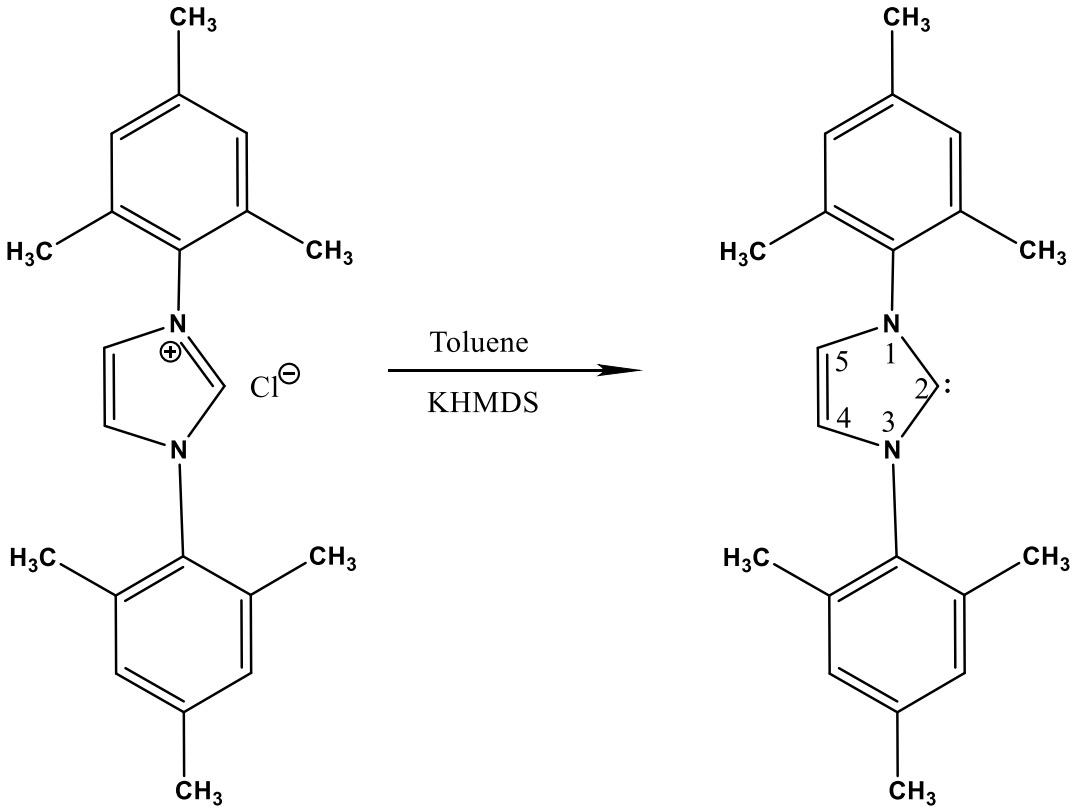

(1) **(2)**

Figure 17. Synthesis of 1,3-bis(2,4,6-trimethylphenyl) Imidazolium Carbene **2**

A 0.5 g quantity of imidazolium salt (IMes-Cl) was weighed out and transferred to a two-neck round bottom flask containing a stir bar and sealed with rubber stopper. The toluene (75 mL) was added to the flask through a cannula to dissolve the salt, but the salt did not completely dissolve in it, hence a cloudy solution was formed. The reaction flask was immersed in a water bath for 30 minutes and heated to 65 ^{o}C, for better dissolution, still no change, it was clamped to a tripod and suspended in the ultrasonic bath for twenty minutes, but the reaction mixture remained cloudy with no change in dissolution. The experiment continued, the 0.5M Potassium

bis(trimethylsilyl)amide (2.6 mL) in toluene was measured out and added to the reaction flask using an oven-dried syringe, to generate the 1,3-bis (2,4,6-trimethyl-phenyl) imidazolium carbene **2**. The mixture was stirred for another thirty minutes for the reaction to complete while closing the two-necked flask from nitrogen and air, and the set-up as shown in **Figure 18**.

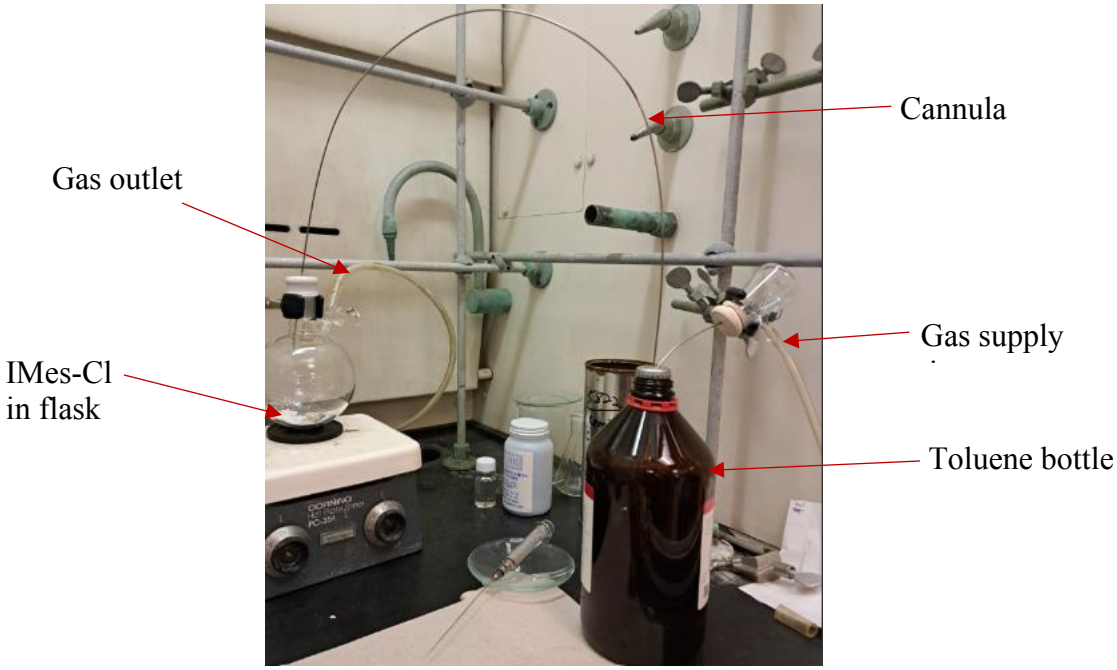

Figure 18. Dissolution of IMes-Cl with Toluene

The second phase (**Figure 19**)**:** Synthesis of 1,3-bis(2,4,6-trimethylphenyl) imidazolium carboxylate **3** from 1,3-bis(2,4,6-trimethylphenyl) Imidazolium Carbene **2**

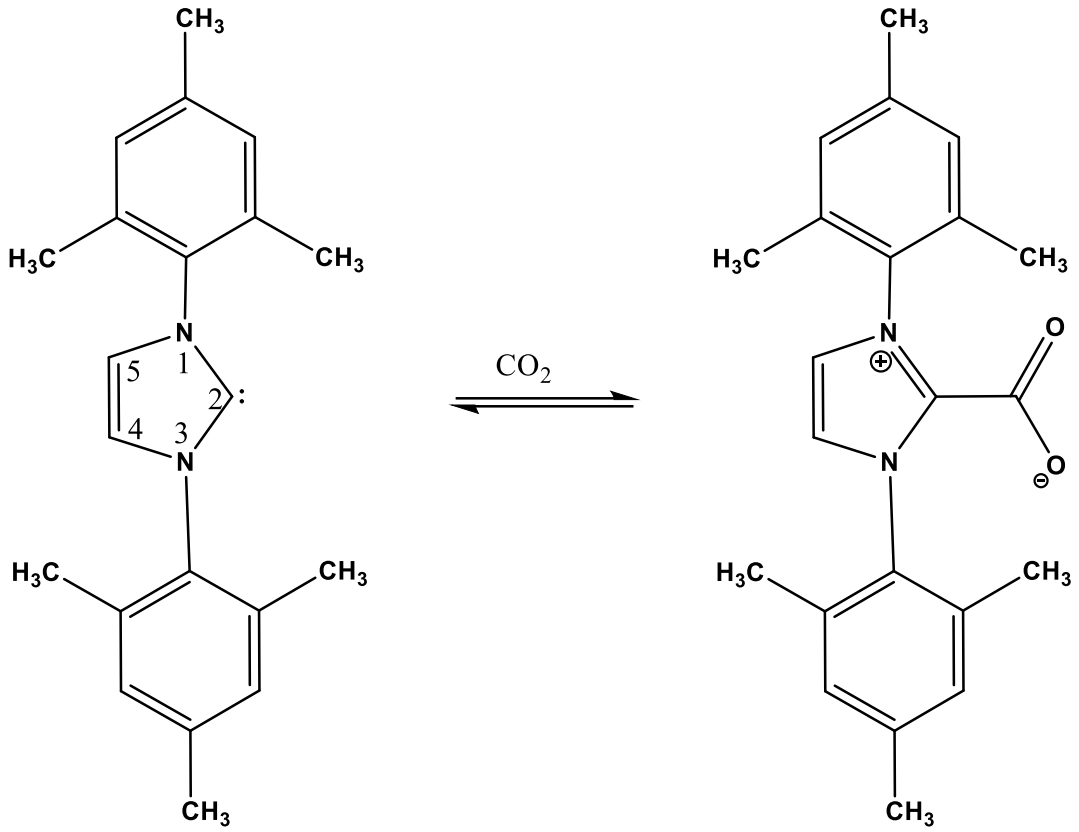

Figure 19. Synthesis of 1,3-bis(2,4,6-trimethylphenyl) Imidazolium Carboxylate **2**

A 1.5 g quantity of oven-dried Celite was weighed out and added to a frit with medium (M) porosity, smeared uniformly into the frit with toluene for good filtration, and then packed tight by drawing off the excess solvent with vacuum filtration. The 1,3-bis (2,4,6-trimethyl-phenyl) imidazolium carbene **2** solution was then filtered through the Celite frit with vacuum. The clear filtrate was immediately transferred to a second two-neck round bottom flask containing stir-bar, purged again with dry nitrogen for about 15 minutes while being stirred, then carbon dioxide was

bubbled through it to generate the 1,3-bis (2,4,6-trimethyl-phenyl) imidazolium carboxylate **3**. The reaction mixture was stirred for forty-five minutes. The precipitated imidazolium carboxylate **3** product was washed with diethyl ether using a fritted funnel with ultra-fine (UF) porosity and pulled through with a vacuum till the slight yellow color vanished. The product was dried in a vacuum desiccator containing calcium chloride and Dri-rite overnight and then weighed. A 58% yield was obtained, and the product was stored in a glass vial inside the desiccator under vacuum.

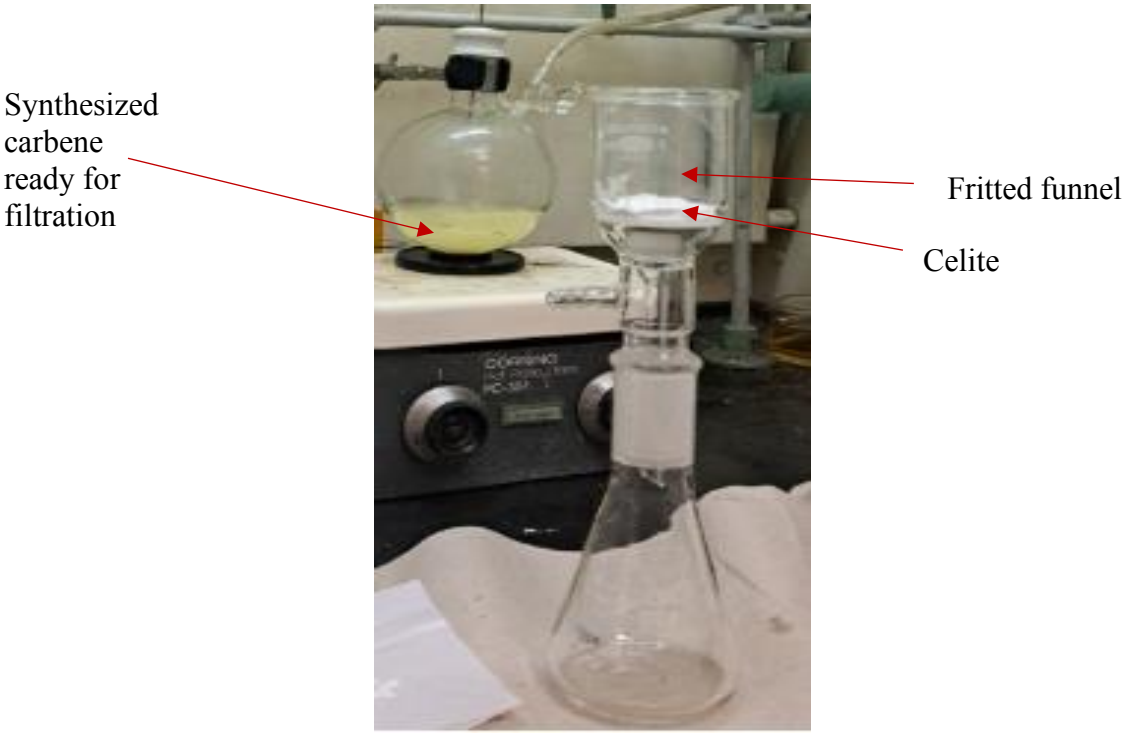

Figure 20. Filtration of the Carbene

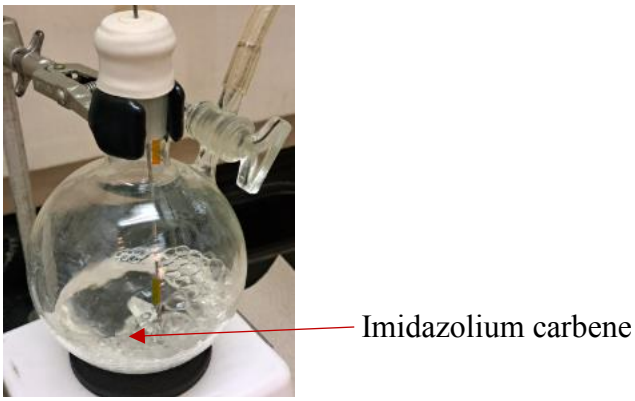

Figure 21. Filtered Carbene Ready for Carboxylation

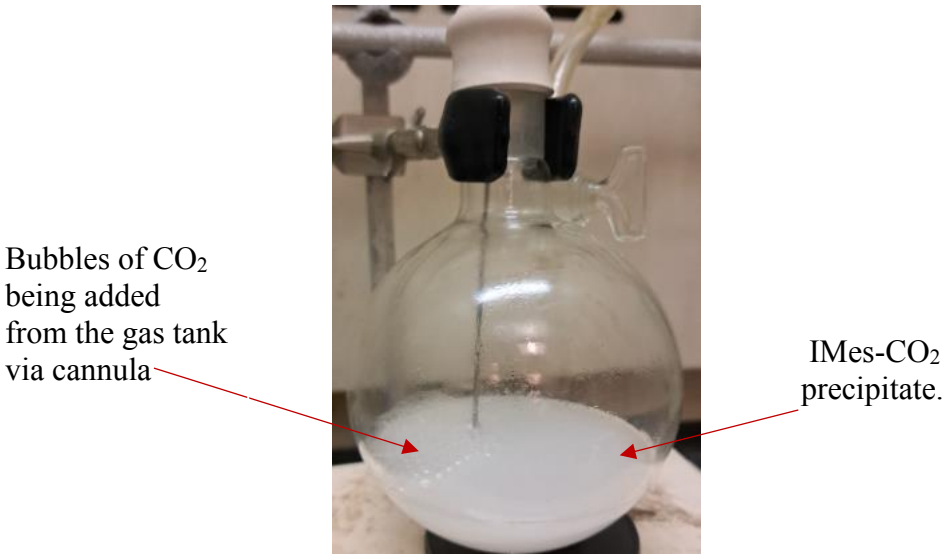

Figure 22. Formation of Compound 3

Alternatively **Figure 23** set-up involving a three-necked flask, needle valve, and capped fritted funnel, was used in transferring the carbene, after its generation while making another round of more 1,3-bis(2,4,6-trimethylphenyl) imidazolium carboxylate **2**. This helped to further reduce the air and water contamination which could occur during the transfer stage as envisaged in the procedure.

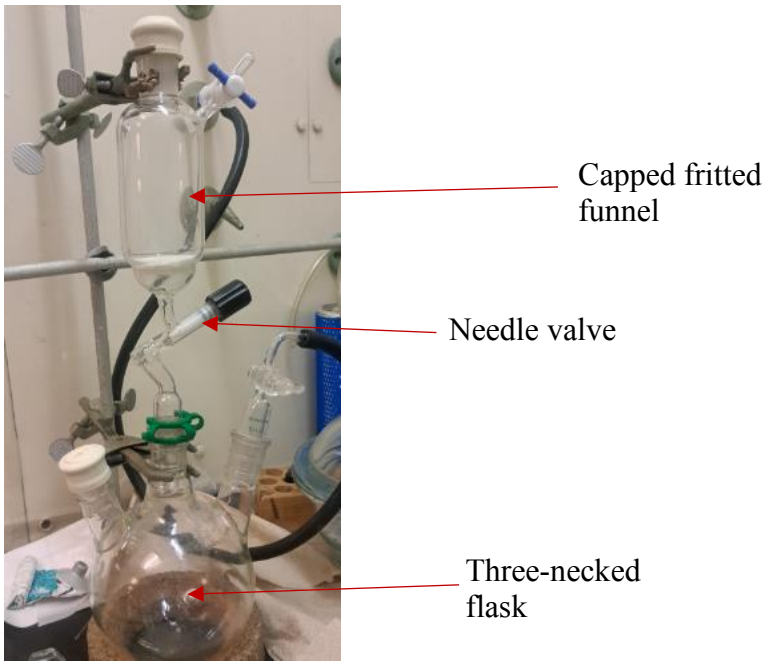

Figure 23. Alternative Set-up for Carbene Transfer

Carboxylate Synthesis Result Analysis

The starting material and the synthetic product were analyzed and verified through nuclear magnetic resonance (NMR) spectroscopy, infrared (IR) spectroscopy, mass spectrometry, and thermal gravimetric analysis (TGA) analytical techniques. The respective spectra and curves obtained were recorded and interpreted.

Nuclear Magnetic Resonance (NMR) Spectroscopy Analysis

The nuclear magnetic resonance spectroscopy analysis was performed using Bruker Ultrashiled 400 instrument.

The NMR Analysis of the Starting Material, Compound **1**.

A 100 mg of the starting material, 1,3-bis (2,4,6-trimethyl-phenyl) imidazolium chloride was weighed out, dissolved in 2ml of deuterated chloroform ($CDCl_3$) for NMR analysis. The NMR Spectra **Figures 24, 25, 26,** and **27** were obtained for its ^{1}H, ^{13}C, COSY, and HSQC results respectively.

The ^{1}H NMR Results of 1,3-bis (2,4,6-trimethyl-phenyl) Imidazolium Chloride

The ^{1}H NMR values obtained (400 MHz, $CDCl_3$, δ ppm): 10.86 (1H, s, H2), 7.64 (2H, s, H1, olefin-Im), 7.02 (4H, s, H4, aromatic), 2.34 (6H, s, H5, para-CH_3), 2.18(12H, s, H3, ortho-CH_3**)**

Figure 24.

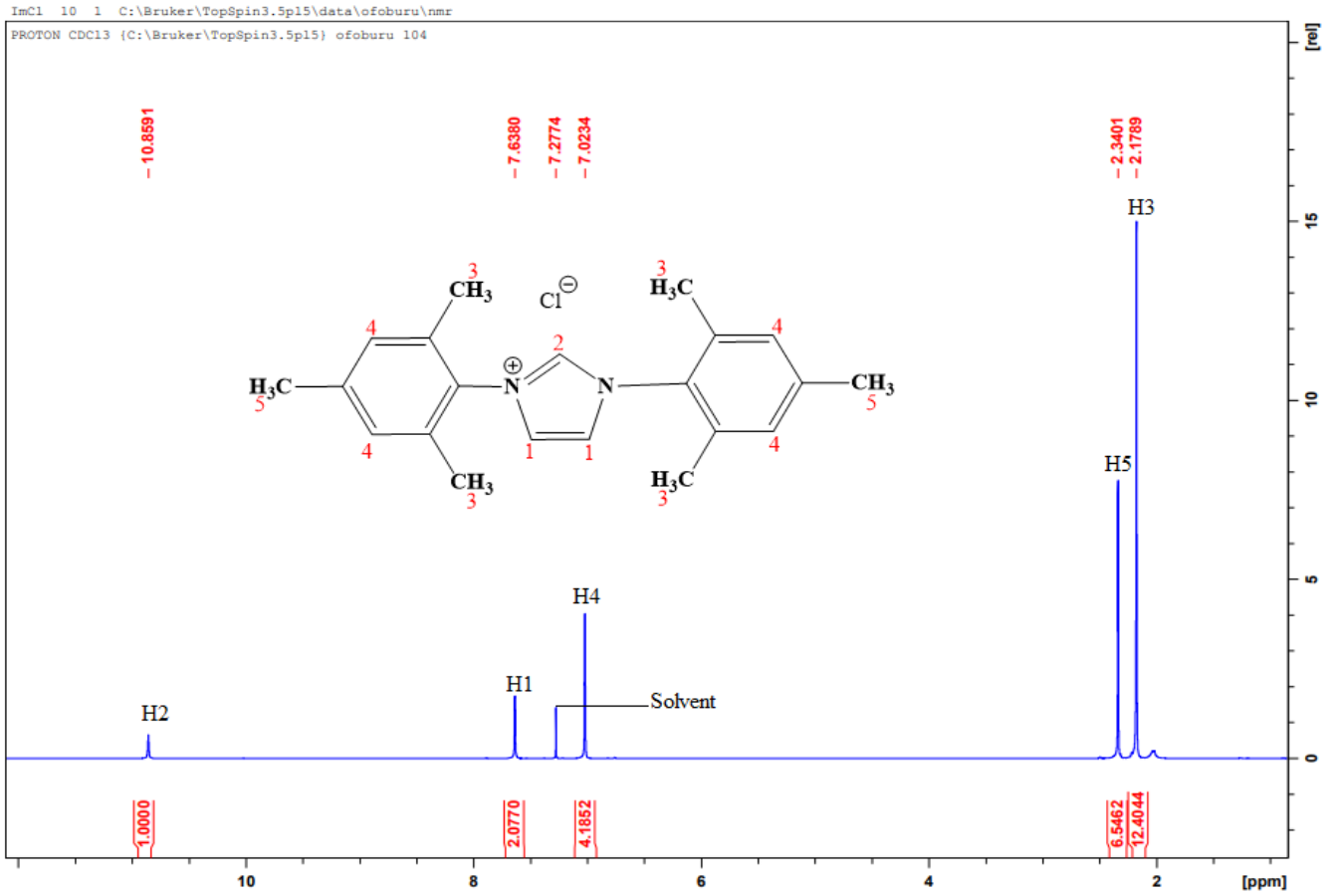

Figure 24. The ^{1}H NMR Spectrum of 1,3-bis (2,4,6-trimethyl-phenyl) Imidazolium Chloride

The ^{13}C NMR Results of 1,3-bis (2,4,6-trimethyl-phenyl) Imidazolium Chloride

The ^{13}C NMR values obtained (400 MHz, $CDCl_3$, δ ppm): 141.32 (C2-Cl), 139.78 (2C, C1, Im), 134.09 (2C, C3, aromatic-imidazole), 130.63(4C, C4, aromatic-ortho CH_3), 129.93 (4C, C6, aromatic-para CH_3), 124.43 (2CH, C7, aromatic), 21.17 (2C, C8, p-CH_3), 17.69 (4C, C5, o-CH_3) **Figure 25.**

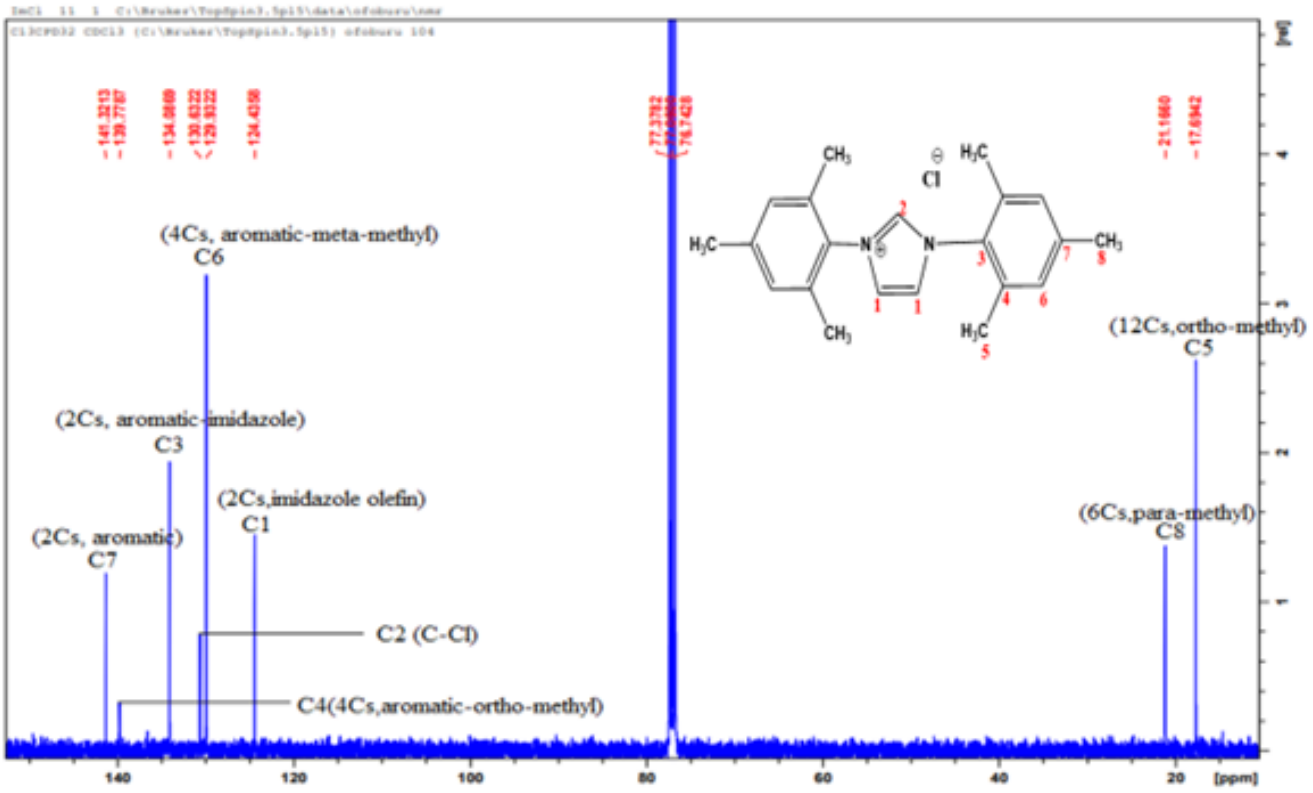

Figure 25. The ^{13}C NMR Spectrum of 1,3-bis (2,4,6-trimethyl-phenyl) Imidazolium Chloride

Figure 25 shows the eight carbon positions of the starting material IMes-Cl properly assigned with the information in the HSQC spectrum. There is currently no peaks at above 150 ppm.

The COSY NMR results of 1,3-bis (2,4,6-trimethyl-phenyl) imidazolium chloride

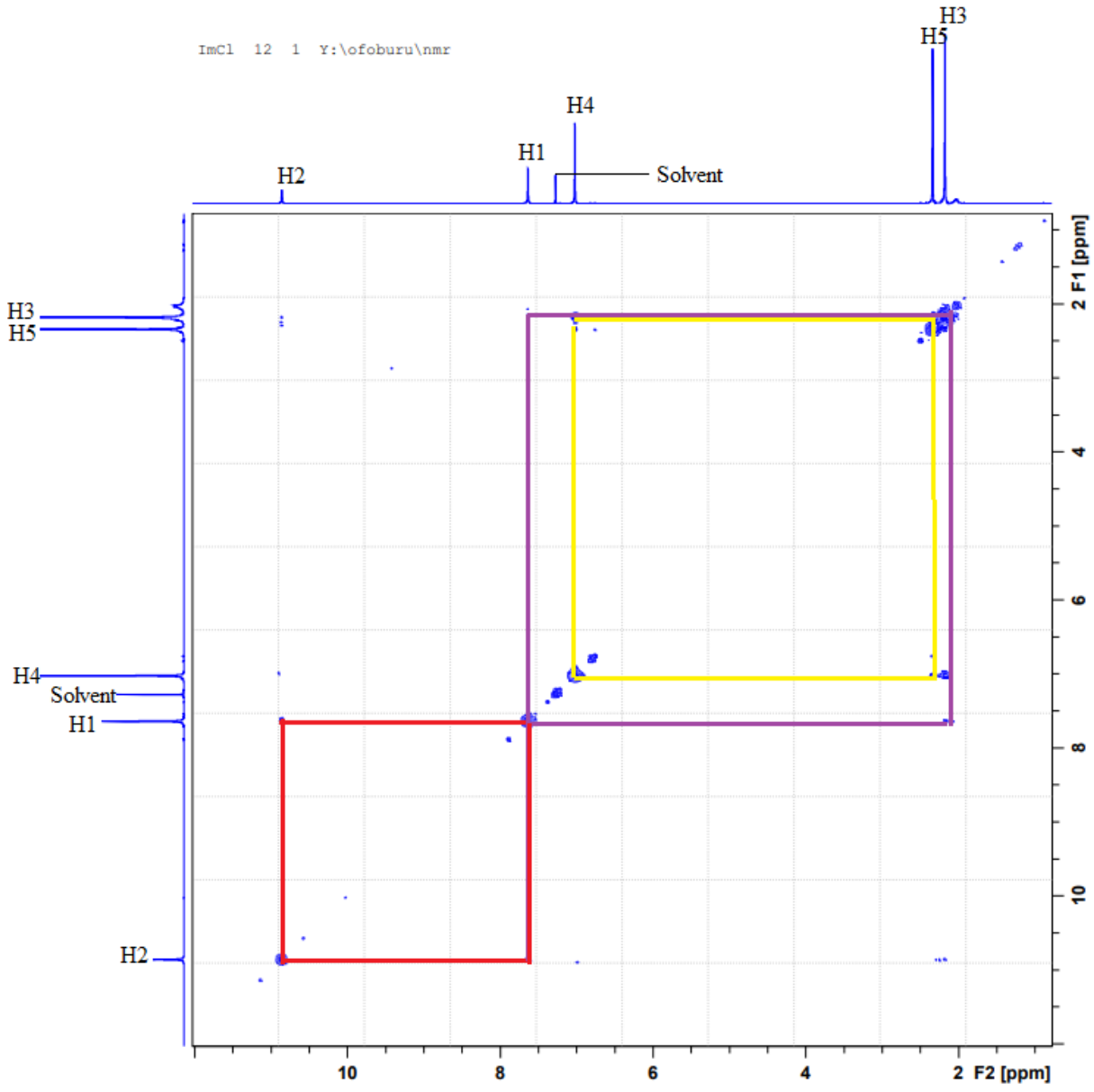

Figure 26. The COSY NMR Spectrum of 1,3-bis (2,4,6-trimethyl-phenyl) Imidazolium Chloride

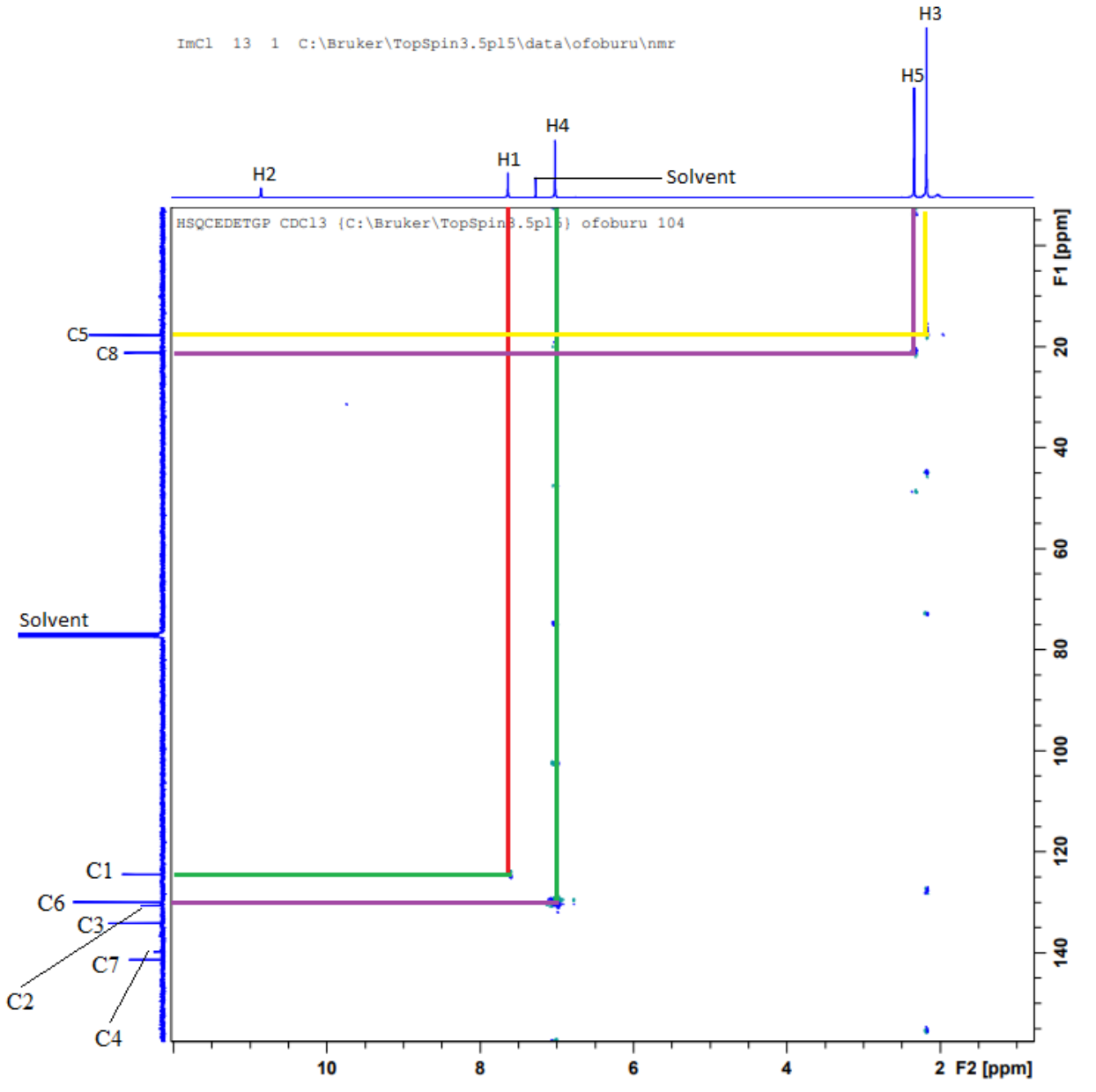

Figure 27. The HSQC NMR Spectrum of 1,3-bis (2,4,6-trimethyl-phenyl) Imidazolium Chloride

Figure 27 shows the correlation between H1 & C1, H4 & C6, H5 & C8, and H3 & C5, thus confirming the proper assignment of carbon peak positions in **Figure 25**.

The NMR Analysis of the Synthetic Product, Compound 3.

A 80 mg of the synthetic product, 1,3-bis (2,4,6-trimethyl-phenyl) imidazolium carboxylate was weighed out and dissolved in mL of deuterated chloroform ($CDCl_3$) for NMR analysis. The NMR Spectra in **Figures 28** and **29** were obtained for its ^{1}H and ^{13}C NMR spectra, respectively.

The ^{1}H NMR results of 1,3-bis (2,4,6-trimethyl-phenyl) imidazolium carboxylate

The ^{1}H NMR values obtained (400 MHz, $CDCl_3$, δ ppm): 7.52 (2H, s, H1, olefin-Im), 6.99 (4H, s, H4, aromatic), 2.32 (6H, s, H5, para-CH_3), 2.20 (12H, s, H3, ortho-CH_3**) Figure 30.**

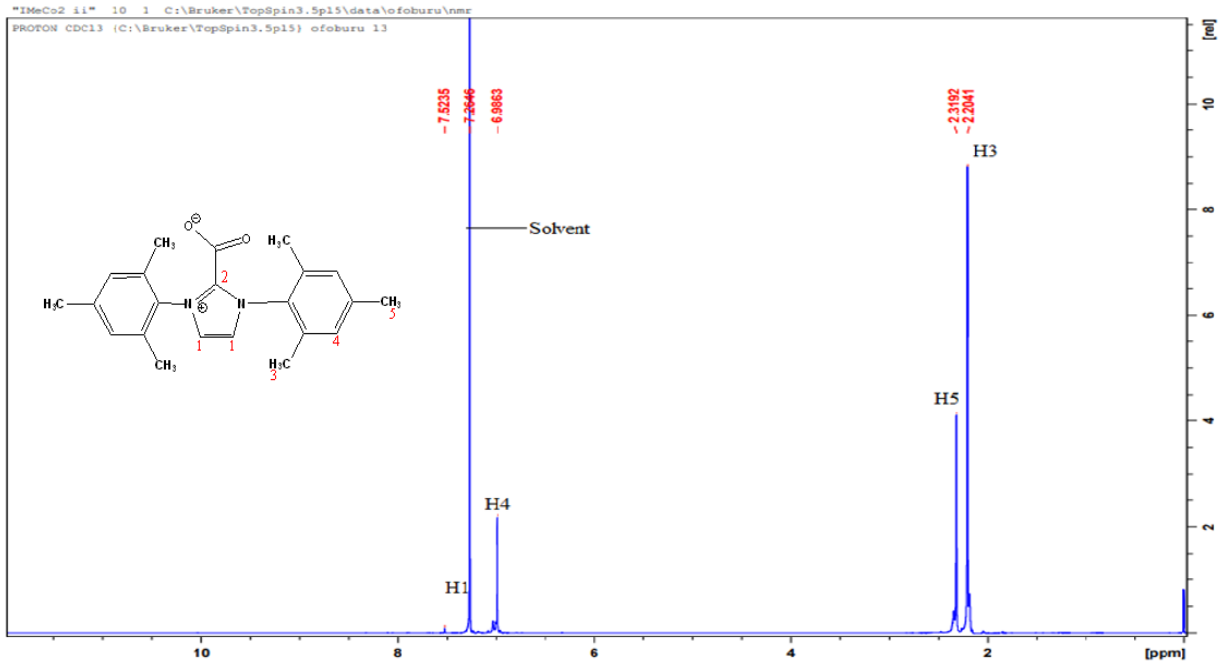

Figure 28. The ^{1}H NMR Spectrum of 1,3-bis (2,4,6-trimethyl-phenyl) Imidazolium Carboxylate

In Figure 28, the H2 peak is not seen indicating that the C2-H2 bond has been reduced for the C9 of CO_2 to bond to C2 position forming the IMes-CO_2. The H1 peak found at the same region with the solvent peak is overlapped within the solvent peak.

The ^{13}C NMR results of 1,3-bis (2,4,6-trimethyl-phenyl) imidazolium carboxylate

The ^{13}C NMR values obtained (400 MHz, $CDCl_3$, δ ppm): 153.46 (CO_2), 147.73 (C2), 140.62 (2Cs, C1, Im), 134.83 (2C, C3, aromatic-imidazole), 131.66 (4C, C4, aromatic-ortho CH_3), 129.92 (4C, C6, aromatic-para CH_3), 129.47 (2CH, C7, aromatic), 21.16 (2C, C8, p-CH_3), 17.57 (4C, C5, o-CH_3) **Figure 29.**

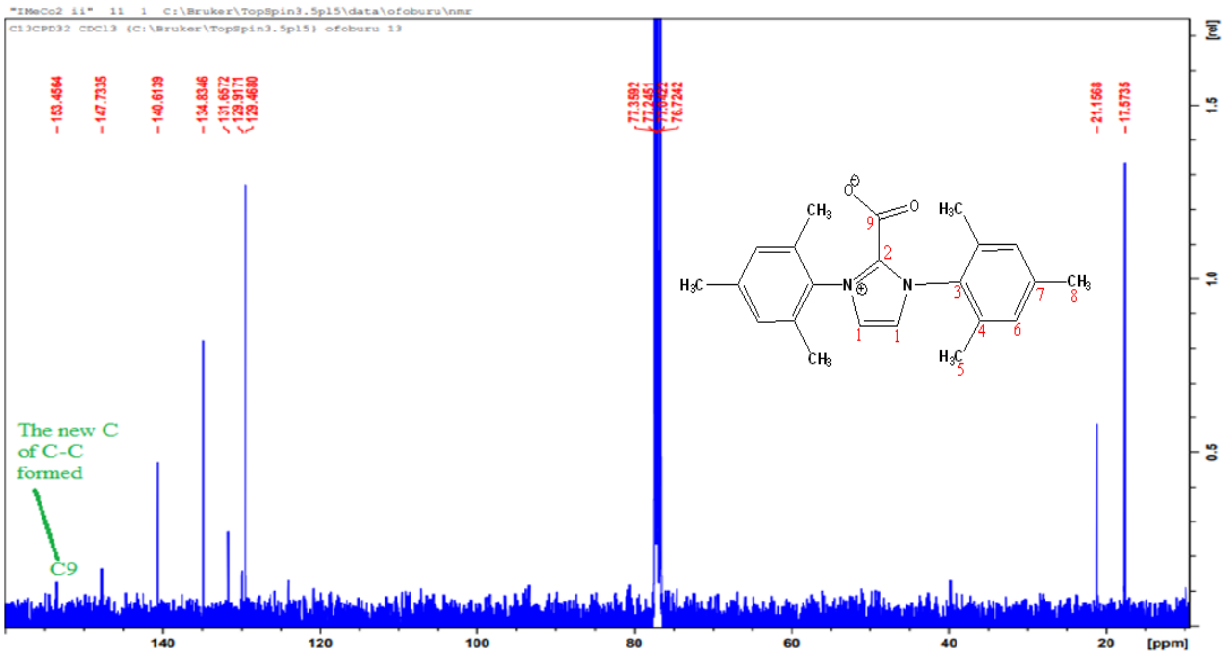

Figure 29. The ^{13}C NMR Spectrum of 1,3-bis (2,4,6-trimethyl-phenyl) Imidazolium Carboxylate

In **Figure 29**, the C9 peak is seen at 153.46 ppm, though the peak is close to the noise level, the expected C=O peak is at above 150 ppm according to literature, which stated the peak to be at 152.8 ppm.[49]

Interpretation of the NMR Results of the Synthesis

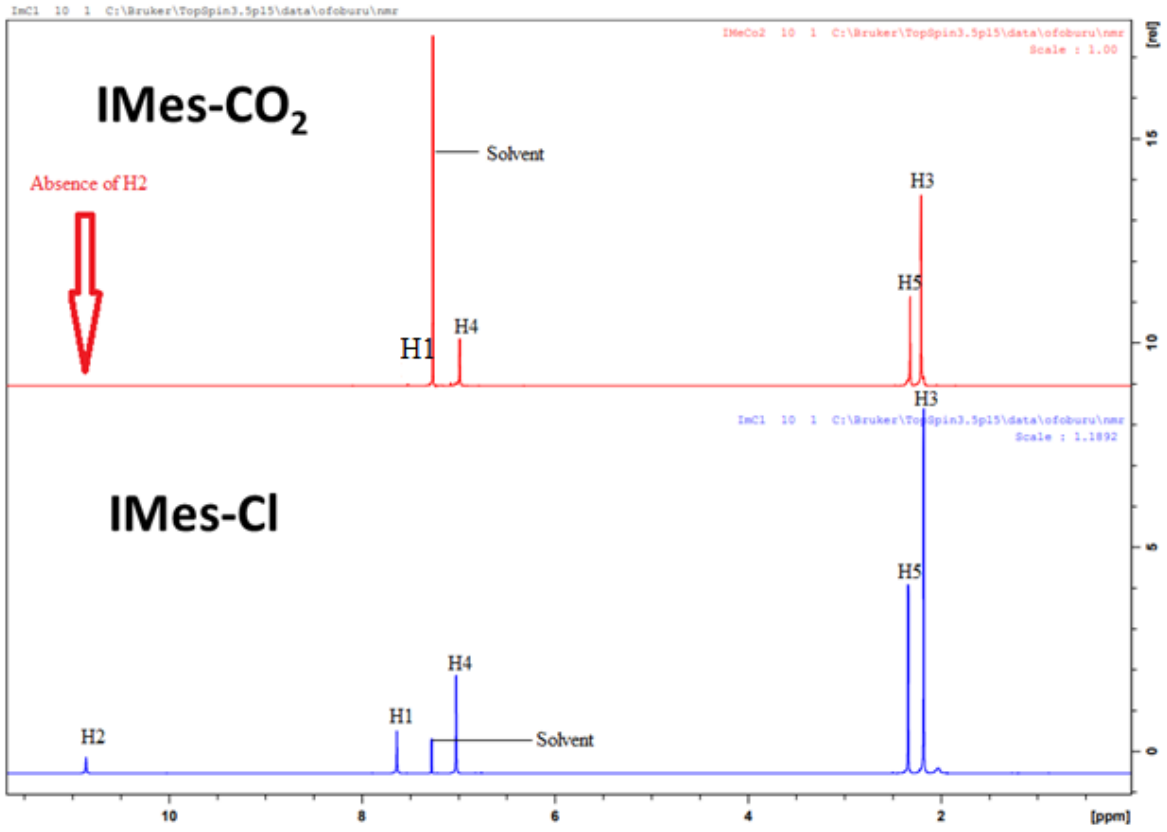

Figure 30. Multiple ^{1}H NMR Spectra of IMes-Cl and IMes-CO_2.

In comparison with the multiple ^{1}H NMR spectra of IMes-Cl and IMes-CO_2., the chemical shifts obtained for the starting material and the product correspond with each other except for the loss of the hydrogen atom at position 2 as seen in the IMes-CO_2 spectrum. The absence of the H2 in the IMesCO_2 indicates a reaction had occurred, leading to the breakage of a bond and subsequently the formation of the C-CO_2 bond, hence confirming the synthesis of the carboxylate.

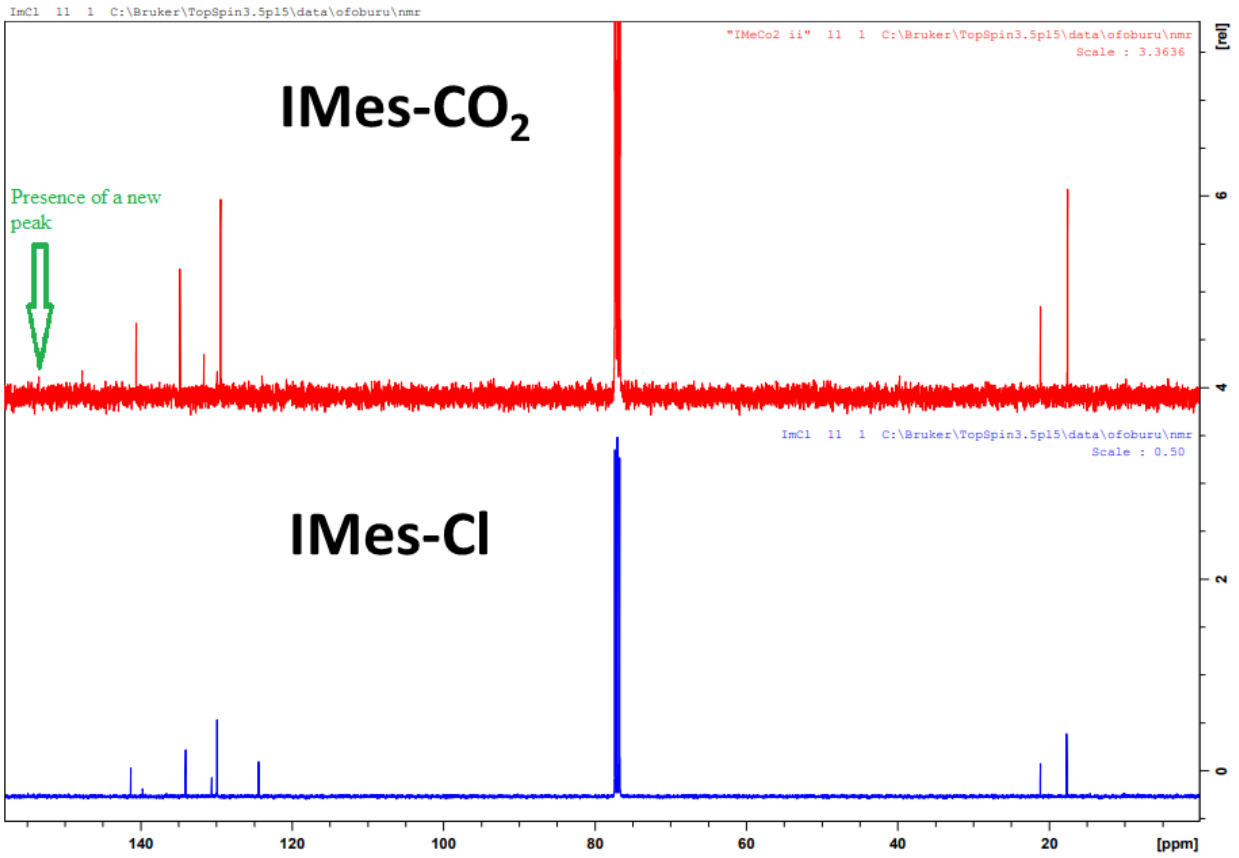

Figure 31. Multiple ^{13}C NMR Spectra of IMes-Cl and IMes-CO_2.

Similarly, as observed in the multiple ^{13}C NMR spectra of IMes-Cl and IMes-CO_2, both spectra relatively correlate with each other except for the appearance of a new peak for the ninth C-atom as seen in the IMes-CO_2 spectrum, though the peak size is so small and very close to the signal to noise ratio. This was attributed to the partial dissolution of IMes-CO_2 in chloroform as the NMR solvent, hence the need to try other solvents such as dichloromethane and dimethyl sulfoxide, in addition to the higher number of scans done overnight but the same peak strength was obtained. The COSY and HSQC spectra showed the coupling and helped to assign the peaks properly.

Infrared (IR) Spectroscopic Analysis of the Synthesis

Infrared spectroscopy is a sensitive analytical technique that uses infrared radiation to identify functional groups based on their characteristic stretching at respective absorbances and frequencies. There are unique carbonyl stretching frequencies for various imidazolium carboxylates shown in **Table 2** as carried out by Van Ausdall.[47]

Table 2. Summary of the C-CO_2 bond lengths, Decarboxylation Temperature, and IR stretching frequencies of some imidazolium carboxylates.

Entry	Carboxylate	C-CO_2 Bond Length (Å)	-CO_2 Temp. (^{o}C)	IR Stretching $^{\nu}co_{asym}$ (cm^{-1})
1	$IMeCO_2$	1.523	162	1653
2	$IEtCO_2$	NA	128	1654
3	I^iPrCO_2	NA	140	1666
4	I^tBuCO_2	NA	71	1629
5	IMe^tBuCO_2	NA	117	1647
6	$IMe_{Me}CO_2$	1.521(3)	182	1669
7	$IEt_{Me}CO_2$	1.535(1)	144	1657
8	$Ii Pr_{Me}CO_2$	1.536	139	1662
9	$I^tBuIprCO_2$	1.525 - 1.544	129	1675
10	$IMesCO_2$	NA	155	1675
11	$IMes_{Me}CO_2$	NA	193	1674
12	$IPrCO_2$	1.536	108	1678
13	$IPr_{Me}CO_2$	1.542(2)	136	1683
14	$SIMesCO_2$	NA	156	1680
15	$SIPrCO_2$	1.535(2)	120	1683

In this study, the Infra-red analysis was carried out with the PerkinElmer FT-IR Spectrometer **Figure 32**.

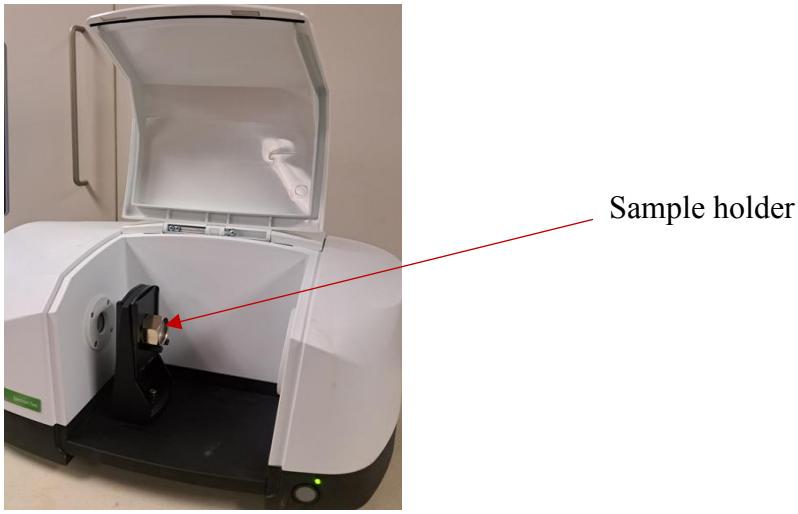

Figure 32. PerkinElmer FTIR Equipment

A 38 mg sample of bis-mesityl imidazolium carboxylate was grounded to a fine powder using a mortar and a pestle. Few drops of Nujol solution were added to the fine powder and mixed together to form a paste. The sample paste was transferred to a disc, made from KBr/NaCl, and water contact was avoided so the sample paste would not be dissolved. The transfer was done using the end of a small spatula, and care was taken to ensure the spatula did not scratch the disc. A second disc was used to press together with the first disc sandwiching the paste to create a film, and the plate holder was used to place and support the disc in the Infra-red spectrometer for analysis.

The IR spectra for Nujol standard, bis-mesityl imidazolium chloride, and bis-mesityl imidazolium carboxylate were obtained and recorded as shown in **Figures 33, 34 and 35,** respectively.

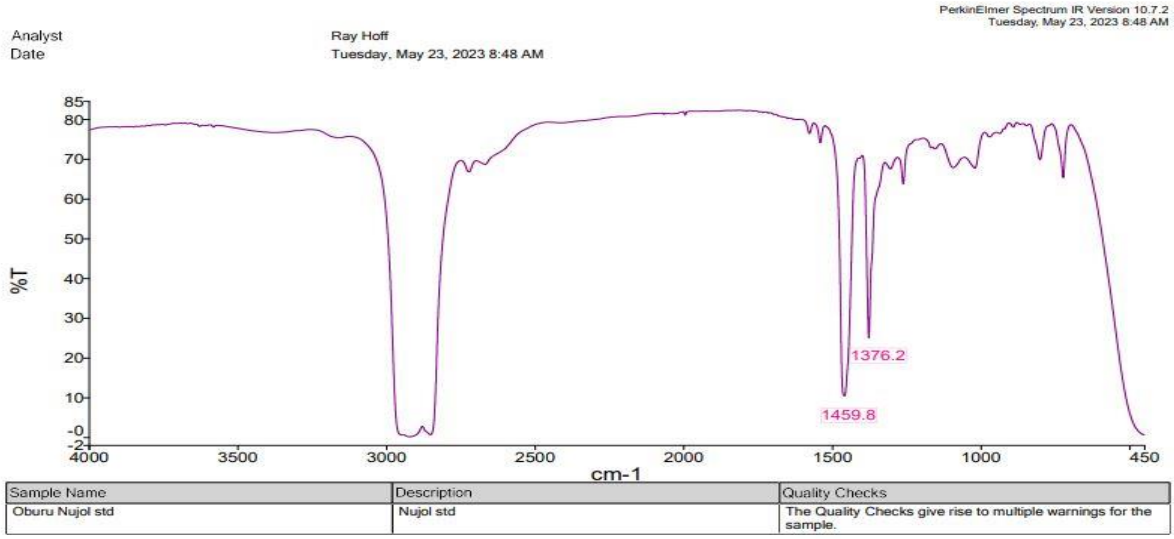

Figure 33. The FTIR Spectrum of Nujol Standard

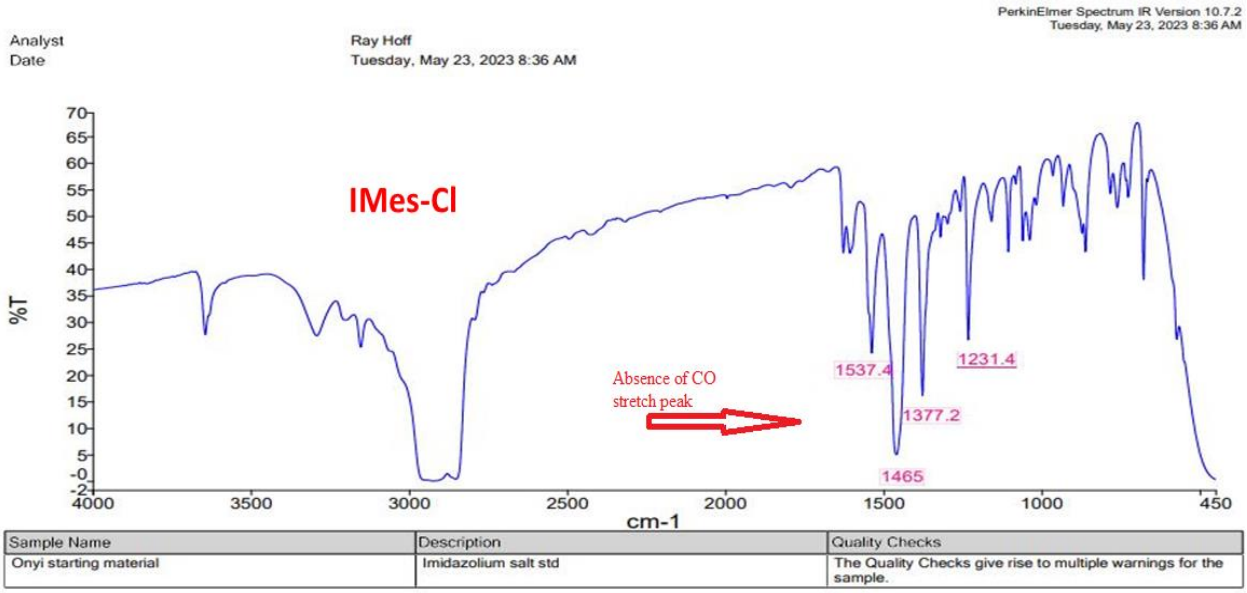

Figure 34. The IR Spectrum of 1,3-bis (2,4,6-trimethyl-phenyl) Imidazolium Chloride

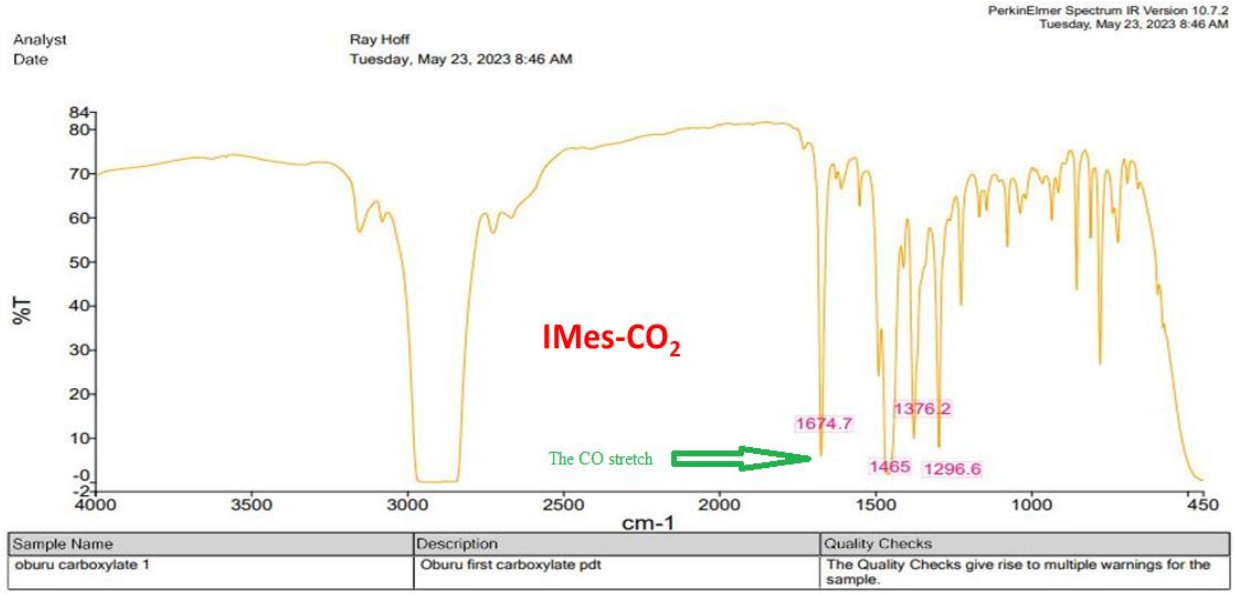

Figure 35. The IR Spectrum of 1,3-bis (2,4,6-trimethyl-phenyl) Imidazolium Carboxylate

Interpretation of the IR results of the Synthesis

The IR results obtained in **Figures 34** and **Figure 35** were compared with the various unique literature IR stretching frequencies of imidazolium carboxylates in **Table 2**.

The presence of a strong peak at 1674.7 cm^{-1} in the IMes-CO_2 IR spectrum in **Figure 35** corresponds with the expected peak at 1675 cm^{-1} for IMesCO_2 in **Table 2,** this confirms the presence of CO_2 which was absent in the starting material. This peak value also corresponds with what Tudose et al. obtained in their past study when they synthesized the same molecule.[49]

Thermogravimetric Analysis (TGA) Analysis of the Synthesis

Thermogravimetric analysis displays the mass of a sample being scanned with an isothermal or dynamic temperature in the air, nitrogen, or oxygen, resulting in a graph of mass versus temperature. This analysis demonstrates the thermal stability of compounds and their respective compositions. The temperature at which the weight loss from the compound begins is vital in establishing how much the compound can hold up under certain conditions. The TGA graph shows the evaporation of materials, the disintegration of the compound, and the presence of carbon black and fillers. The TGA analysis was carried out with the TA TGA Q50 Thermogravimetric Analyzer **Figure 36** and it was set to analyze samples to the maximum temperature of 600 ^{o}C with an aluminum pan but at higher temperatures with platinum pan.

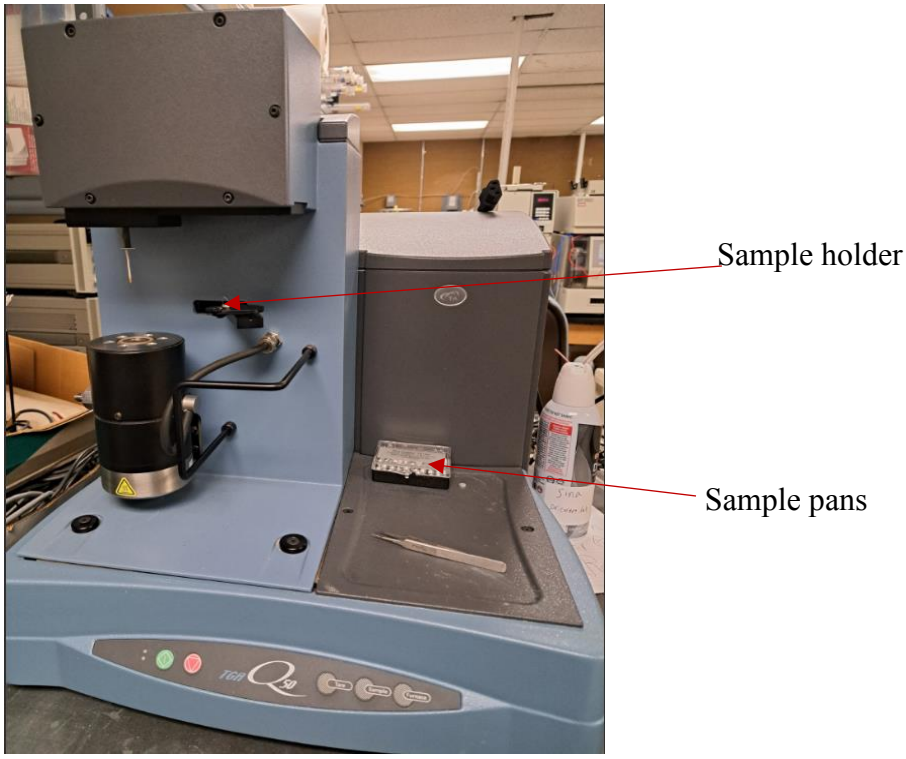

Figure 36. TA TGA Q50 Instrument.

About 3.3 mg of IMes-Cl was weighed out, loaded on the aluminum crucible, and analyzed. **Table 3** shows the individual fragments, their molar masses, and mass percentages of the total molecular mass of the starting material.

Table 3: Individual Fragments, Molecular Masses, and Mass Percentages of the Total IMes-Cl

Individual fragments	**Molecular mass (g)**	**Mass Percentage of IMes-Cl (%)**
Cl	35.5	10.46
Imidazole	66	19.44
Bis-mesitylene /Mesitylene	238 / 119	70.10 / 35.05
Total Mass of IMes-Cl	**339.5**	**100**

Similarly, about 3.6 mg of IMes-CO_2 was analyzed and **Figures 37. 38** and **39,** show the structures for the proposed major fragmentations in the analysis.[50] and in accordance with **Table 4** that shows the individual fragments, their molar masses and mass percentages of the total molecular mass of IMes-CO_2.

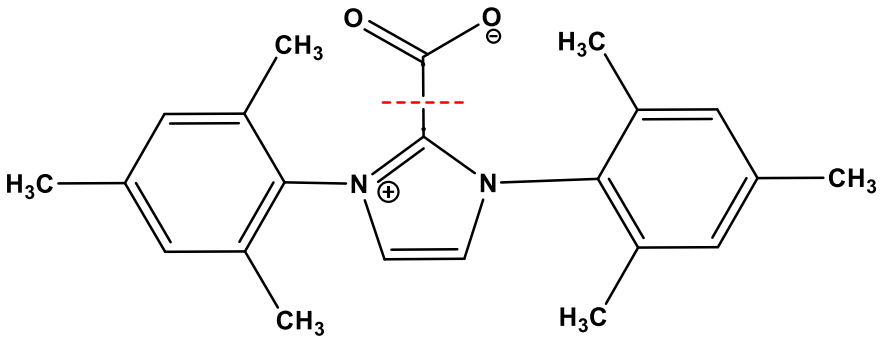

Figure 37. The Fragmentation Structure of CO_2

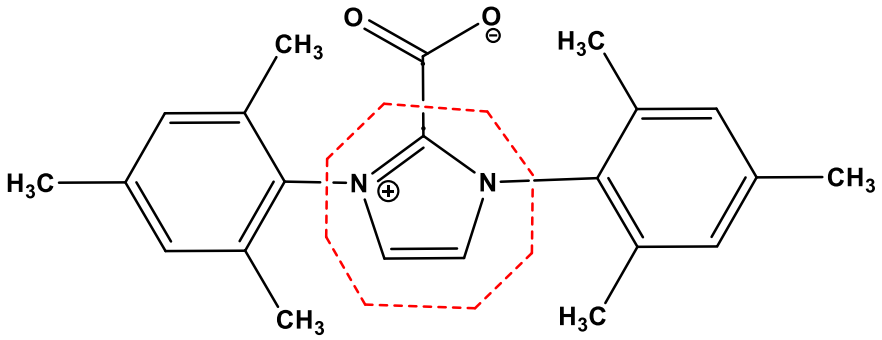

Figure 38. The Fragmentation Structure of Imidazole

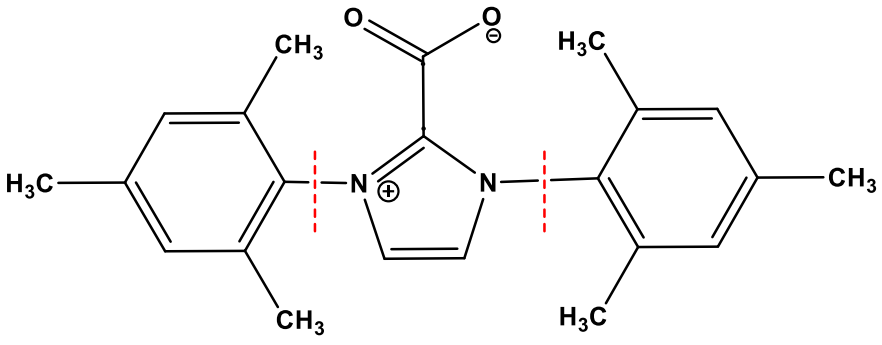

Figure 39. The Fragmentation Structure of Bis-mesitylene

Table 4. Individual Fragments, Molecular Masses, and Mass Percentages of the Total IMes-CO_2

Individual fragments	**Molecular mass (g)**	**Mass Percentage of IMes-CO_2 (%)**
CO_2	44	12.64
Imidazole	66	18.97
Bis-mesitylene /Mesitylene	238 / 119	68.39 / 34.20
Total Mass of IMes-CO_2	**348**	**100**

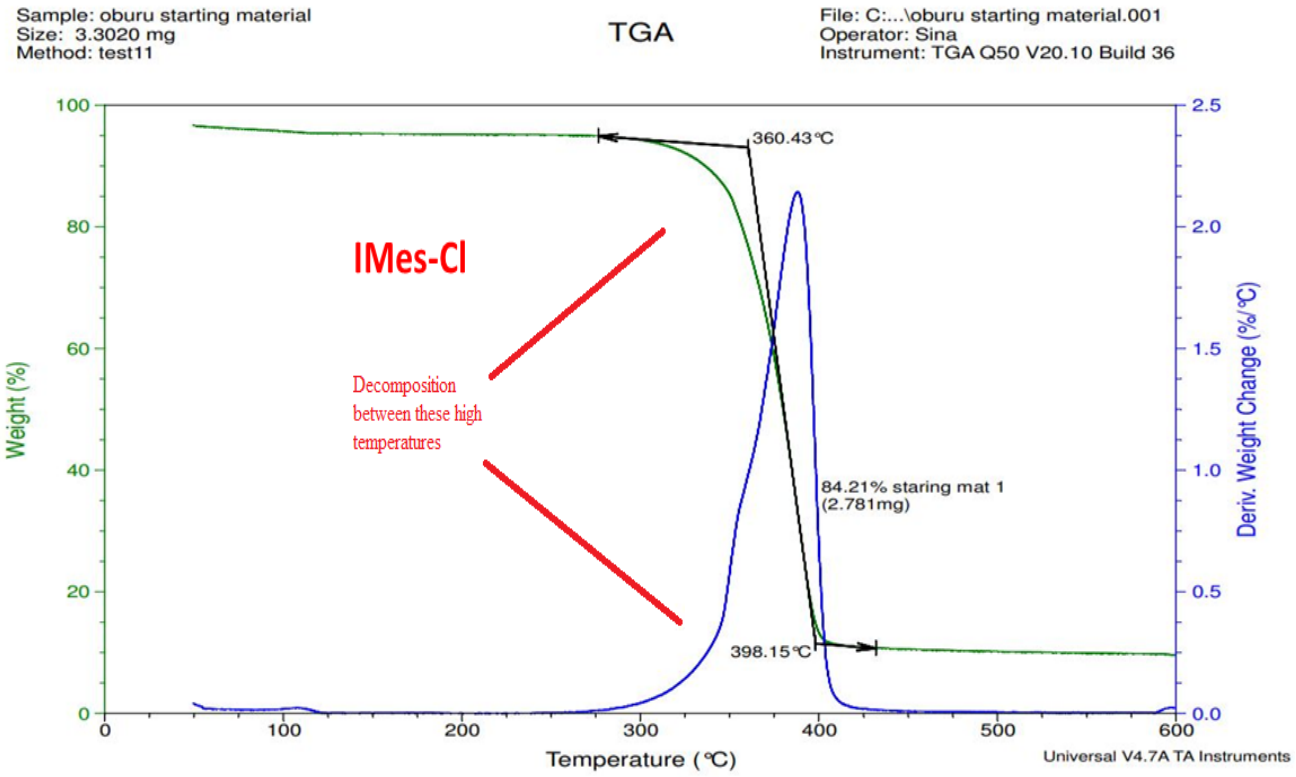

Figure 40. The TGA Curve of 1,3-bis (2,4,6-trimethyl-phenyl) Imidazolium Chloride

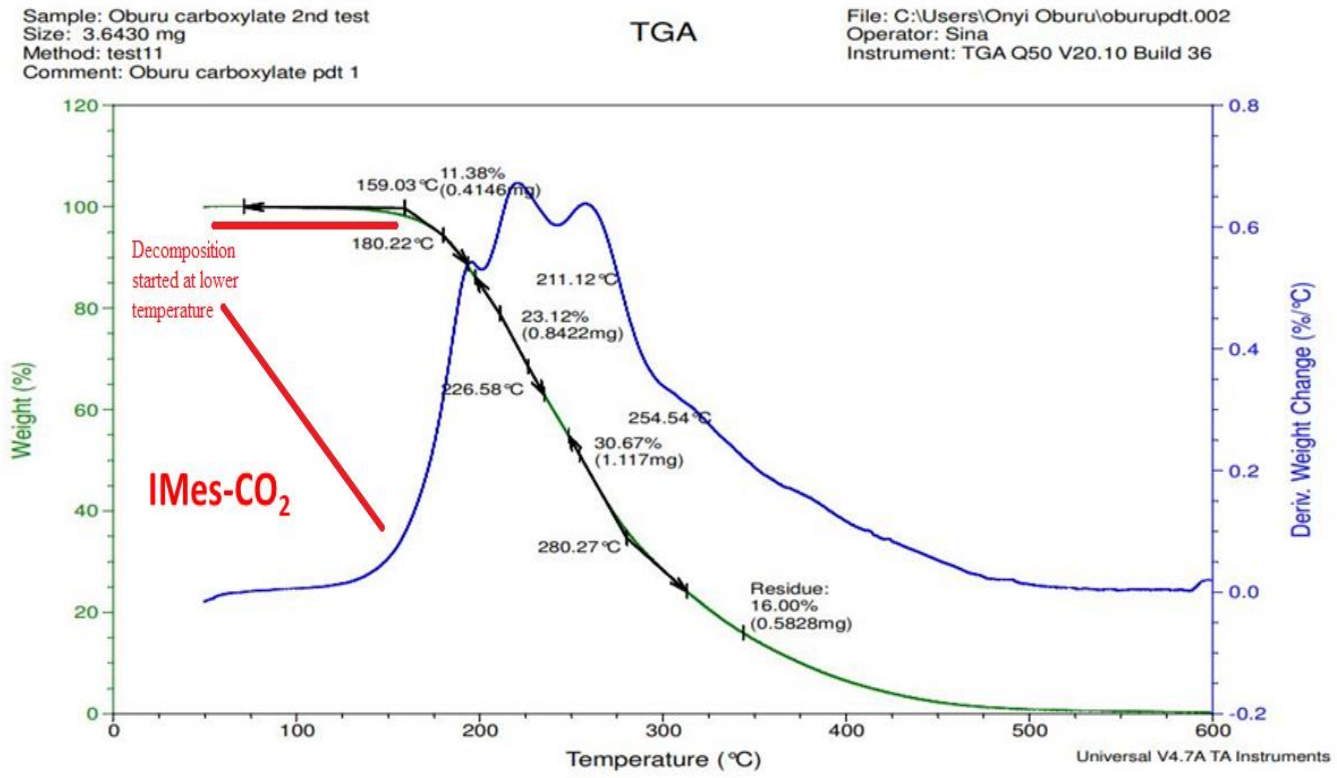

Figure 41. The TGA Curve 1,3-bis (2,4,6-trimethyl-phenyl) Imidazolium Carboxylate

Interpretation of the TGA Results of the Synthesis.

The TGA curve of IMes-Cl in **Figure 40** shows a major transition state of 84.21% (2.781 mg) weight decomposition between the temperatures of 360.43 ^{o}C and 398.15 ^{o}C. This could correspond to the loss of the chloride and the two mesitylene groups simultaneously within the same timeframe as their total weight sum corresponds to the observed weight loss in the curve. Also, the TGA curve for the IMes-CO_2 in **Figure 41** shows three transition states that could be attributed to the three major fragments, i.e. CO_2, imidazole, and bis-mesitylene/mesitylene respectively as shown in **Table 4.** The thermal gravimetric analysis demonstrated the thermal

stability of the IMes-CO_2, as the decomposition peaked between the temperatures of 159.03 ^oC and 180.22 ^oC, which is close to the IMes-CO_2 C-CO_2 bond decomposition temperature of 155 ^oC shown in **Table 2**. The amount of the sample being analyzed affects the results of the analysis as a higher amount increases the decarboxylation temperature and verse versa. [26]

Van Ausdall also observed that methylation of the backbone increases the basicity of a carbene relative to that of the unsaturated parent carbene, when his N-substituent was the (2,4,6-trimethyl) phenyl group, the decarboxylation temperature of the group with the methylated backbone was higher (193 ^oC) than that of the Imidazolium carboxylate (155 ^oC). [47]

Mass Spectrometry Analysis of the Synthesis

The thermal decomposition of the imidazolium-CO_2 was also carried out manually and the detection signals were measured using the Inficon Ecotec E3000 single quadruple mass spectrometer with a leak detector **Figure 42**. The mass spectrometer analyses as the leak detector sniffs/detects the presence of a gas that comes in touch with it, and the gas is drawn into the spectrometer through a turbo molecular pump. The internal pressure of the spectrometer is typically set between 4-10 millibars for proper measurements, otherwise the turbo Molecular pump will not be able to maintain the required vacuum. In carrying out the measurements, the molecular masses of up to four gases of interest are programmed into the mass spectrometer and the detector probe is positioned close to the sample which is usually the source of the gas.

Figure 42. The Single Quadruple Mass Spectrometer

Figure 43. The Mass Spectrometry Screen Showing a Jump in the ppm at Molar Mass of 44g, Indicating that CO_2 is Released from the Sample.

A 30 mg of 1,3-bis (2,4,6-trimethyl-phenyl) imidazolium carboxylate was weighed out and transferred to a glass test-tube inside a beaker. The test-tube was further clamped to a tripod stand and the beaker was placed on the Corning laboratory stirrer/hot plate and connected with an Omega benchtop thermocouple. The mass spectrometer sniffer was also clamped to the tripod stand and placed at the tip of the test-tube to measure any gas outlet. At the detection of any of the gases, the resulting reading in parts per million (ppm) unit, is shown on the MS screen and the corresponding volume of the respective molecular mass increases in ppm **Figure 43**, thus indicating the exact gas that is being released from the sample. The heat was powered on and readings were observed on the MS screen from room temperature to about 200 ^{o}C.

The signals received on the mass spectrometer were recorded and the curve obtained **Figure 44**.

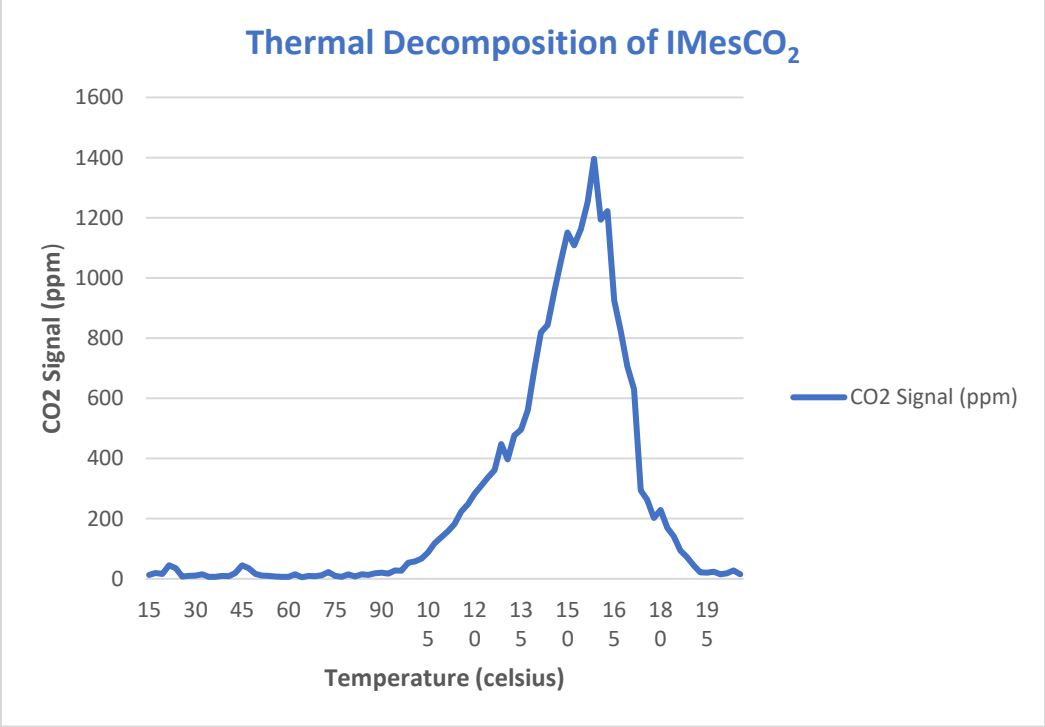

Figure 44. MS Curve of the 1,3-bis(2,4,6-trimethylphenyl) Imidazolium Carboxylate at Thermogram at m/z = 44.

Interpretation of the MS Results of the Synthesis

The mass spectrometer was powered on and readings were observed on the screen from room temperature to about 200 ^{o}C. The signals received in **Figure 44,** showed the highest CO_2 detection peak obtained between 150 – 165 ^{o}C, and this reflected a major raise in ppm at the corresponding 44g molecular mass set on the spectrometer, hence indicating the presence of CO_2 from IMes-CO_2. In comparison, we observed that the **Figure 44** MS curve is not quite in agreement with the TGA curve in **Figure 41** since the onset of CO_2 evolution began at 100 ^{o}C in the former while the latter held out until 155 ^{o}C. This suggested to us that the IMes-CO_2 in **Figure 44** had become hydrated and its release of water when heated up accompanied by the release of CO_2.

Chapter Four

Hydrogenation Reactions of IMes-CO_2

The choice of the metal catalyst used in our hydrogenation reactions at high pressure and room temperature was made based on Trassati's volcano plot on the metal-hydrogen bond strength **Figure 45.**[50]

At varying reaction conditions but at room temperature we carried out a series of reactions:

1) Direct reduction of IMes-CO_2 with hydrogen gas in the presence of a Pd/C catalyst, at 25 atmospheres for 72hours.
2) Direct reduction of IMes-CO_2 with hydrogen gas in the presence of a Pd/C catalyst, at 30 atmospheres for 72 hours.
3) Direct reduction of CO_2 with hydrogen gas in the presence of a Pd/C catalyst, at 30 atmospheres for 72hours
4) Direct reduction of CO_2 with hydrogen gas without any catalyst at 30 atmospheres for 72 hours.
5) Direct reduction of CO_2 with hydrogen gas in the presence of a Pd/C catalyst for 24 hours at 30 atmospheres.
6) Reduction of IMes-CO2 and CO2 together with hydrogen gas in the presence of a catalyst for 72 hours at 30 atmospheres.
7) Continuously stirring Pd/C catalyst in dichloromethane only for 72 hours in a glove bag
8) Continuously stirring IMes-CO_2 in dichloromethane only for 72 hours in a glove bag.

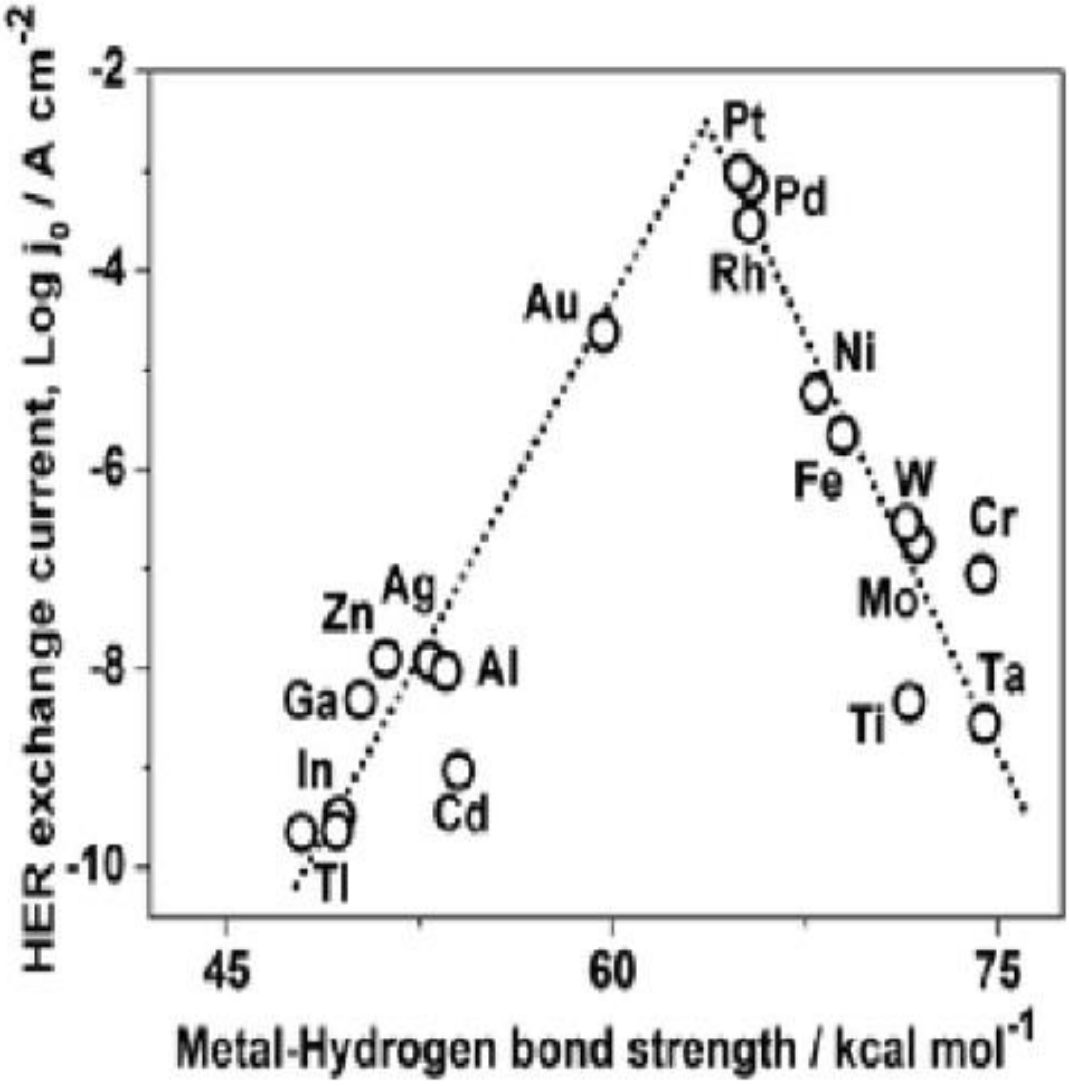

Figure 45. Trassati's Volcano Plot on the Metal-Hydrogen Bond Strength.

It has been established to a larger extent that modifying the structures of organic compounds and subsequently altering their mobilities in the medium when with catalytic metals such as palladium, gold, Silver, copper or graphite produces great reactions.[19]

Palladium on carbon, commonly known as Pd/C is the form of palladium used as a catalyst in chemical processes, in which the palladium metal is supported on carbon to increase its surface area and activity.[51] In addition to the activated carbon support, palladium metal catalysts are also supported on other different kinds of metals, oxides, or sulfides, and have been demonstrated to be beneficial in many organic reactions such as Schiff bases and imines reduction.[51] The most popular among the Pd-based catalysts is the Pd/c catalyst due to its very high benefit as it has shown greater catalytic activities in a variety of chemical reactions[51] This type of catalyst is heterogenous in nature and can be easily refined, recycled, and recovered at the end of a reaction.[53] The Pd/C catalysts are known to exist in the form of nanoparticles, they are highly efficient in reduction and coupling reactions and their catalytic performances are influenced by some of the palladium's properties such as oxidation state, moisture content, and distribution.[54] The use of palladium on carbon (Pd/C) catalyst in organic synthesis started as far back as 1972, when Heck et al. first used it in the Heck coupling reaction, after which it became popularly applicable in cross-coupling reactions.[53] Nonetheless, a wide range of reduction reactions have been carried out successfully in the presence of a heterogeneous Pd/C catalyst, among which is the chemoselective hydrogenation of a quinoline derivatives, which are cyclic as IMes-CO_2 to tetrahydroquinolines.[54]

Though, this work is the first attempt to reduce Imes-CO_2 to methanol through the use of hydrogen gas and Pd/C catalysis, similar conditions as those used by Patti and Pedotti, were adopted in the reaction procedure.

Sample Preparation and Reaction Set-up

The Pd/C sample preparation was done in a glove bag, as it was weighed out and suspended in freshly dispensed dichloromethane (DCM).

Apparatus

One-liter Parr non-stirred reactor pressure vessel, petri-dish, stirrer, stir bar, stirring rod, Craftsman micro adjusting torque wrench, Parker pipe bender. Parker pipe cutter, teflon tape, measuring cylinder, beakers, weighing balance, two-necked compression and pipe fittings, nitrogen tank, CO_2 gas tank, and hydrogen gas tank.

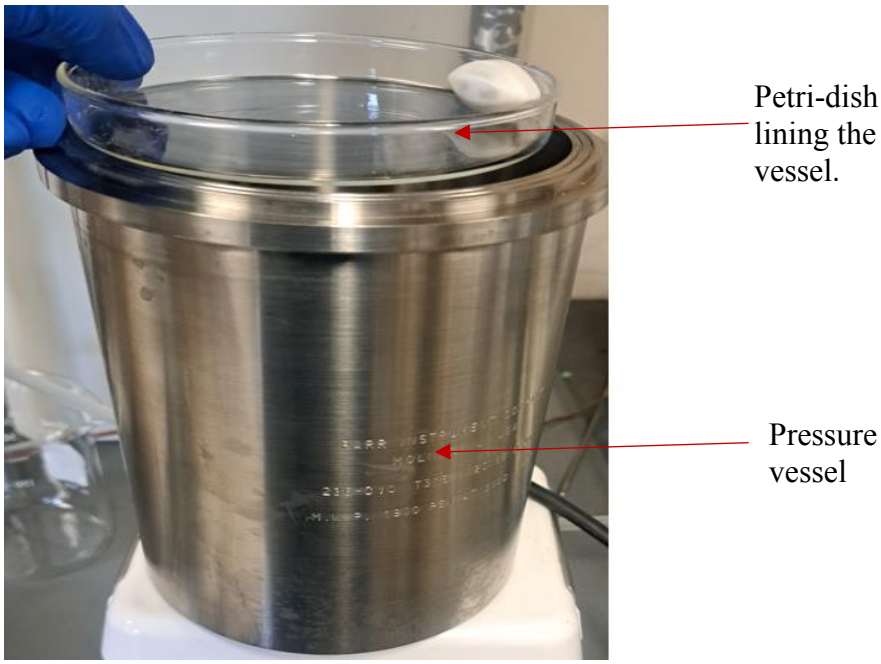

Figure 46. The One-liter Parr Non-stirred Reactor Pressure Vessel

Safety and Handling

Pd/C is highly flammable, thus to avoid a fire that could result from exposure to air, a glove bag was used to prepare the catalyst. The bag was rigorously purged with nitrogen gas to chase out any air within it before preparing the catalyst. The Pd/C was put first in the beaker before pouring the DCM on it otherwise a vapor from the solvent could cause a fire. The powder papers used in weighing PD/C were soaked in water and kept safely labeled in a bottle. A fire extinguisher was available close by and the reaction workup was done in the hood.

General Procedure

The glove bag contained a weighing balance, freshly dispensed DCM in a two-necked flask, spatula, and two 400 ml beakers. A 61 mg of 10% palladium on carbon catalyst was weighed out at the ratio of 3.28: 1 for IMes-CO_2: Palladium on carbon catalyst and suspended in a freshly dispensed 40 ml dichloromethane collected with a two-neck flask. The reaction mixture was stirred with the stirring rod, removed from the glove bag and transferred to the one-liter reactor vessel lined with a petri dish containing a stir bar. The nuts of the vessel were precisely tightened with a torque wrench set to 25 ft-lb. When the CO_2 gas was not a reactant, the system was purged with nitrogen gas instead for ten minutes to chase out any air in the system. The CO_2 gas was bubbled through its connected pipe from the tank to the reactor vessel till it reached the 10 atm on the pressure gauge and was shut off, and its tank properly closed. The H_2 gas was then bubbled through its connected pipe from the tank to the reactor till the total pressure gauge on the reactor vessel read the desired pressure. The H_2 supply was shut off with its tank properly closed and the reaction was allowed to run for the set period ass shown in **Figure 47.**

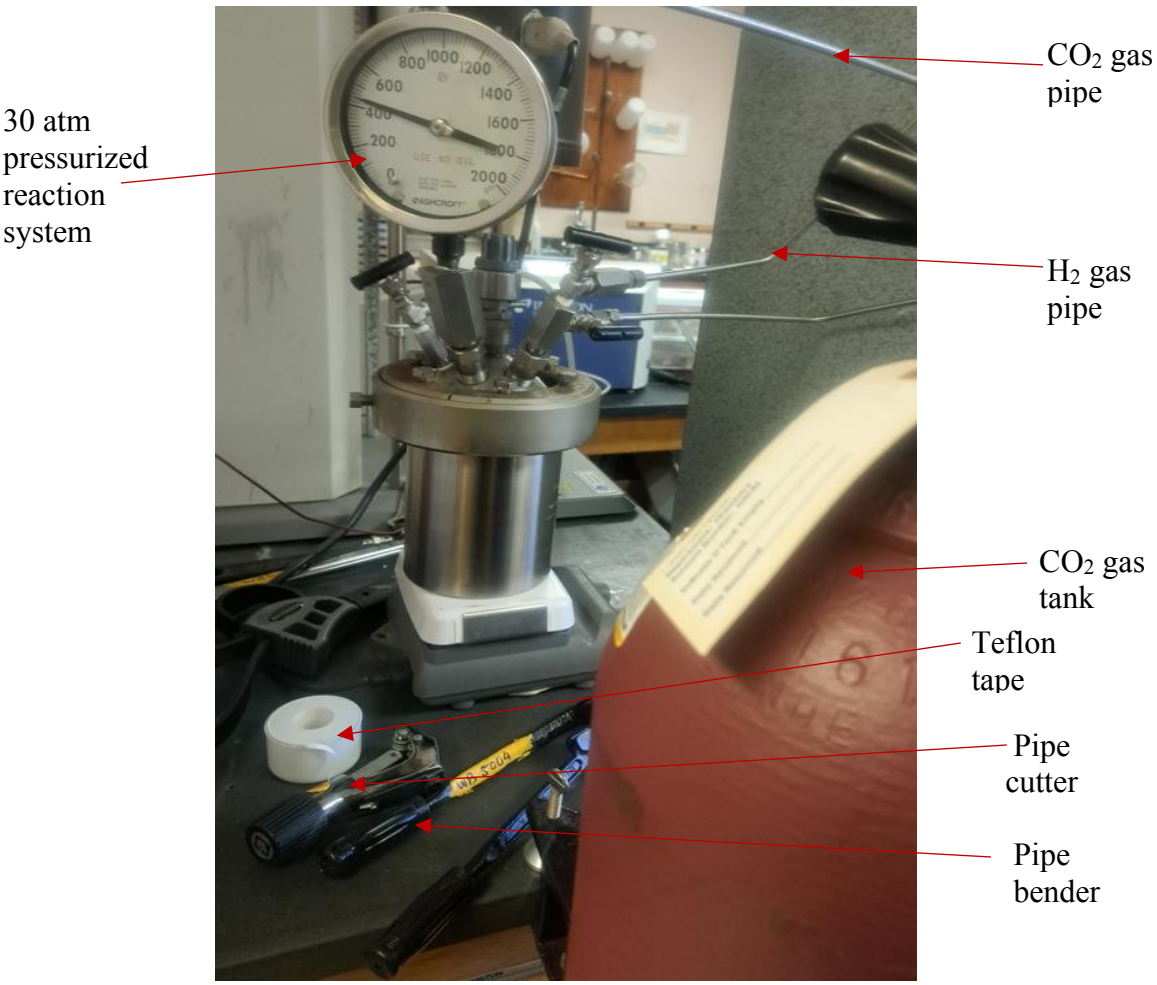

Figure 47. The Hydrogenation Reaction Set-up to Run.

After the desired set period, the reaction was stopped, the vessel was disassembled and its contents were filtered through a fritted funnel with celite under vacuum if catalyzed, otherwise, filtration was not needed. After the filtration process, the Pd/C on the celite was diluted in water and kept safely labeled bottle while the filtrate was collected for analysis using the NMR and IR techniques.

All the hydrogenation reactions in this work were carried out with the same procedure and experimental setup but with a little adjustment to fit the exact reactants and conditions per experiment.

NMR & IR Results of the Hydrogenation Products as per Set Reaction Conditions

NMR & IR Results from the Pd/C Catalyzed IMes-CO_2 + H_2 at 25 Atmospheres after 72 Hours.

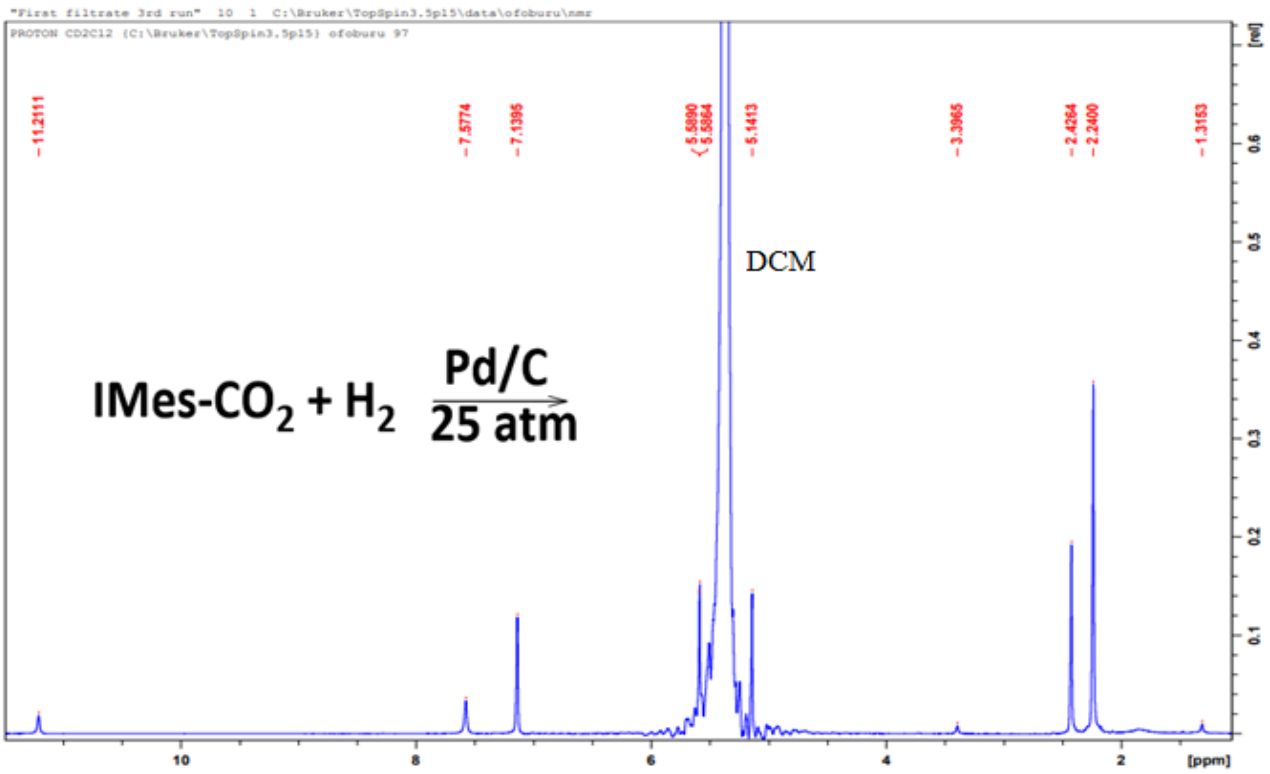

Figure 48. The ^{1}H NMR Spectrum of the Product of IMes-CO_2 + H_2 at 25 Atm after 72 Hours

In **Figure 48,** the appearance of a peak at 3.40 ppm could be taken for the OH of a reduction product but the peak is a septet which is characteristic of isopropanol. While the peak at 1.32 ppm could be OH from water trace. Also, the peaks at 2.42 ppm and 2.24 ppm are for the H5 and H3 of IMes respectively as seen in **Figures 24** and **28**.

The absence of a peak above 160 ppm in **Figure 49**, also confirmed that -CO_2 from IMes-CO_2 was lost but no methanol or any reduction product was formed with it. The peaks at 20.85 – 17.43 are the C8 and C5 of IMes respectively as also seen in **Figures 25** and **29**

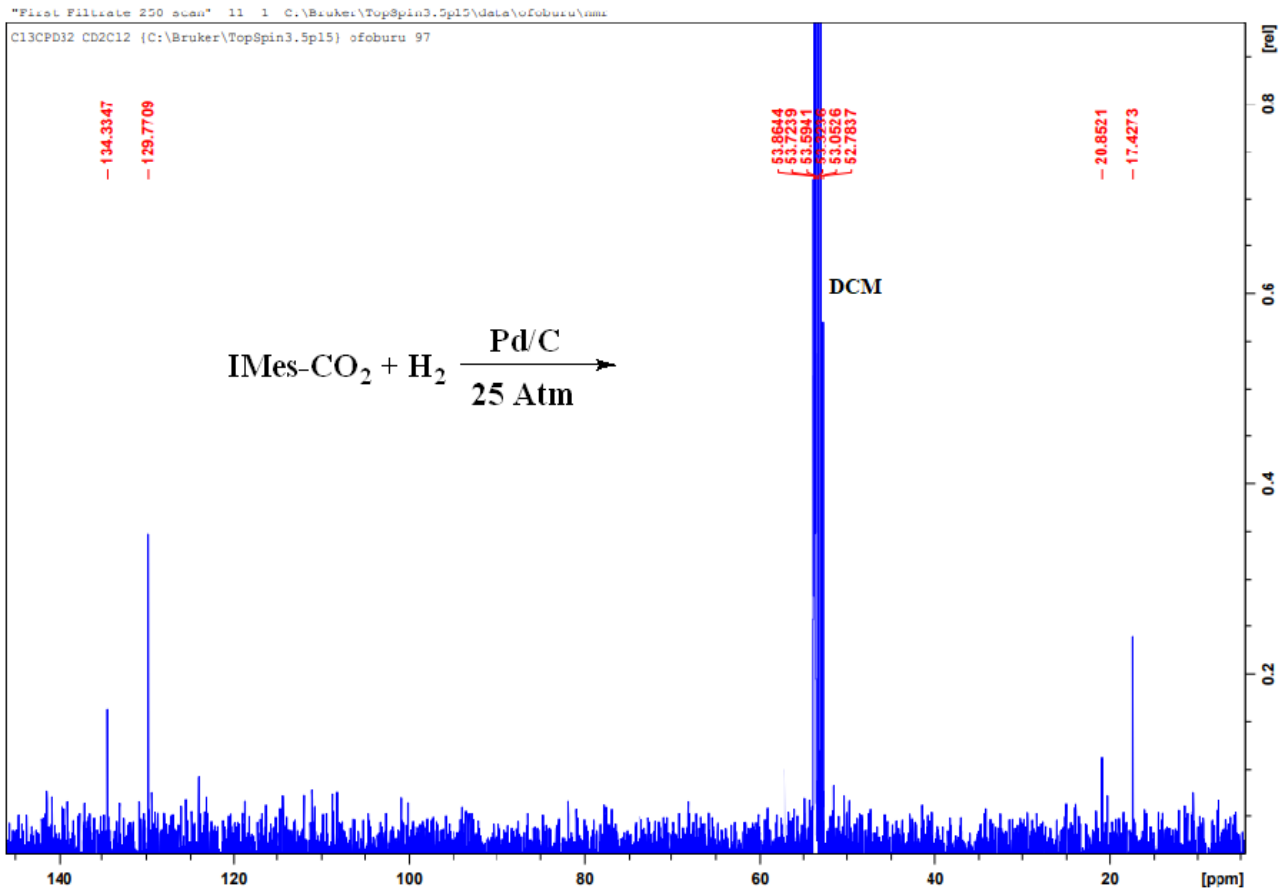

Figure 49. The ^{13}C NMR Spectrum of the Product of IMes-CO_2 + H_2 at 25 Atm after 72 Hours

In **Figure 49**, the peaks seen are those of the IMes-H, indicating that CO_2 has been lost as no peak was seen above 150 ppm.

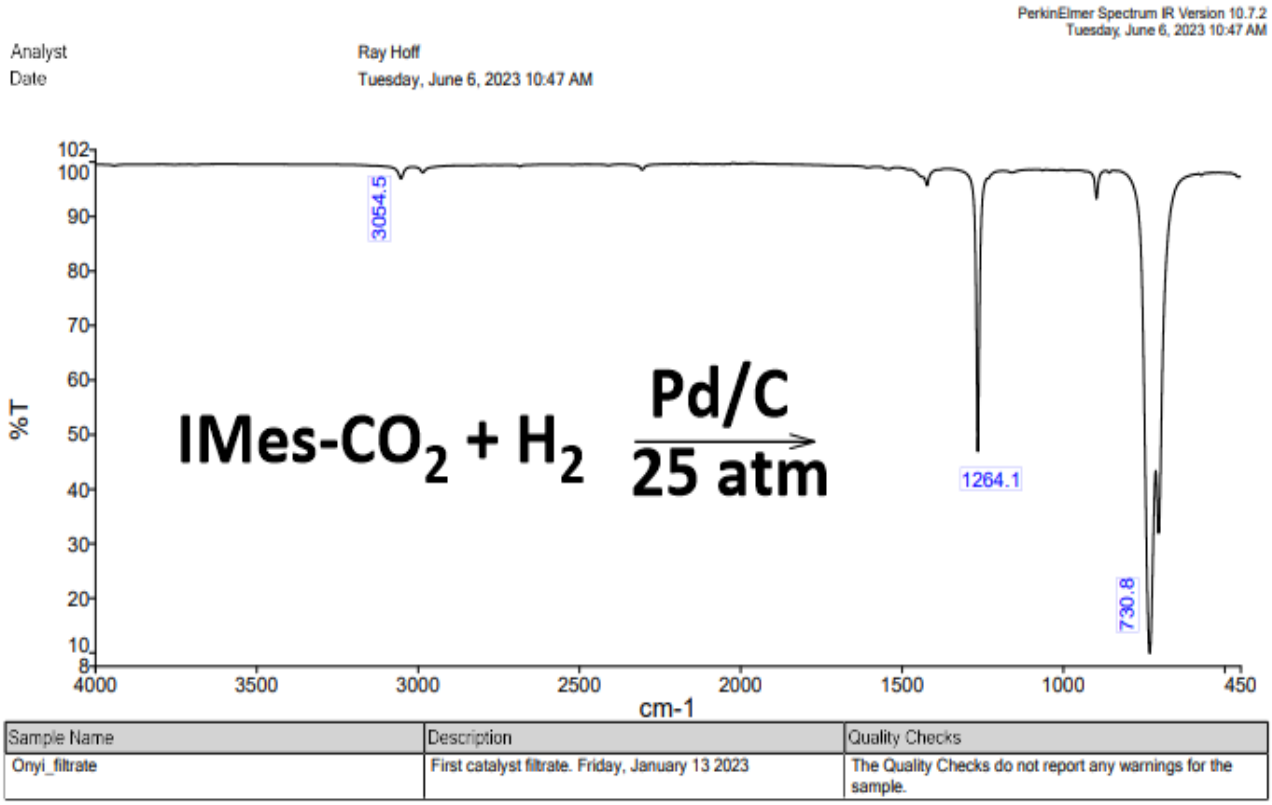

Figure 50. The IR Spectrum of the Product of IMes-CO_2 + H_2 at 25 Atm after 72 Hours

In **Figure 50**, the IR spectrum further reconfirmed the loss of the -CO_2 from the IMes-CO_2, as the CO bond stretch peak at 1675 cm^{-1} was no longer there. There was also no additional peak of a reduction product seen at above 3000 cm^{-1}, thus no reduction product was made.

NMR & IR Results from the Pd/C Catalyzed IMes-CO_2+ H_2 at 30 Atmospheres after 72 hours.

Though this reaction was done at 30 atmospheres, similar results were obtained as the reaction done at 25 atmospheres but with more distinct peaks at 4.0 – 3.95 ppm and 1.01-1.34 ppm in **Figure 51** showing clearly that the compounds present were not methanol and water traces. The peak at 1.01 – 1.34 ppm was a doublet and not an OH broad peak as would have been for water.

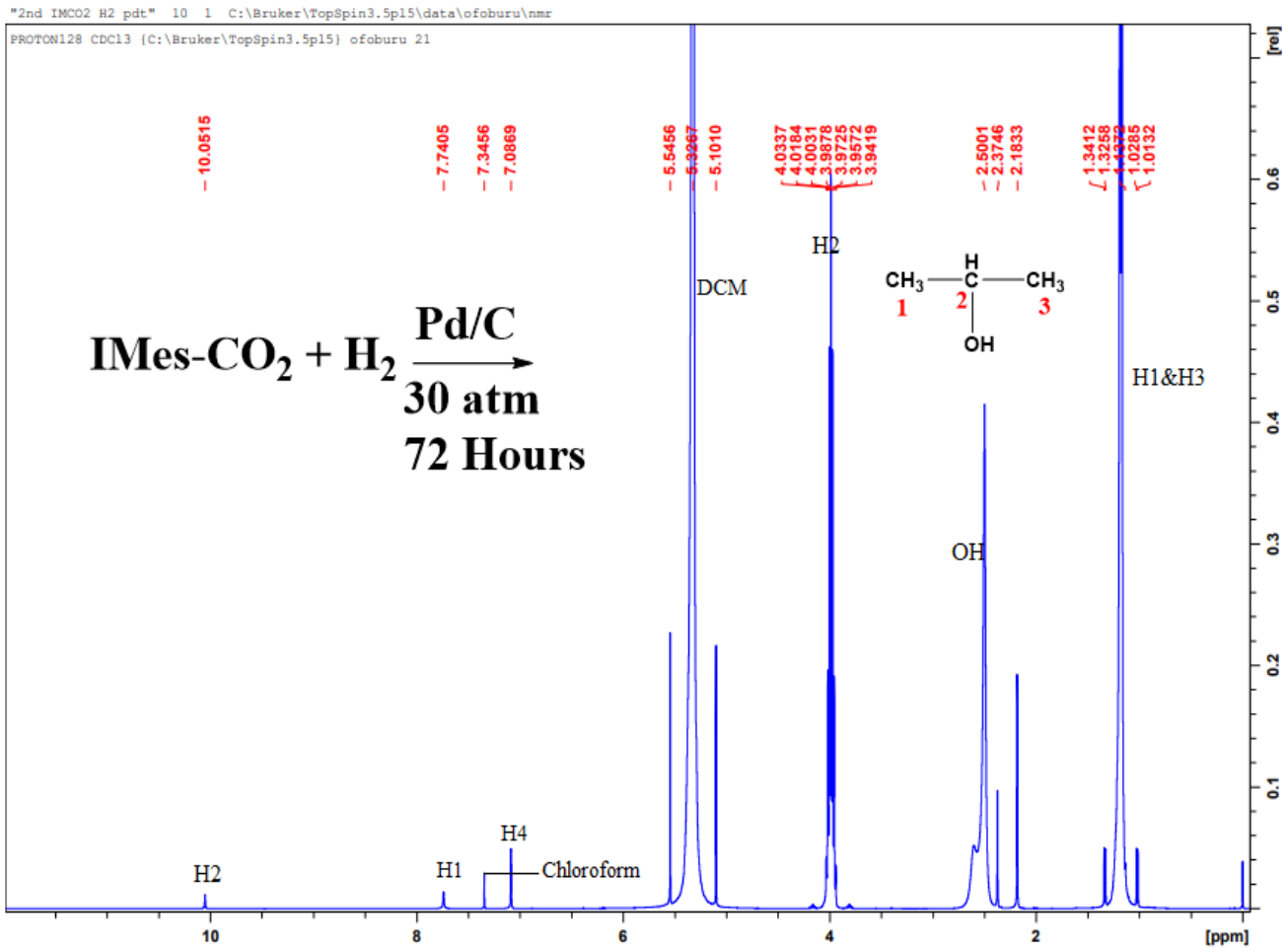

Figure 51. The ^{1}H NMR Spectrum of Product of IMes-CO_2 + H_2 at 30 Atm after 72 Hours

In **Figure 51**, the H2 reappeared at above 10 ppm as seen in the 1H NMR spectrum of IMes-Cl. In addition to the aromatic and olefin protons, there are three other new peaks at 4.0 – 3.90 ppm (septet), 2.50-2.18 ppm (OH broad) and 1.34-1.01 ppm (doublet). These peaks are characteristic isopropanol peaks, thus indicating the presence of isopropanol in the reaction system.

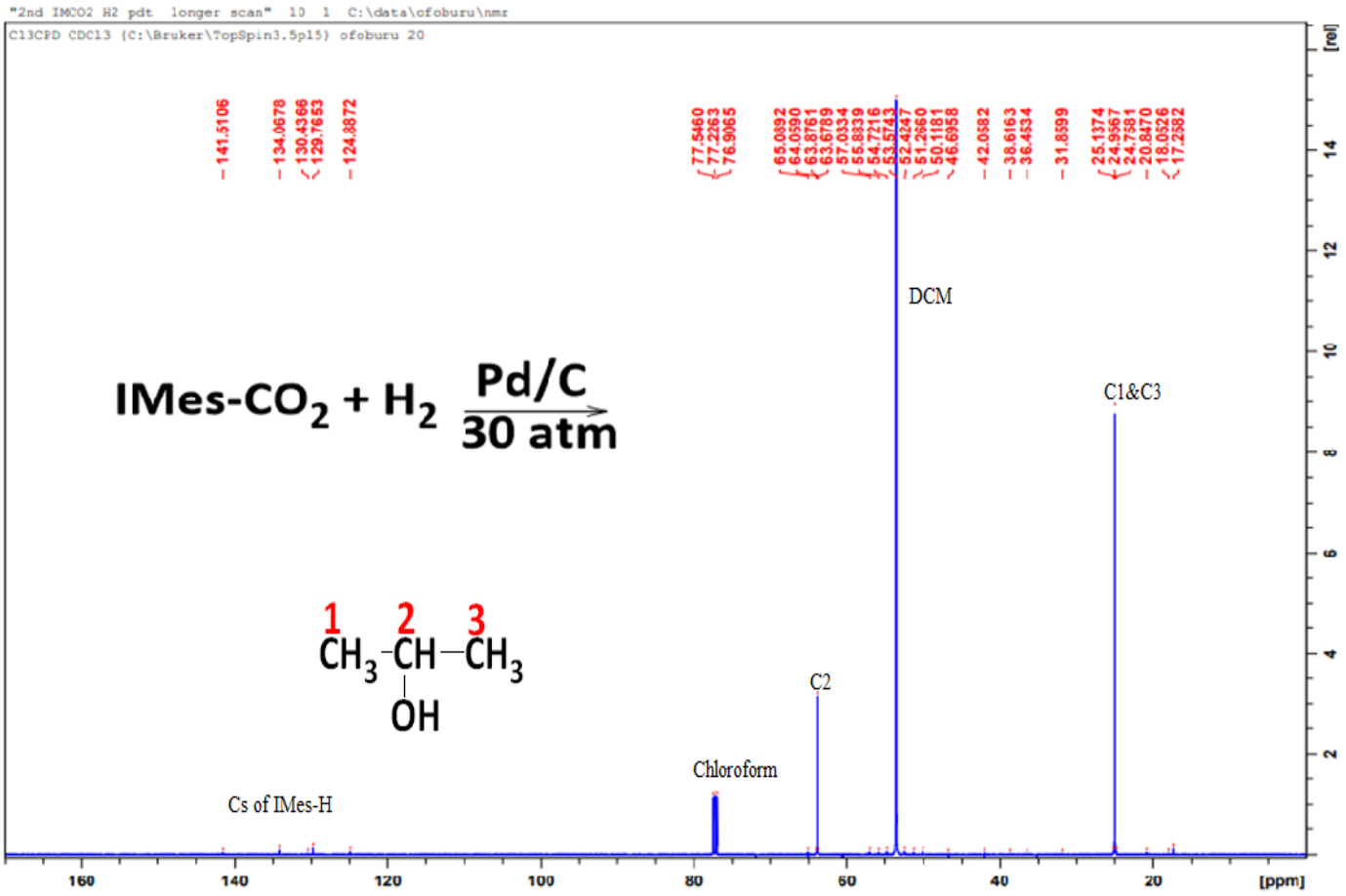

Figure 52. The ^{13}C NMR Spectrum of Product of IMes-CO_2 + H_2 at 30 Atm after 72 Hours

Also, no peak was seen above 160 ppm in **Figure 52,** confirming the absence of a reduction product. The aromatic carbons of IMes-H are at the region as indicted within the spectrum.

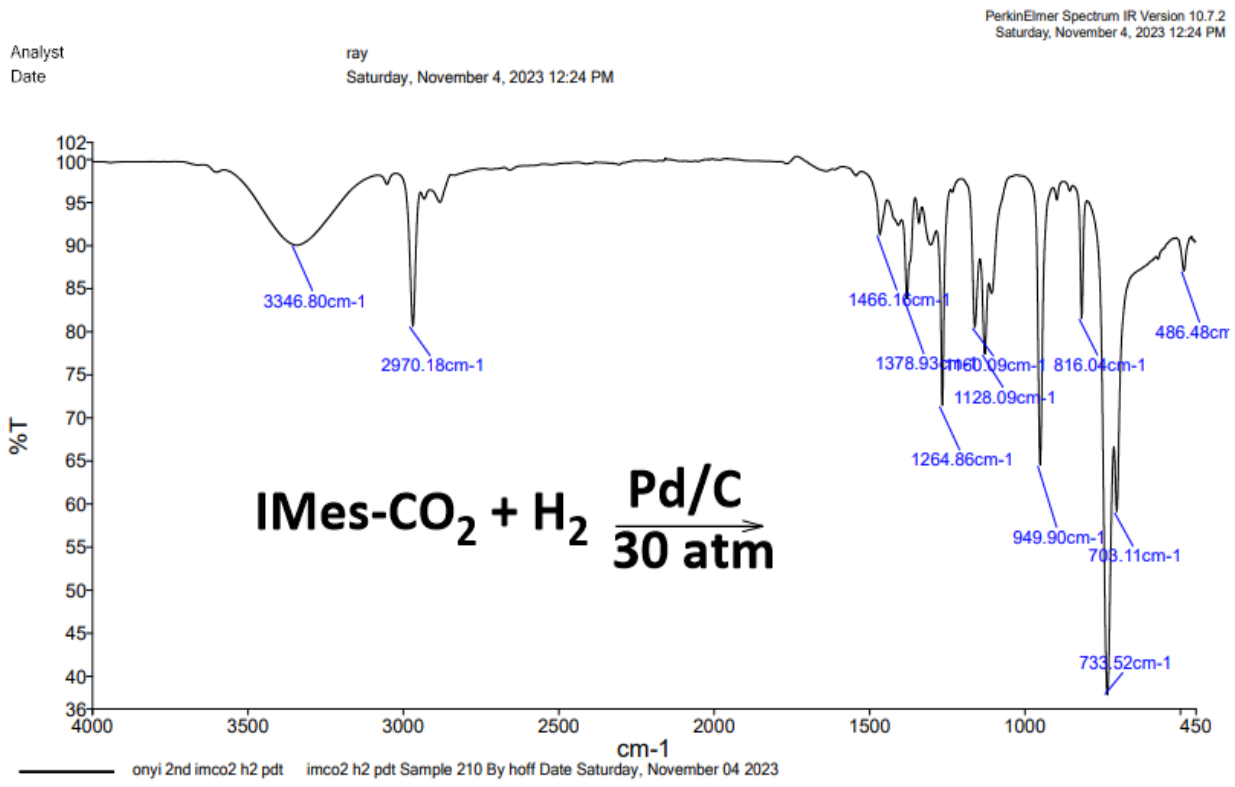

Figure 53. The IR Spectrum of Product of IMes-CO_2 + H_2 at 30 Atm after 72 Hours

In **Figure 53,** the broad peak at 3346.80 cm-1 is above all the peaks obtained from running the IR of some expected reduction products such as the formic acid, methanol, oxalate, and bicarbonate.

NMR & IR Results from the Pd/C Catalyzed $CO_2 + H_2$ at 30 Atmospheres after 72 Hours.

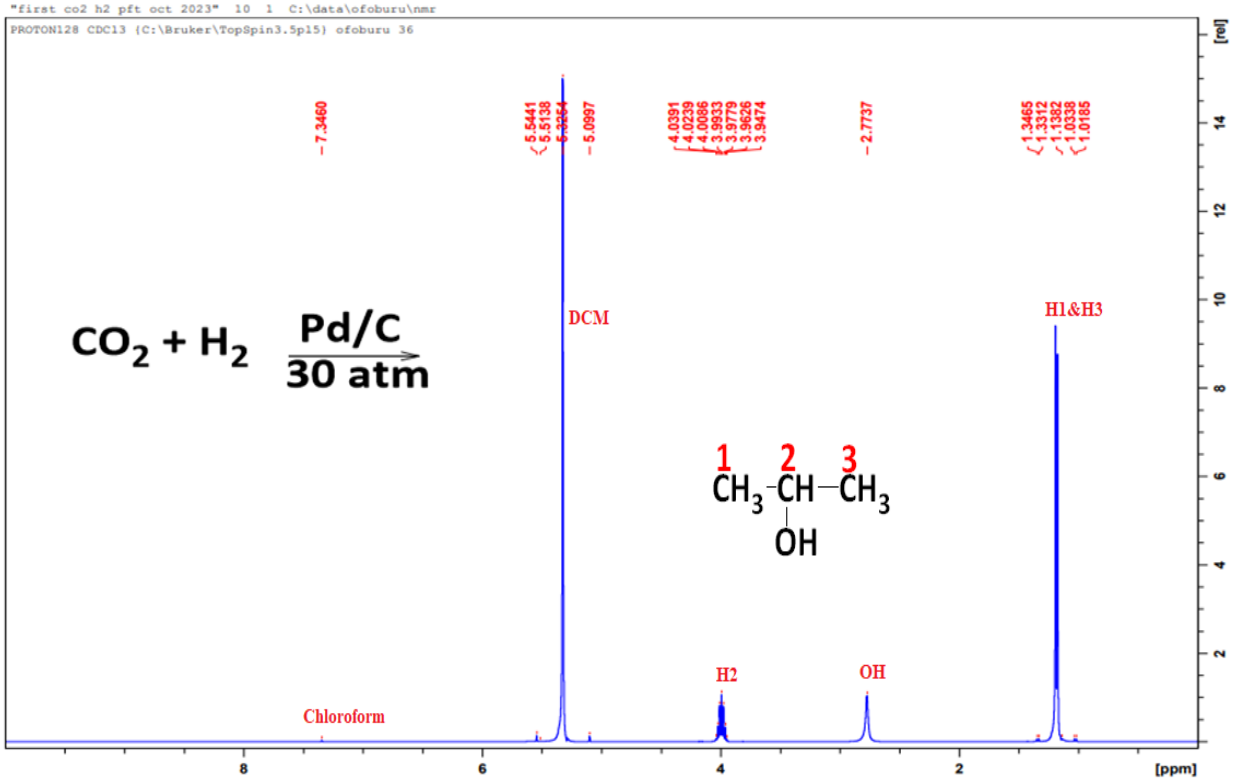

Figure 54. The ^1H NMR Spectrum of the Product of Pd/C Catalyzed $CO_2 + H_2$ at 30 Atm after 72 Hours

In **Figure 54,** the spectrum clearly shows the peaks of isopropanol and not any of the reduction products. No peaks for the IMes as IMes-CO_2 was not part of the reaction.

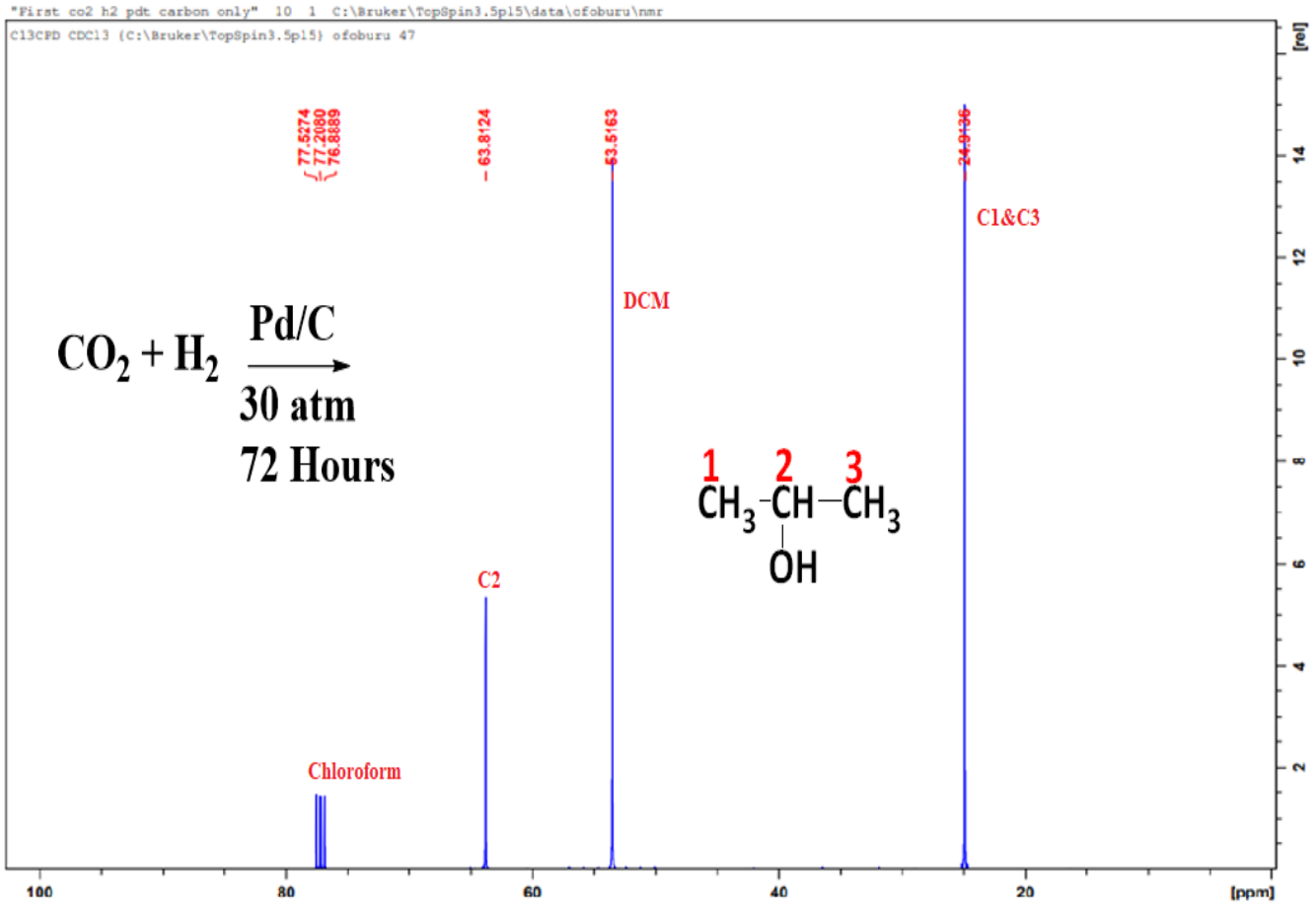

Figure 55. The ^{13}C NMR Spectrum of the Product of Pd/C Catalyzed $CO_2 + H_2$ at 30 Atm after 72 Hours

Figure 55 clearly shows the signals of isopropanol with the C-OH peak at 63.81 – 65.03 ppm, and the two methyl carbon position at 25.09 – 24.71 ppm.

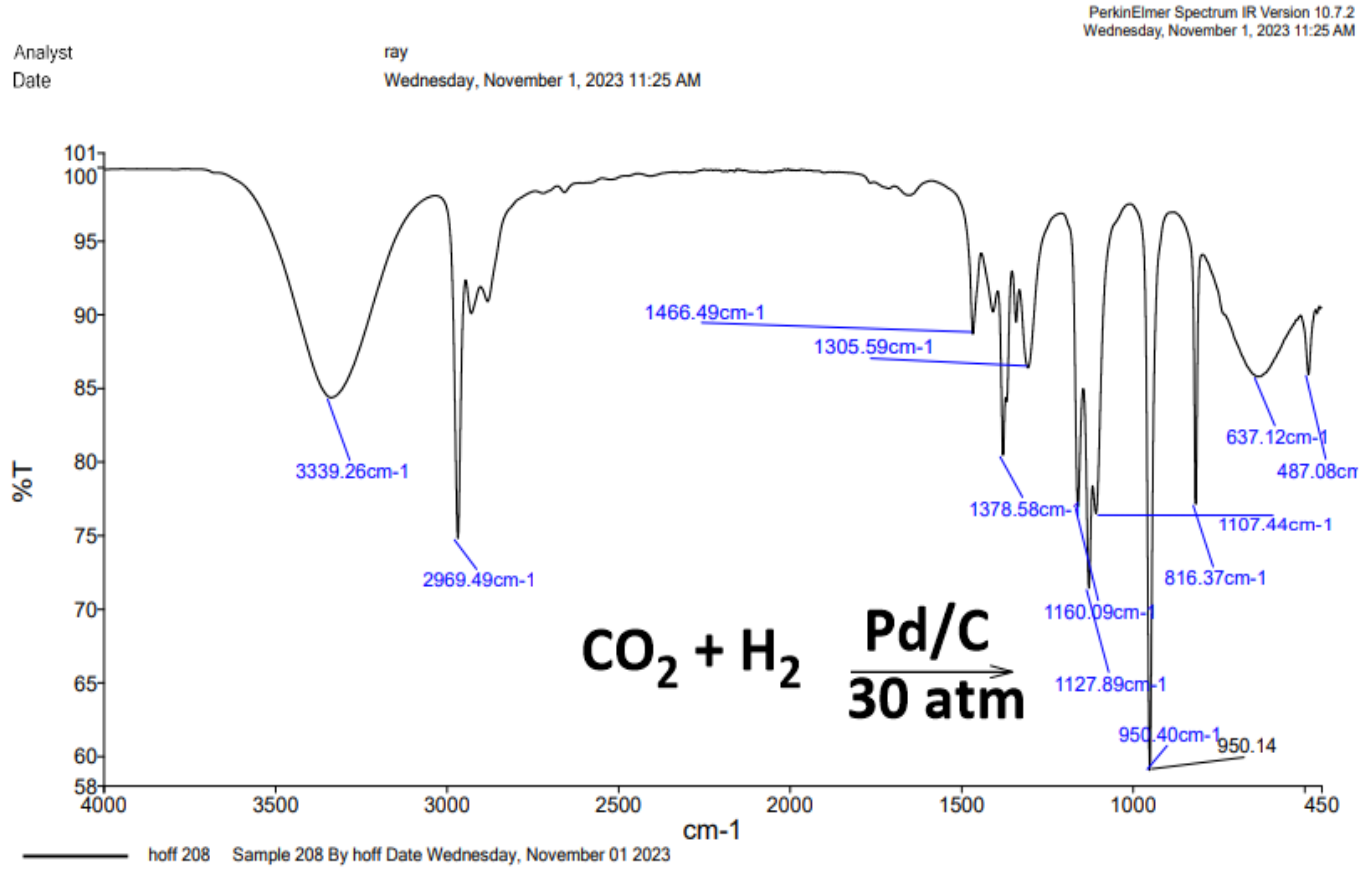

Figure 56. The IR Spectrum of the Product of Pd/C Catalyzed CO_2 + H_2 at 30 Atm after 72 Hours

There is also the presence of the broad peak at 3339.26 cm-1 in Figure **56**, as seen in all the reactions involving the Pd/C catalyst.

NMR & IR results from Uncatalyzed $CO_2 + H_2$ at 30 atmospheres after 72 Hours.

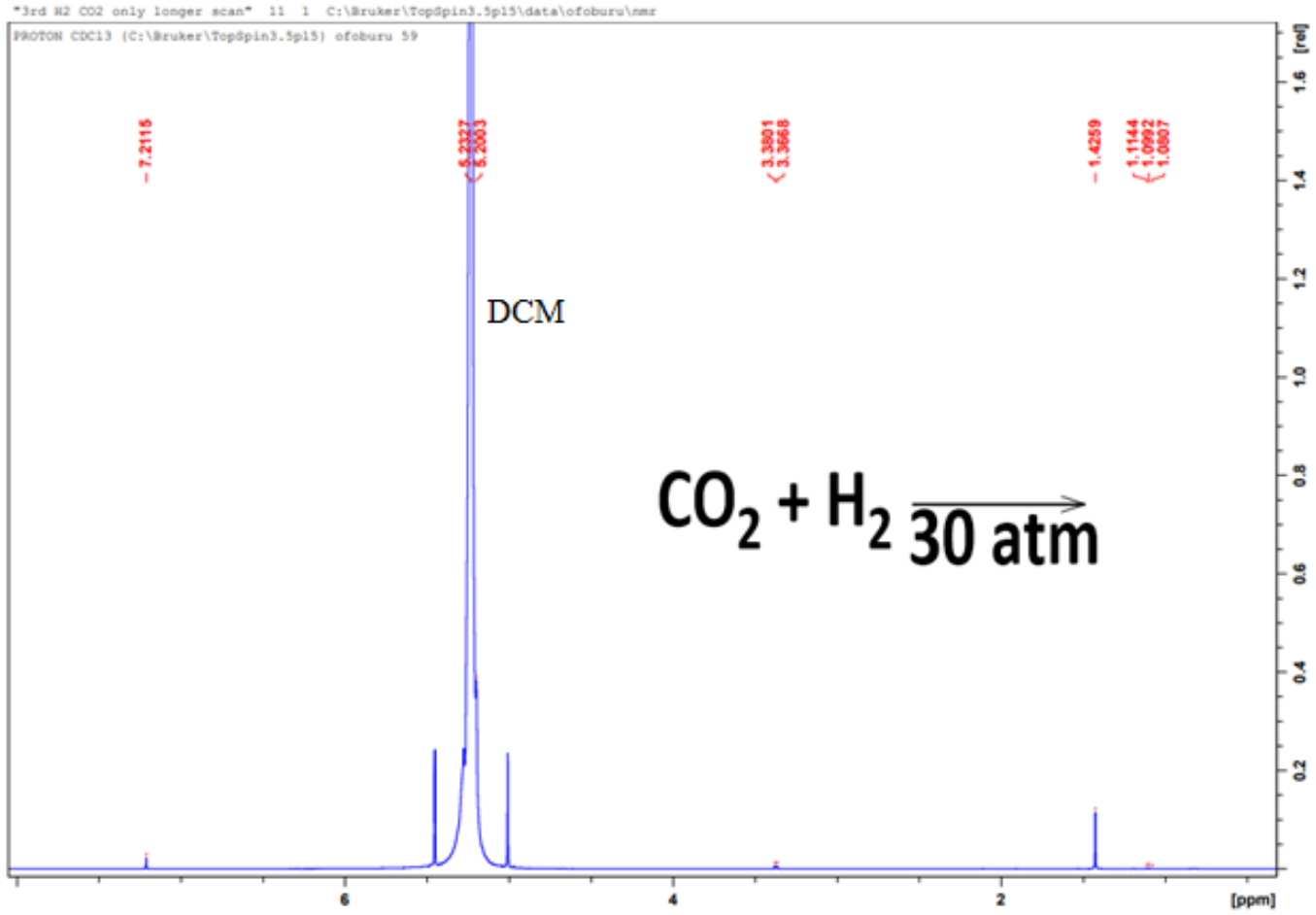

Figure 57. The ^{1}H NMR Spectrum of Uncatalyzed $CO_2 + H_2$ at 30 Atm after 72 Hours

Figure 57, does not show any of the isopropanol peaks, and this was because there was no Pd/C catalyst involved in this reaction. This result was an indication that the isopropanol was not made in the previous reaction but must have been related with the catalyst.

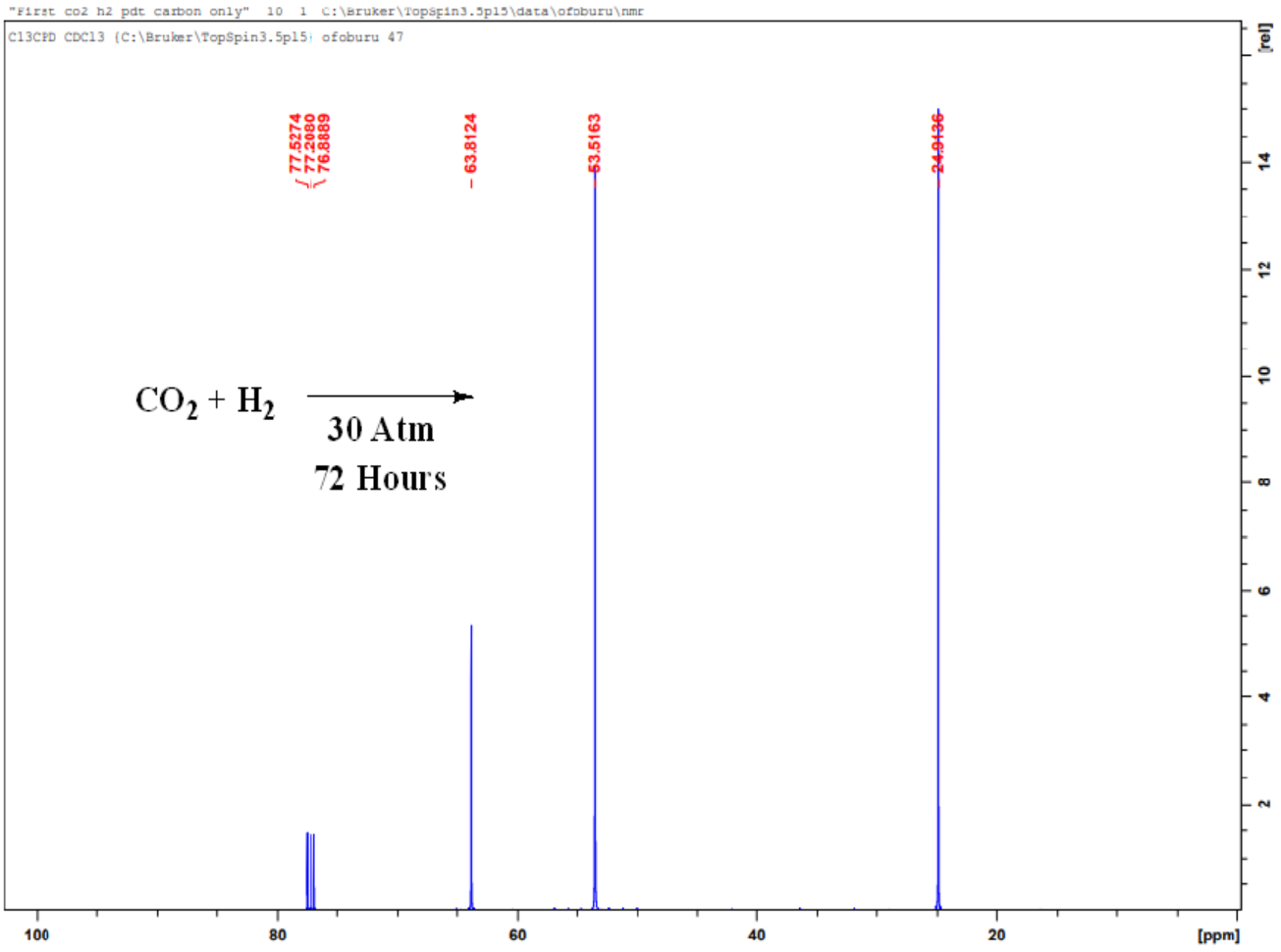

Figure 58. The ^{13}C NMR Spectrum of Uncatalyzed $CO_2 + H_2$ at 30 Atmospheres after 72 Hours

In Figure 58, no additional peaks were seen aside the peaks of DCM and chloroform solvents at 77.40 – 76.76 ppm and 56.94 – 50.03 ppm respectively. The peaks for isopropanol were not seen as Pd/C catalyst was not involved in the reaction.

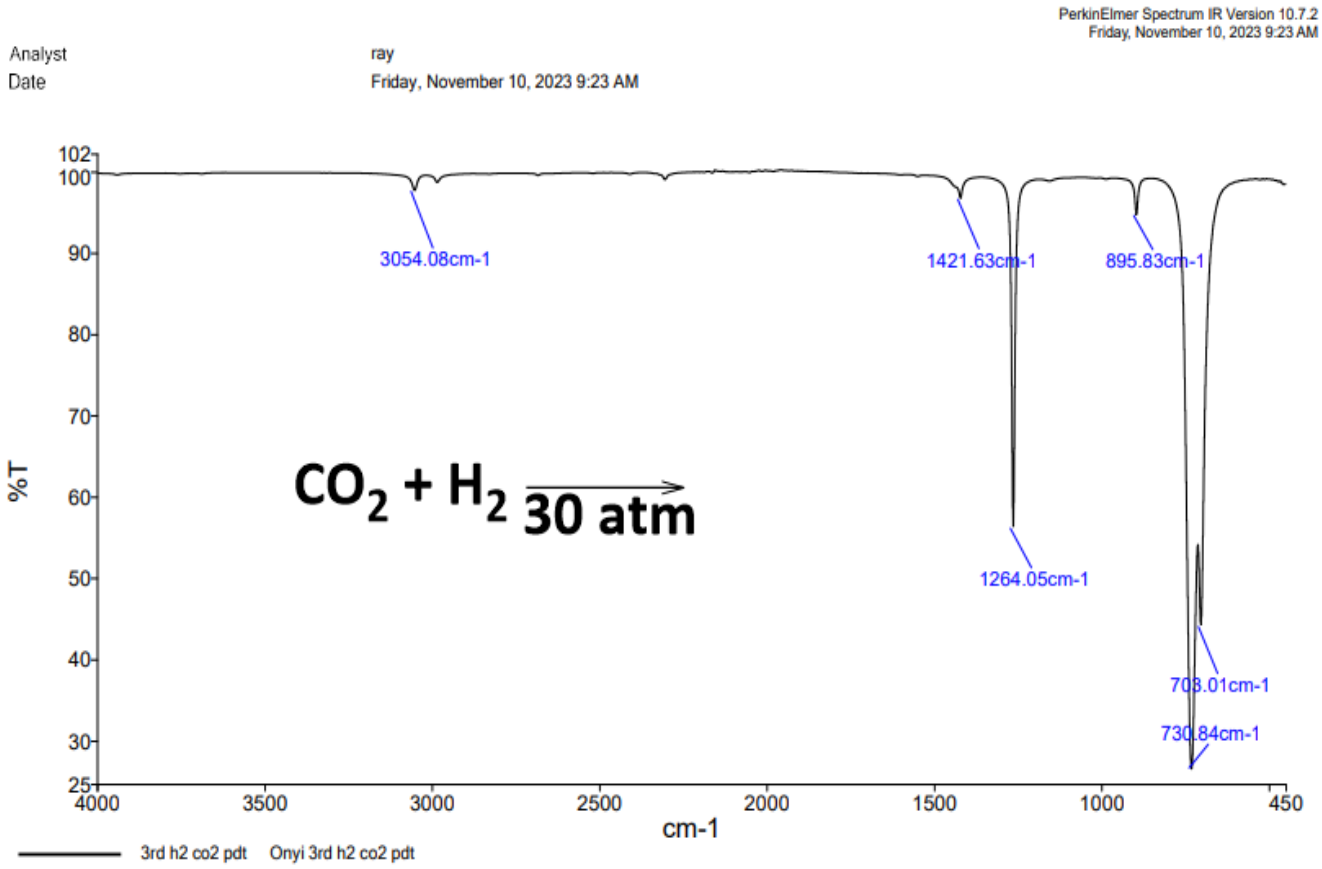

Figure 59. The IR Spectrum of Uncatalyzed CO_2 + H_2 at 30 Atmospheres after 72 Hours

The spectrum in **Figure 59,** showed the peaks of dichloromethane only without the broad peak at 3339.26 seen in results from reactions involving Pd/C catalyst.

NMR & IR Results from the Pd/C Catalyzed $CO_2 + H_2$ at 30 Atmospheres after 24 Hours.

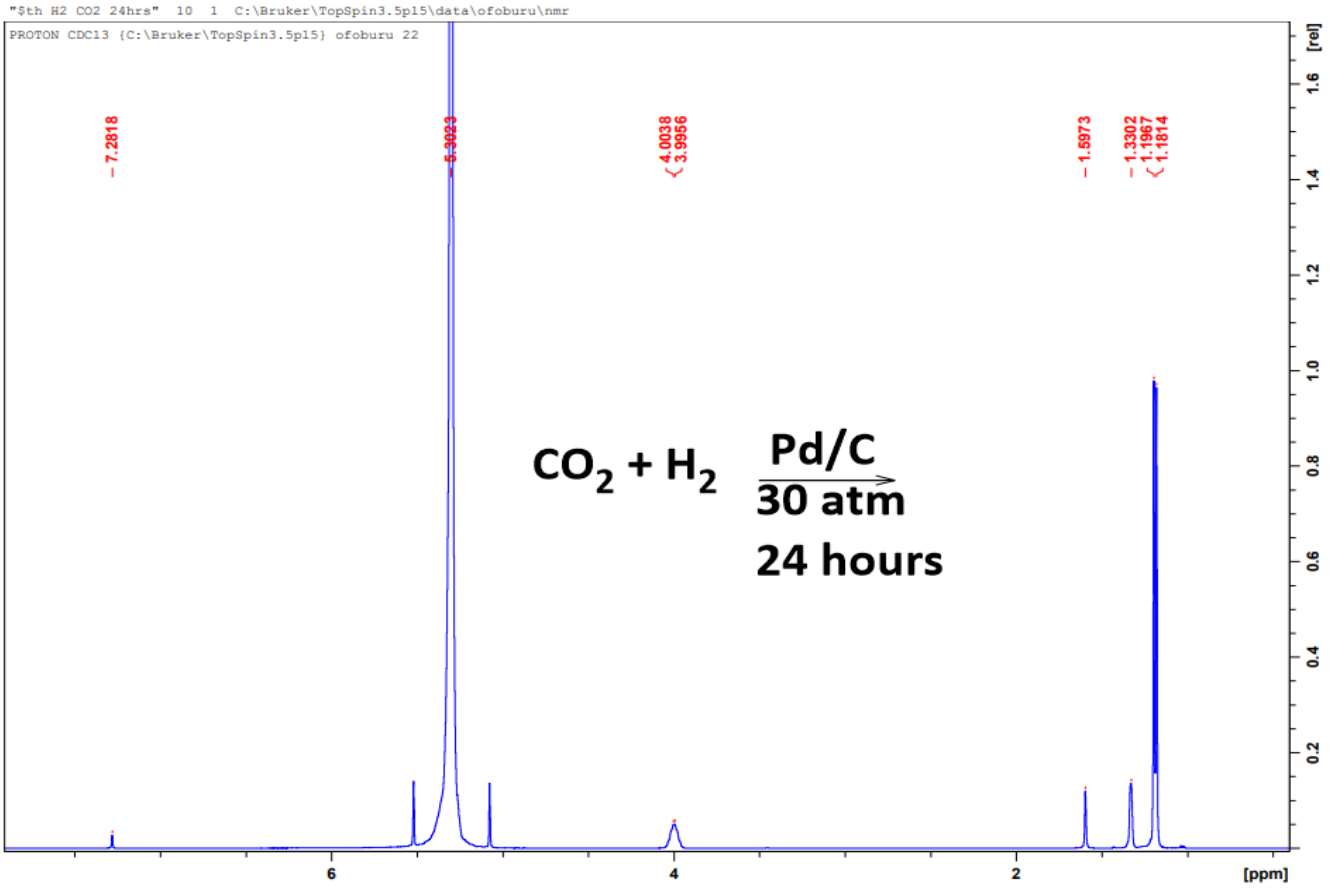

Figure 60. The ^1H NMR Spectrum of Pd/C Catalyzed $CO_2 + H_2$ at 30 Atmospheres after 24 Hours

The result displayed in **Figure 60**, was from a reaction ran for 24 hours instead the usual 72 hours. Nonetheless, the peaks for isopropanol were seen indicating its present in the reaction system.

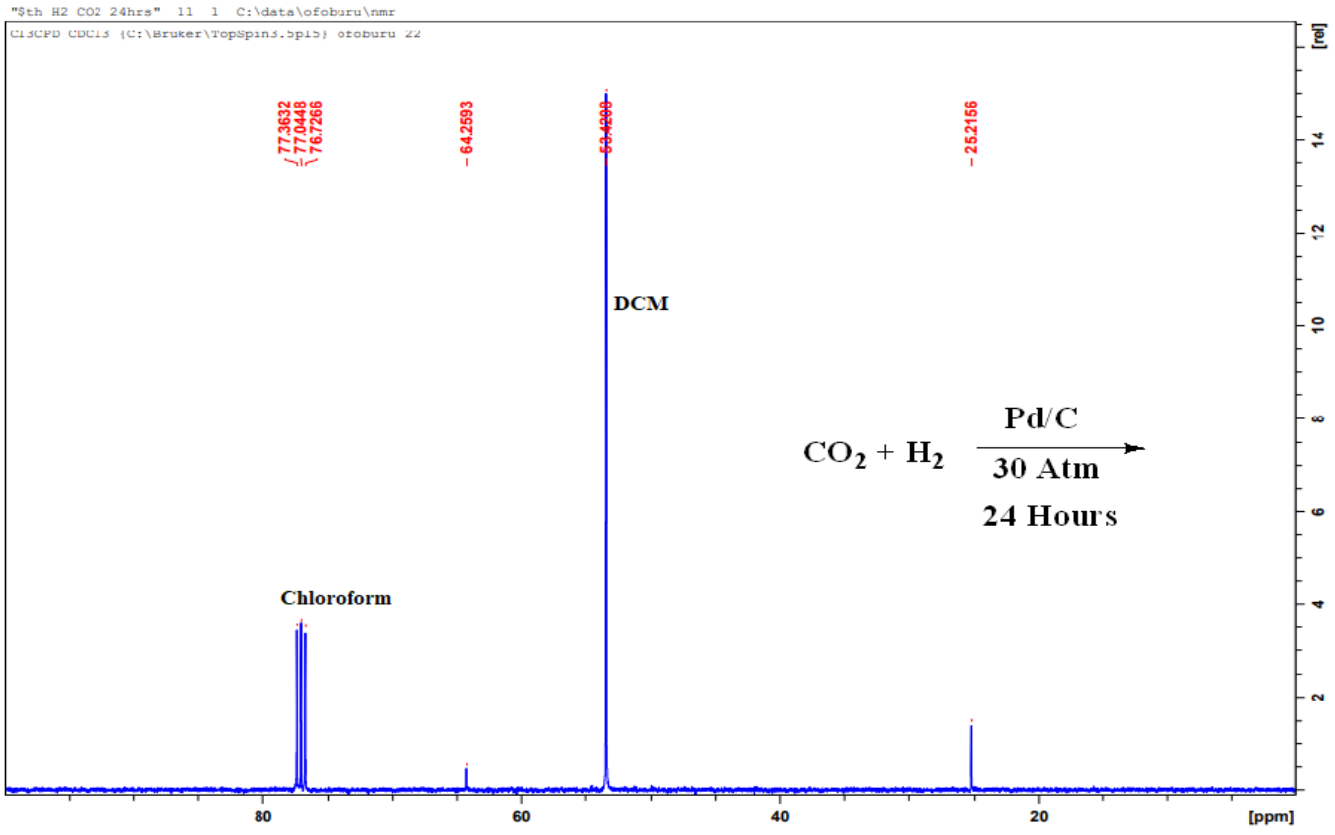

Figure 61. The ^{13}C NMR Spectrum of Pd/C Catalyzed $CO_2 + H_2$ at 30 Atmospheres after 24 Hours

Figure 61 also confirms the presence of isopropanol from a reaction ran for 24 hours only instead the usual 72 hours as with the rest of the reactions.

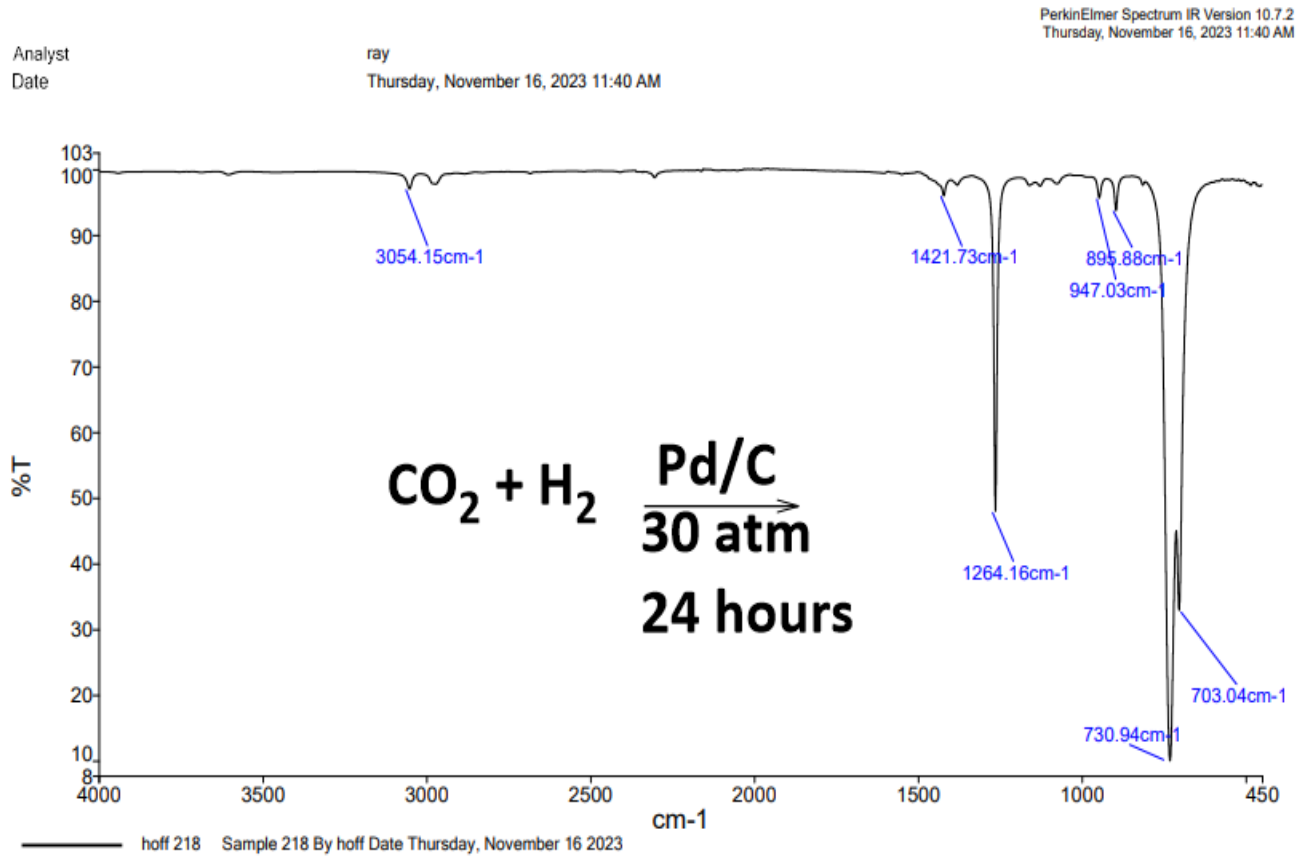

Figure 62. The IR Spectrum of Pd/C Catalyzed CO_2 + H_2 at 30 Atmospheres after 24 Hours

Though the Pd/C was involved in the reaction, **Figure 62** showed no broad peak as seen in other reactions involving the catalyst because the reaction instead the characteristic DCM peak was seen at 3054.15 cm^{-1}.

NMR & IR Results from Pd/C Catalyst Stirred in DCM under N_2 gas for 72 Hours

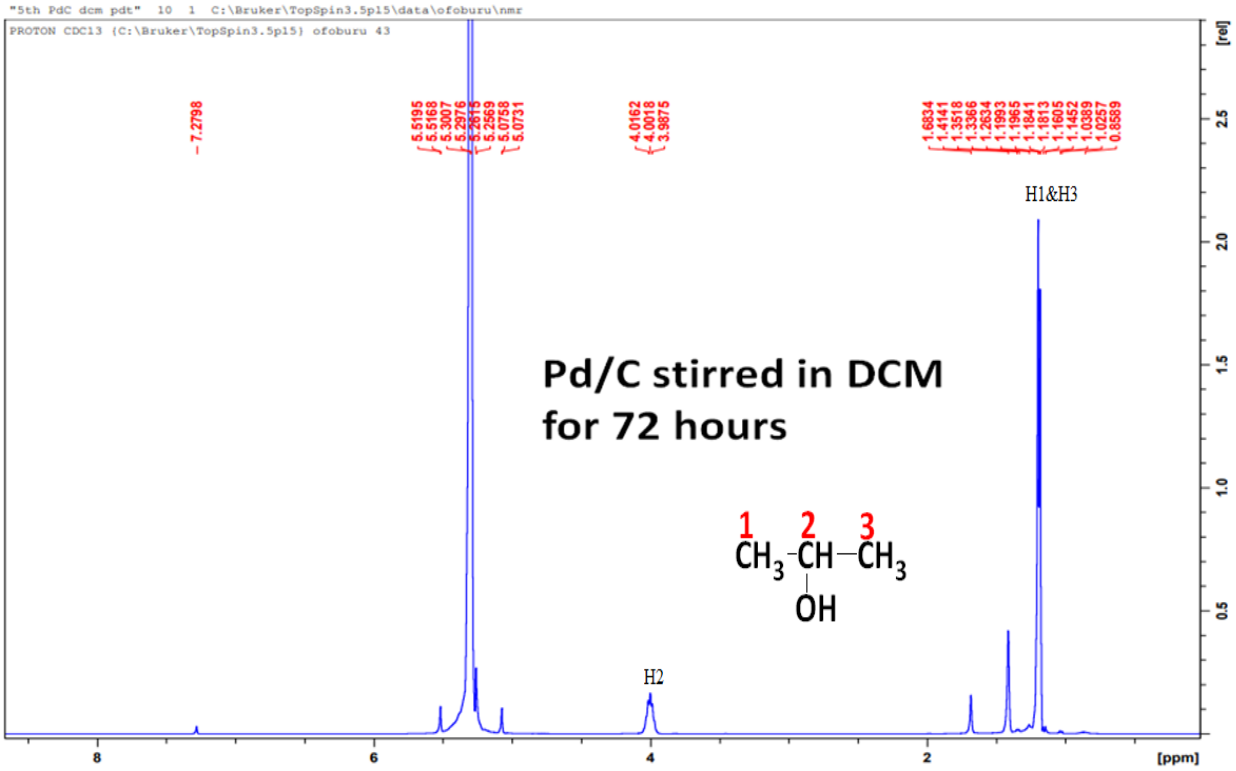

Figure 63. The ^{1}H NMR Spectrum of Pd/C Stirred in DCM for 72 Hours.

Figure 63 displays the results of the control experiment indicating the presence of isopropanol with the peaks at 4.0 ppm and 1.68 ppm for the H2 and H3 positions.

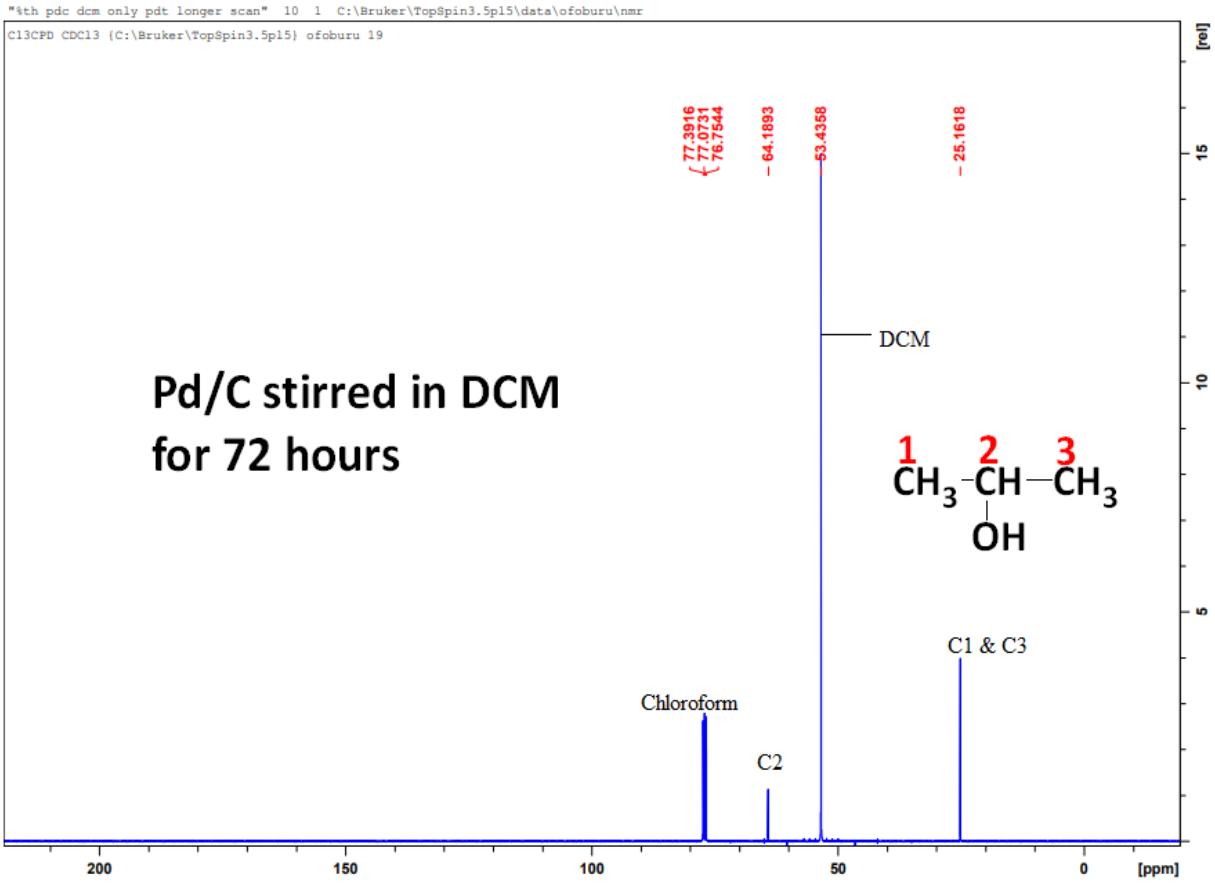

Figure 64. The ^{13}C NMR Spectrum of Pd/C Stirred in DCM for 72 Hours.

Figures 63, 64, and **65** results obtained from the control experiment confirmed the source of the isopropanol with all the relevant peaks showing at same positions as seen in previously Pd/C catalyzed reactions.

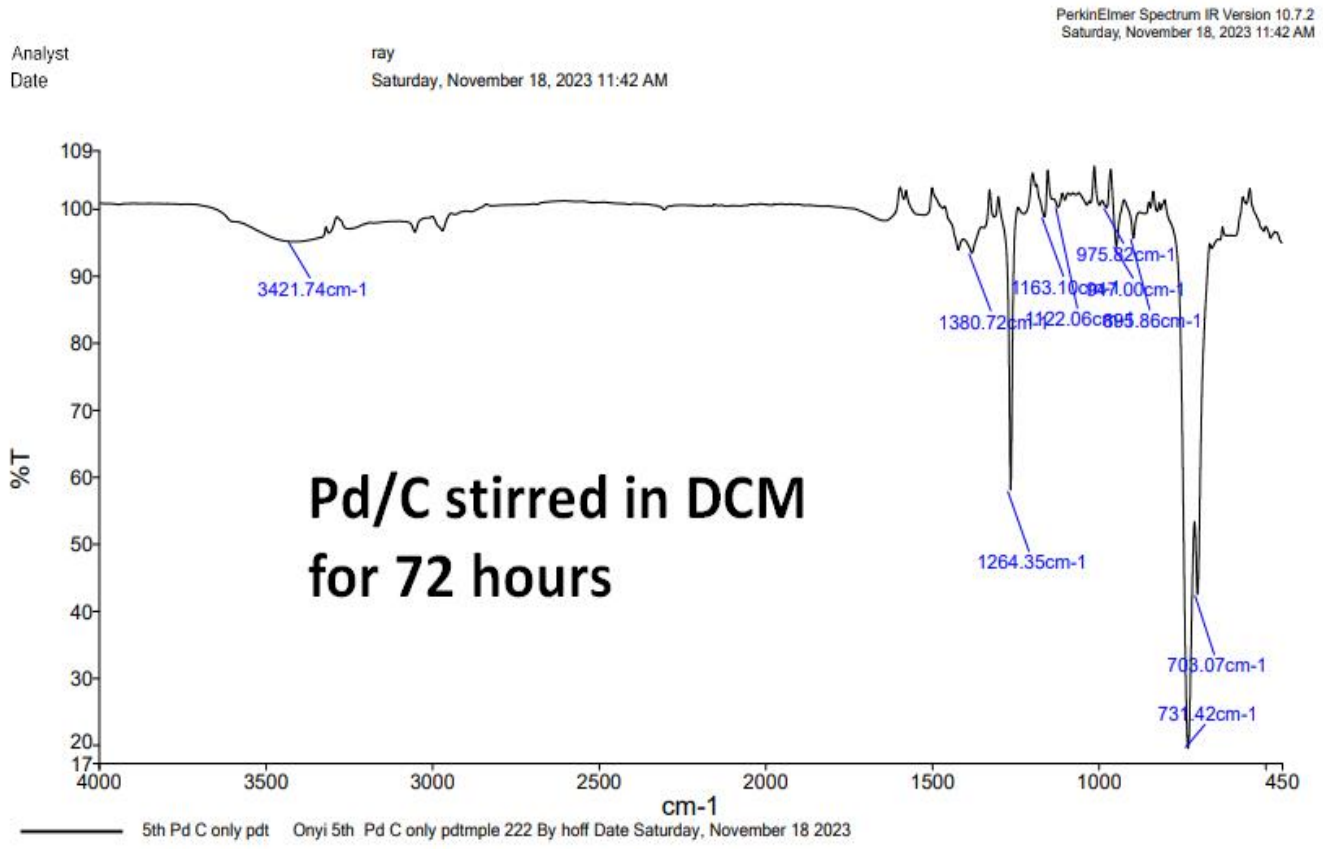

Figure 65. The IR Spectrum of Pd/C Pd/C Stirred in DCM for 72 Hours.

Figure 65 also shows the broad peak at above 3300 cm^{-1} within the alcohol IR region as seen in all the reactions involving the Pd/C catalyst.

NMR & IR Results from the Pd/C Catalyzed IMes-CO_2 + CO_2 + H_2 at 30 Atmospheres after 72 Hours

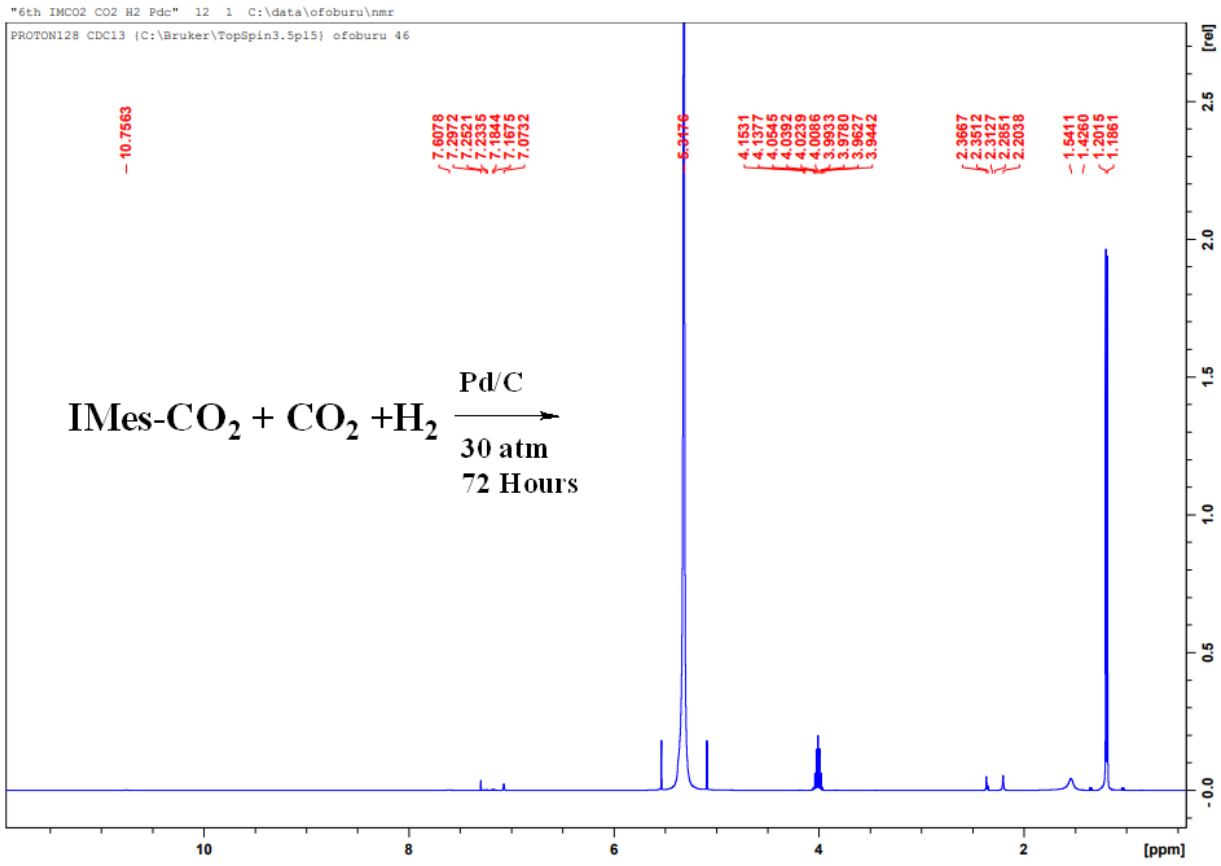

Figure 66. The ^{1}H NMR Spectrum of the Pd/C Catalyzed IMes-CO_2 + CO_2 + H_2 at 30 Atmospheres after 72 Hours

The results displayed in **Figure 66**, is same with the results obtained when the IMes-CO_2 was pressurized with only H_2 gas. The H2 hydrogen reappeared at above 10 ppm and the IMes hydrogens were also present confirming no further reduction occurred.

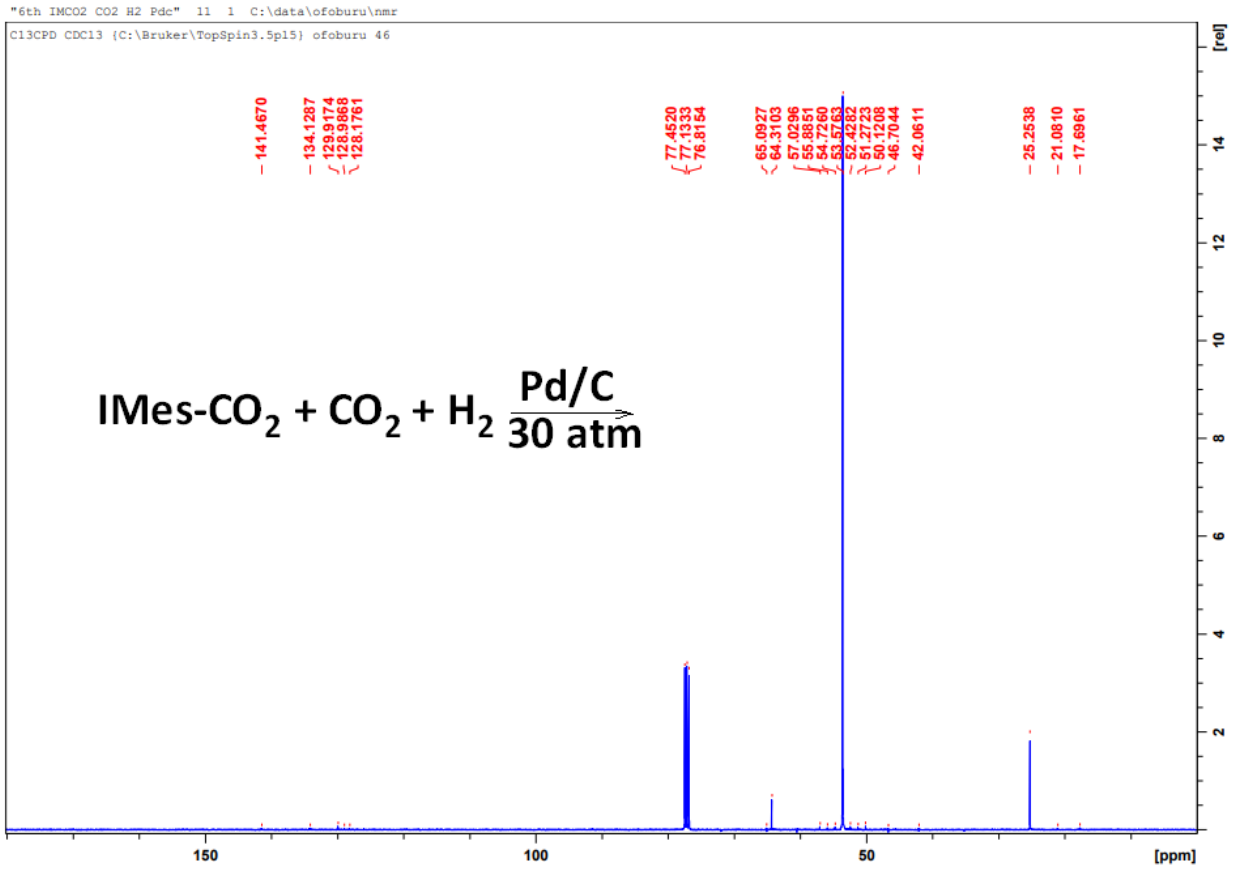

Figure 67. The ^{13}C NMR Spectrum of the Pd/C Catalyzed IMes-CO_2 + CO_2 + H_2 at 30 Atmospheres after 72 Hours

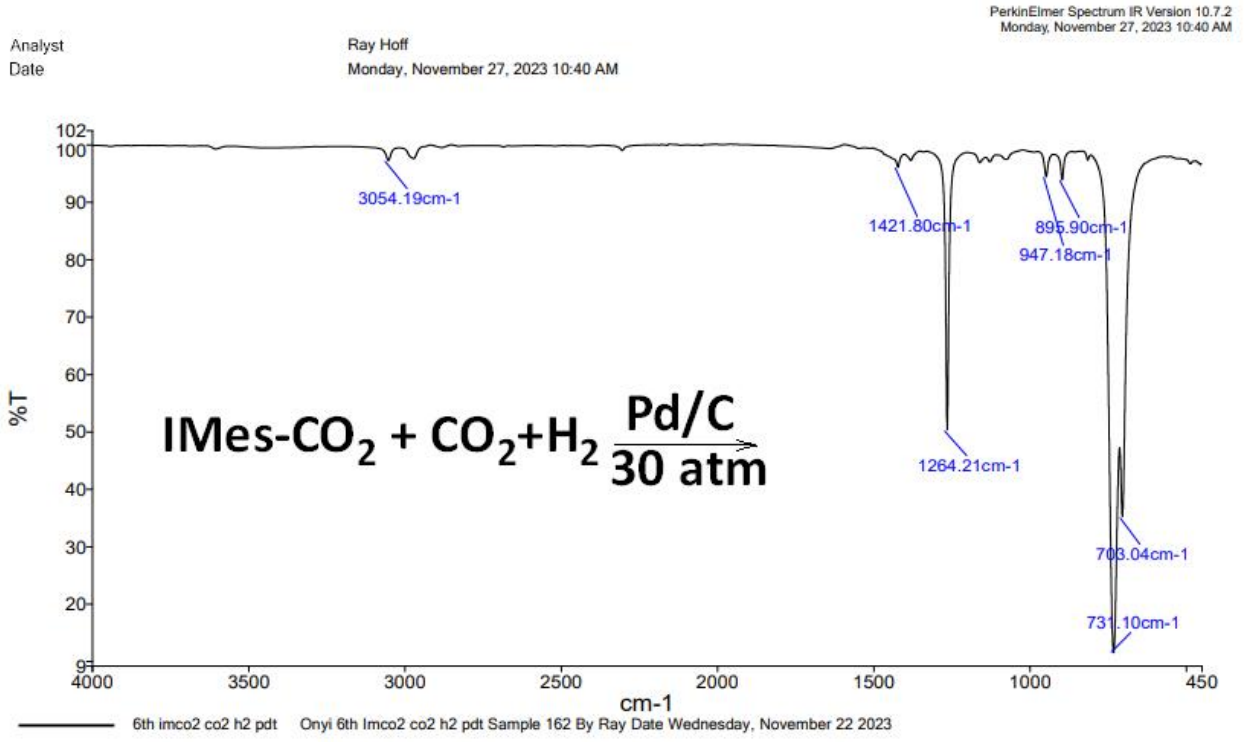

Figure 68.The IR Spectrum of the Pd/C Catalyzed IMes-CO_2 + CO_2 + H_2 at 30 Atmospheres after 72 Hours

Figure 68 further confirmed that the C2-CO_2 bond was broken and the CO_2 was lost at the end of the reaction as the C=O bond peak at 1675 cm^{-1} was lost and no additional peak was seen within the region of the reduction products.

NMR & IR Results from the Uncatalyzed IMes-CO_2 + CO_2 + H_2 at 30 Atmospheres after 72 Hours

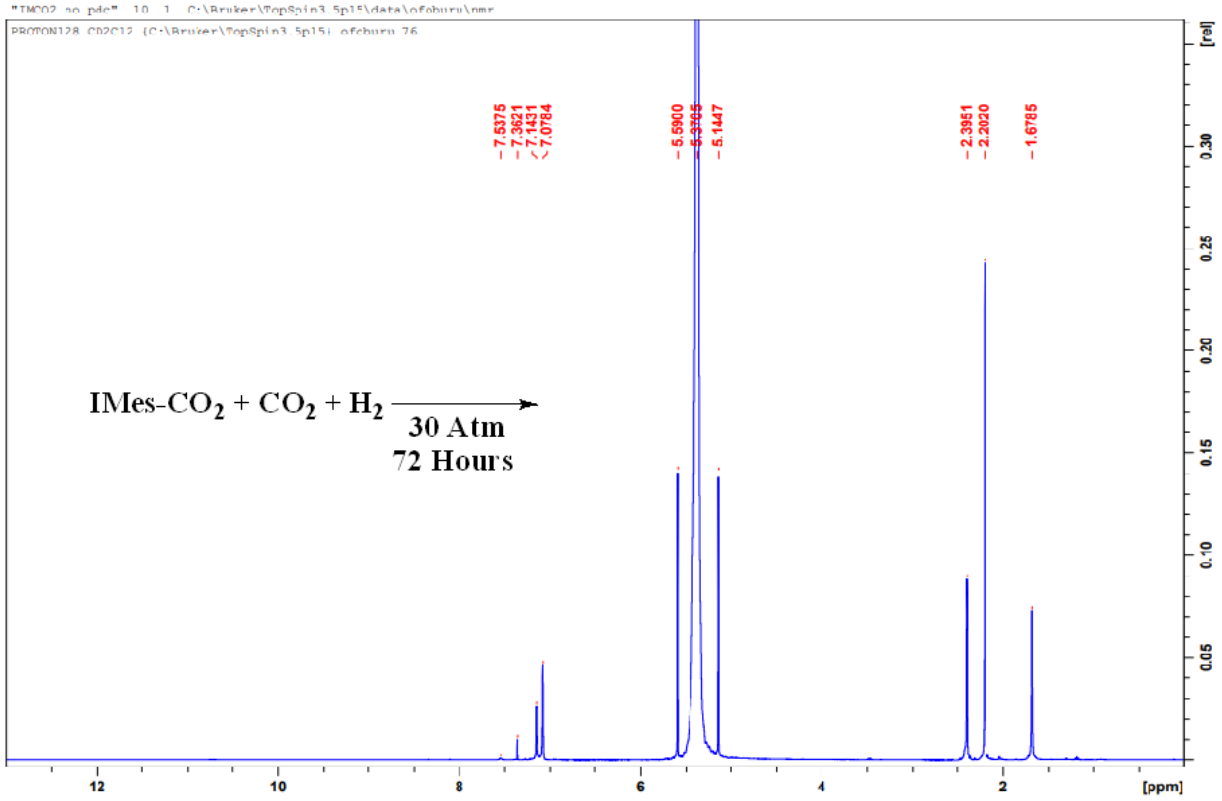

Figure 69. The ^1H NMR Spectrum of the Uncatalyzed IMes-CO_2 + CO_2 + H_2 at 30 Atmospheres after 72 Hours

This results spectrum in **Figure 69**, showed in that IMes holds on tightly to the IMes-CO_2 if pressurized with CO_2 in the absence of a catalyst. The peak at 1.68 ppm could be the OH of water trace in the system.

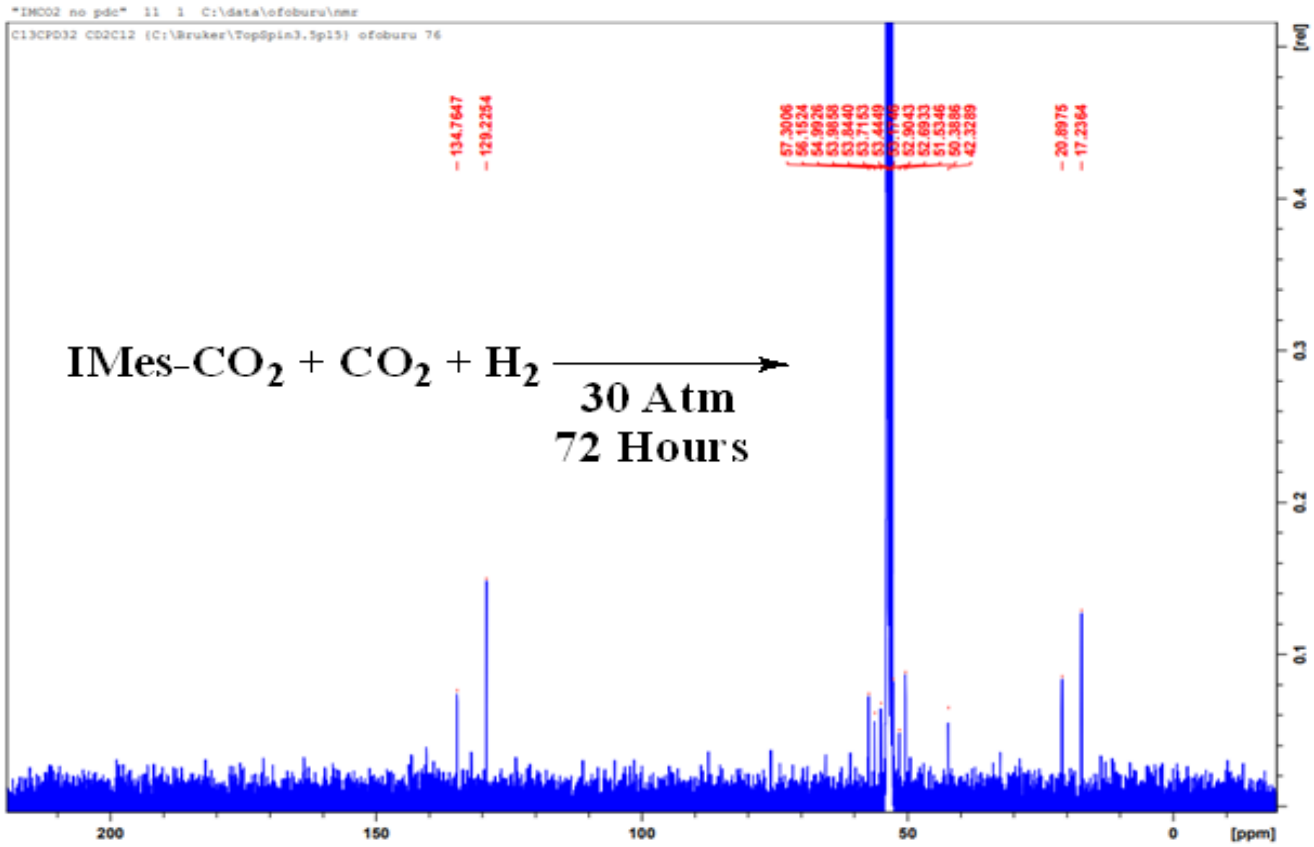

Figure 70. The ^{13}C NMR Spectrum of the Uncatalyzed IMes-CO_2 + CO_2 + H_2 at 30 Atmospheres after 72 Hours

In **Figure 70**, none of the peaks seen in reactions involving Pd/C catalyst was seen here because the catalyst was not involved in this reaction. Hence the peaks present are those of IMes-CO_2 which is still attached to the CO_2 due to the pressurized CO_2 background supplied to it.

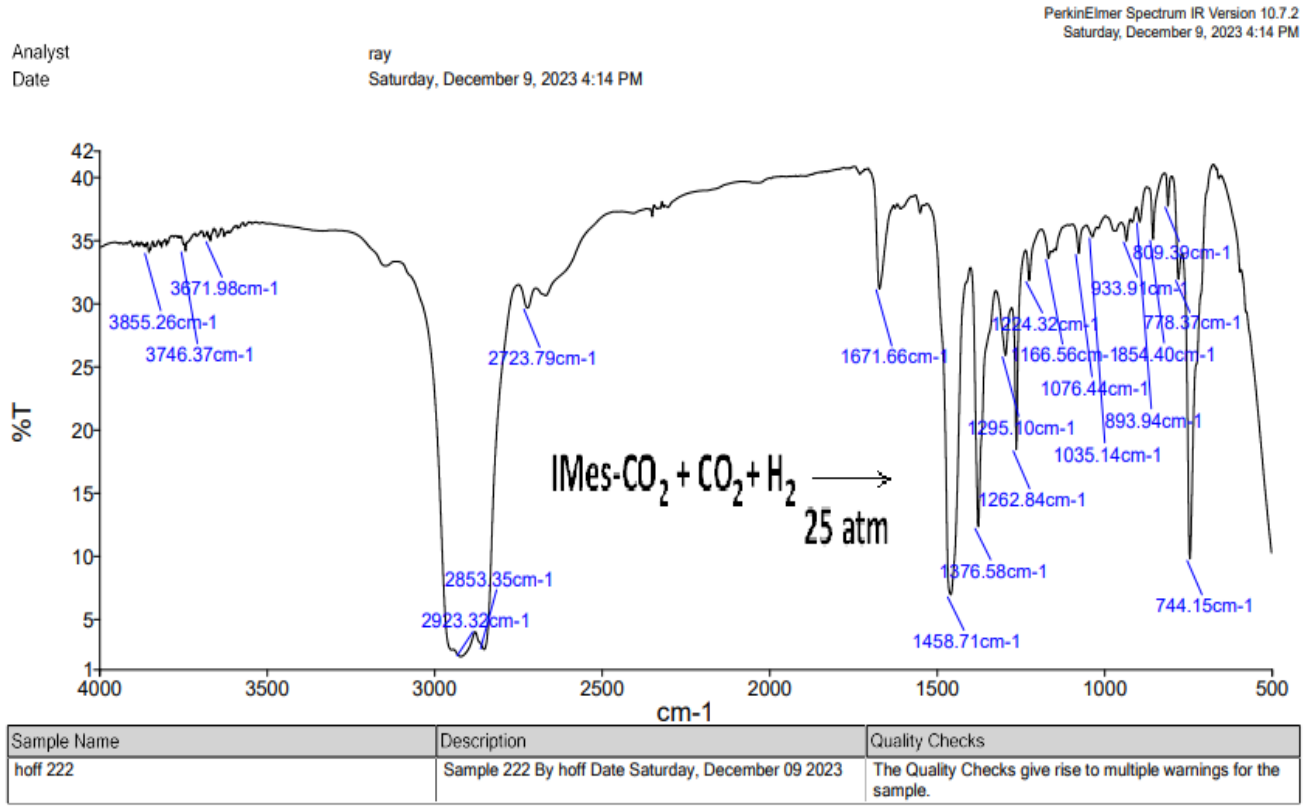

Figure 71. The IR Spectrum of the Uncatalyzed IMes-CO_2 + CO_2 + H_2 at 30 Atmospheres after 72 Hours.

In **Figure 71**, the peak at 1671.66 cm^{-1} further confirms that the CO_2 is still attached to IMes-CO_2 due to the pressurized CO_2 background supplied to it. Also, catalyst was not present to reduce the C-CO_2 as seen in the reactions involving the Pd/C catalyst.

NMR & IR Results of IMes-CO_2 Stirred in DCM Under N_2 for 72 Hours

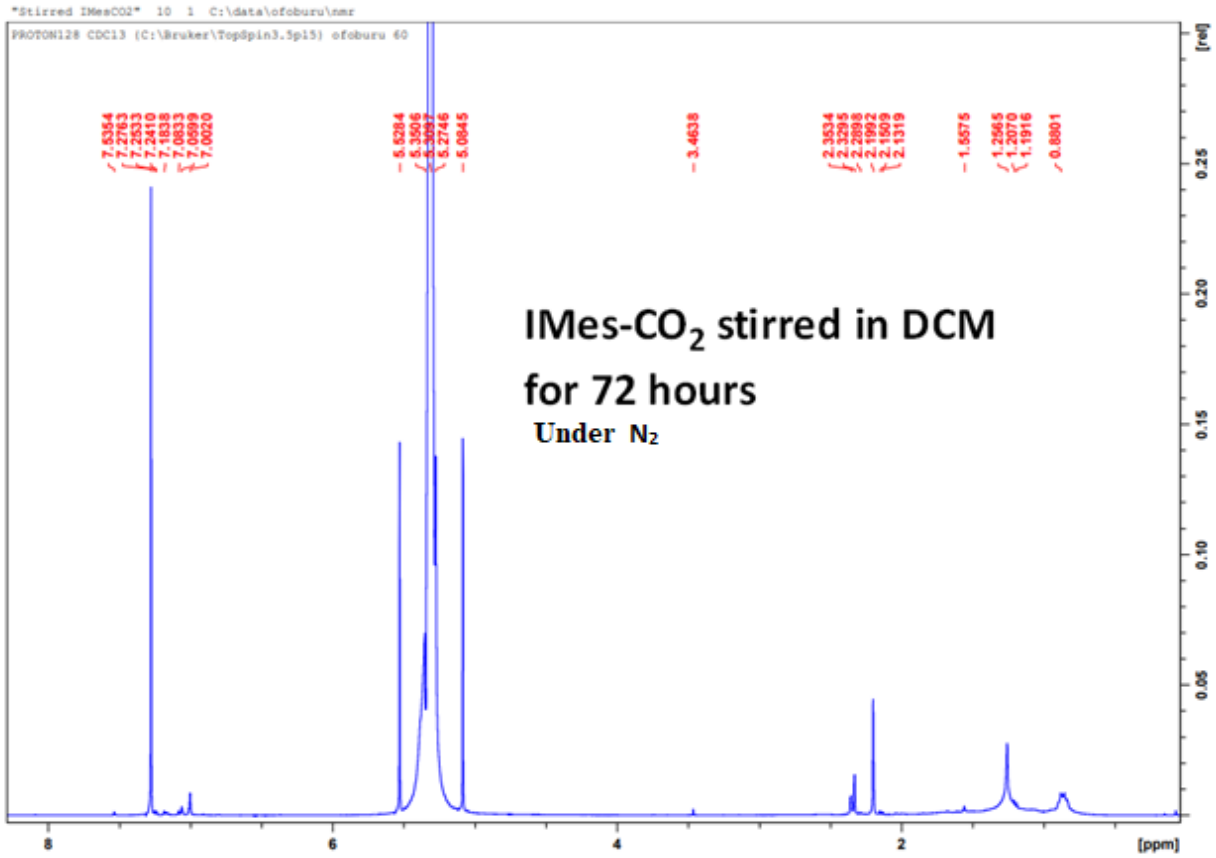

Figure 72. The ^{1}H NMR Spectrum of the Product of IMes-CO_2 Stirred in DCM under N_2 for 72 Hours

The results obtained from the control experiment in **Figure 72** showed that IMes can slowly dissociate itself from IMes-CO_2 if not pressurized with CO_2.

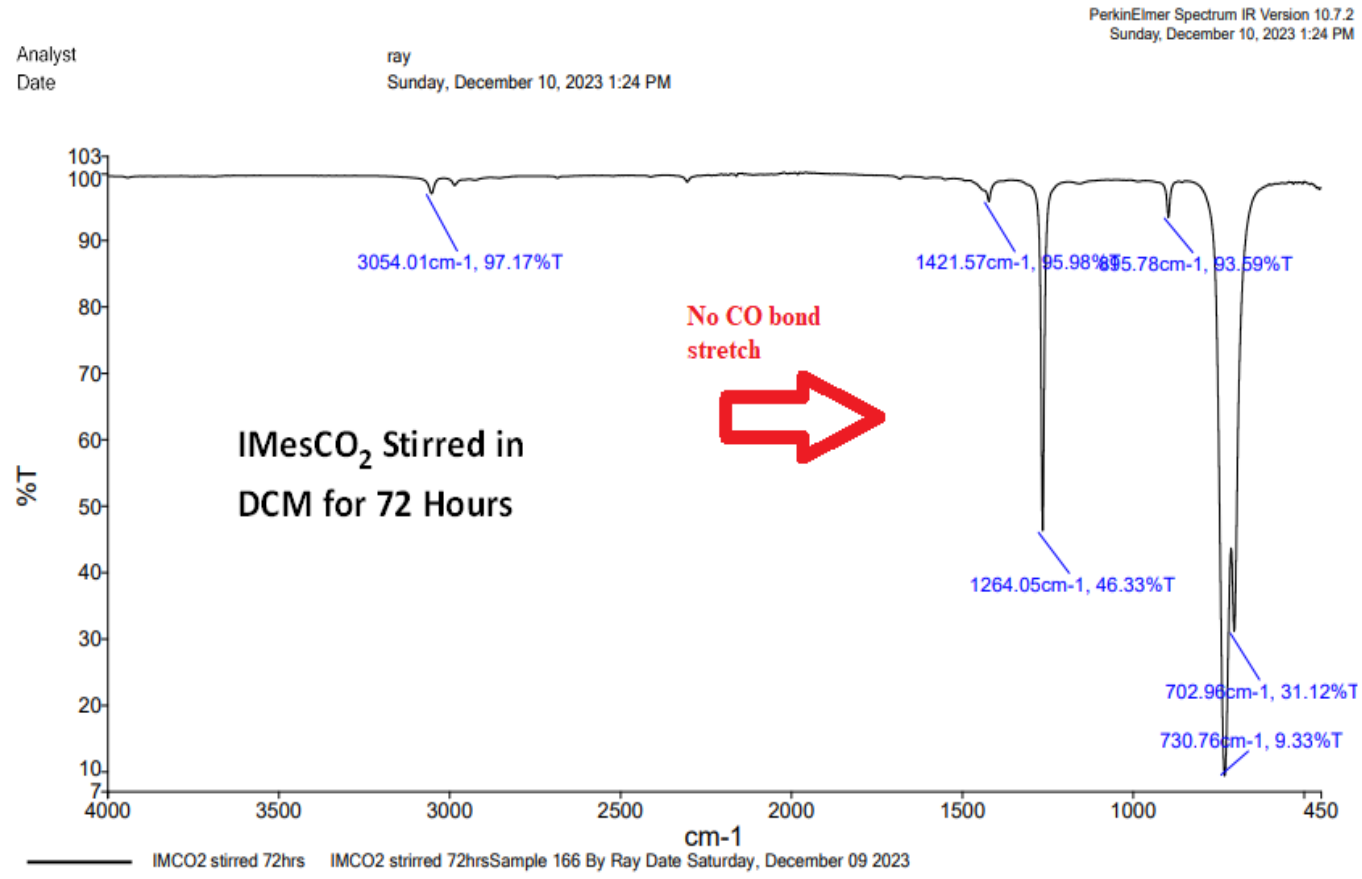

Figure 73. The IR Spectrum of the Product of IMes-CO_2 Stirred in DCM under N_2 for 72 Hours

In **Figure 73**, the CO IR stretch was not seen, thus indicating that IMes can slowly dissociate itself from IMes-CO_2 when not pressurized in a CO_2 background. Absence of the CO bond and no additional peak indicates that the CO_2 left the reaction system with no further reactions.

Multiple ^{1}H and ^{13}C NMR Spectra of IMes-CO_2 Reactions

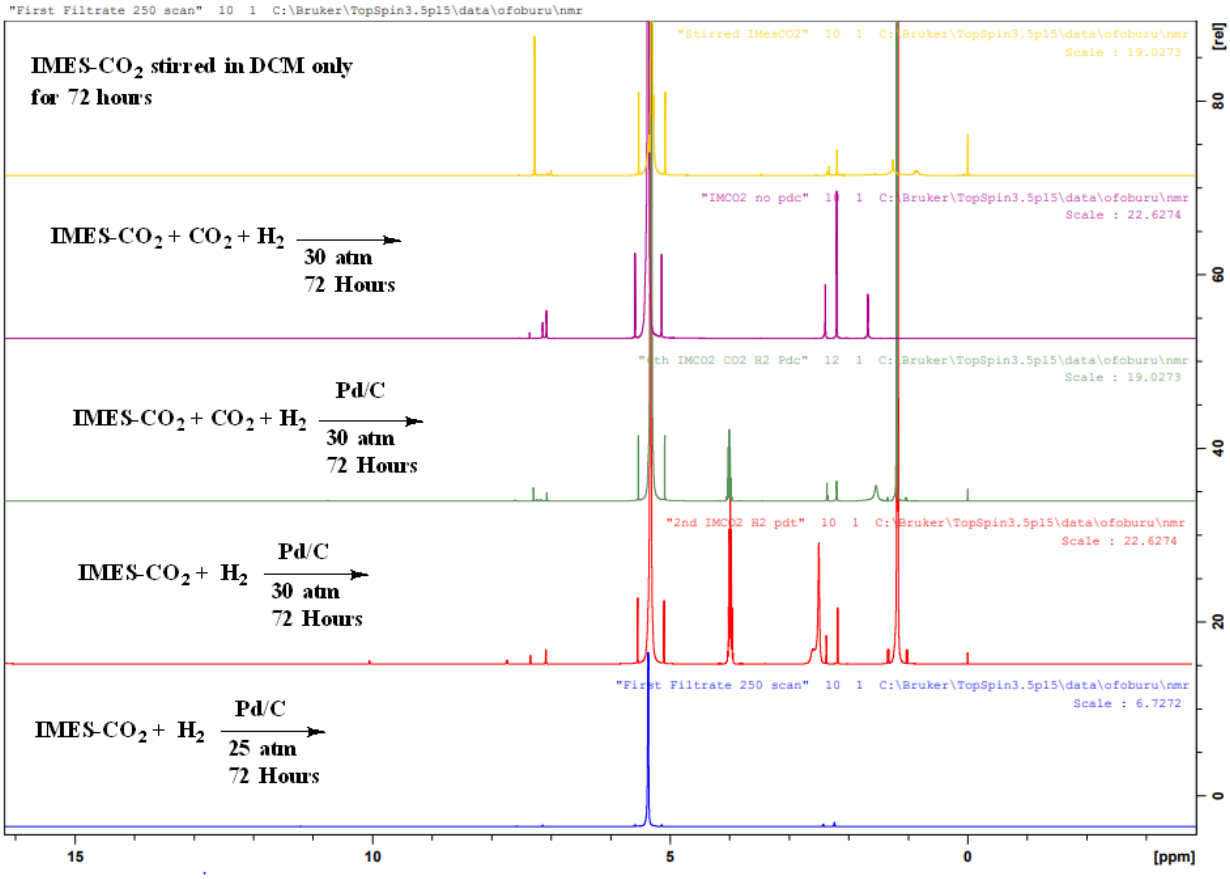

Figure 74. Multiple ^{1}H NMR Spectra Comparing products of IMes-CO_2 Reactions

The combined spectra in **Figures 74** and **75** compare the various peaks observed in ^{1}H and ^{13}C NMR spectra respectively of all the IMes-CO_2 reactions with and without the Pd/C catalyst.

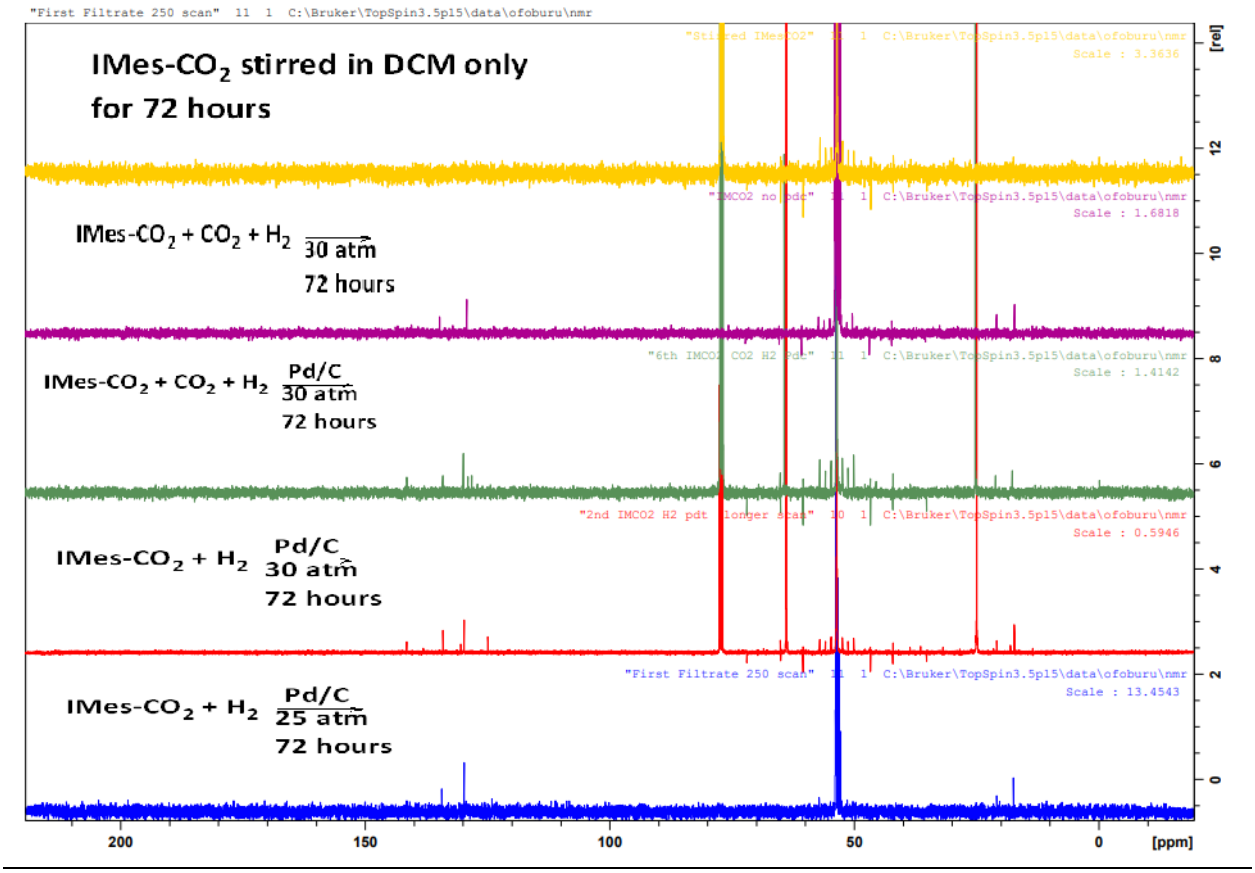

Figure 75. Multiple ^{13}C NMR Spectra Comparing Products of IMes-CO_2 Reactions

The H2 peak was seen in all reactions involving the Pd/C catalyst, but in the absence of the catalyst, the H2 hydrogen was not present. This confirms that the catalyst rehydrogenates the C2 carbon.

Chapter Five

Discussion and Conclusion

Synthesis of Bis-mesityl Imidazolium Carboxylate

We synthesized IMes-CO_2 frequently during this study, as each synthetic cycle only produced a 50 - 58% yield, just enough for one hydrogenation reaction. Nuclear magnetic resonance spectroscopy, infrared spectroscopy, thermogravimetric analysis, and mass spectrometry techniques were used to analyze and characterize the products. In confirming the synthesis of IMes-CO_2, the characteristic ^{13}C-NMR peak for the attached CO_2 at 153.46 ppm (**Figure 29)** was weak and barely resolvable above background but the IR and TGA results in **Figures 35 and 41,** respectively, were more convincing. **Figure 35** showed the presence of the characteristic C=O stretch at 1674.7 cm^{-1}, and **Figure 41** showed the onset of CO_2 release at about 155 ^oC as expected from the literature. Quantitatively, the synthetic yield was found to be highly dependent on the extent of IMes-Cl dissolution in toluene before the addition of KHMDS. Efforts to dissolve it by rigorously stirring for 72 hours and heating it in a water bath to about 80 ^oC for 2 hours still did not yield complete dissolution. Though most of our syntheses were productive, we did witness three unproductive syntheses where the supposed carbene solution remained clear and did not form any solids under CO_2 that would indicate formation of IMes-CO_2. Initially, the first two were thought to have resulted from contaminated CO_2 being supplied from an almost empty tank, but the third instance happened with a fresh LaserStar™ 5.0 gas cylinder, which is 99.999% pure. Therefore, purity of the CO_2 gas was not the issue. The NMR spectra obtained of the supposed carbene solution in **Appendix B,** showed peaks for the toluene solvent at 2.72 ppm, 7.52 ppm, 7.61 ppm, and 7.62 ppm, and the conjugate acid of KHMDS at 1.44 and 0.49 ppm, but nothing attributable to IMes-H, suggesting that the IMes-Cl did not dissolve enough to be

protonated by KHMDS and was filtered out completely on the Celite during the carbene filtration process**.**

Hydrogenation Reactions of Bis-mesityl Imidazolium Carboxylate

The transformation of carbon dioxide into useful products is certainly a complex process, depending on the versatility of the catalytic system and reaction conditions. The synthesized IMes-CO_2 underwent hydrogenation reactions at varying reaction conditions and some of its unique characteristics were discovered. Some of the products expected from these reactions include formic acid/formate, formaldehyde, methanol, bicarbonate, and oxalic acid, so their NMR and IR spectra were obtained and compared to those of the pressure vessel filtrates post reaction, after the Pd/C catalyst had been filtered out. During the direct reaction with hydrogen gas in the presence of a Pd/C catalyst, the pressurized IMes-CO_2 lost its CO_2, as the C=O bond stretch at 1675 cm^{-1} disappeared in the IR spectra in **Figures 50, 53,** and **68**, and the CO_2 peak at 153.46 ppm in the ^{13}C-NMR spectrum was also not present (**Figures 49, 52,** and **67)**. It appears that the Pd/C catalyst was able to break the C-C bond and rehydrogenated the C2 with one hydrogen, hence the reappearance of the H2 peak at 11.21 ppm, 10.05 ppm, and 10.76 ppm, along with the aromatic H4 peaks at 7.14 ppm, 7.08 ppm and 7.07 ppm, and the IMes methyl peaks at 2.42 ppm and 2.24 ppm, 2.37 ppm and 2.18 ppm, & 2.31 ppm and 2.20 ppm as seen in **Figures 48, 51,** and **66,** respectively. The released CO_2 probably escaped the reaction system and did not react with either the molecular hydrogen or the adsorbed hydrogen on the surface of the Pd/C catalyst, as no peak was seen above 150 ppm in their respective ^{13}C NMR spectra. Furthermore, when IMes-CO_2 was stirred alone in dichloromethane for 72 hours under N_2 gas, the ^{1}H NMR results obtained showed that the CO_2 adduct can break off from the adduct if there is no background pressure of CO_2 supplied to it, as seen in **Figure 72**. Using the ACD NMR predictor, it was found that if both of

the carbene electrons were separately rehydrogenated, saturating the C2 bonding and thus interrupting the imidazolium π-electron conjugation, the H2 peak would be expected to appear within the range of 5.43-4.83 ppm, which was not the case, thus confirming the regeneration of the IMes-H. Nonetheless, there were peaks around this range but they were identified as another compound present in the reaction.

At the end of all the reactions involving Pd/C catalyst, a signature for isopropanol was seen in their ^{1}H NMR spectra (**Figures 48, 51, 54,** and **66)**, with the characteristic H2 (1H, septet) peak at 4.0 -3.9 ppm, OH (1H, broad) at 2.77 - 2.50 ppm, and CH_3(6Hs, doublet) at 1.35-1.01 ppm. A control experiment was carried out by stirring Pd/C in dichloromethane alone for 72 hours, and the NMR results of the filtrate shown in **Figures 63** and **64** confirmed that isopropanol was not made from the reaction but was already present as a contaminant on the Pd/C catalyst. The catalyst is often fabricated by chemical reduction of aqueous Pd (II)Cl_2 in the presence of carbon powder; isopropanol must have been added as a sacrificial reducing agent, and some of the excess remained adsorbed on the carbon support.

The infrared and thermogravimetric results obtained after storing IMes-CO_2 for a period of four months under a vacuum showed that the compound can be stable when preserved under such conditions. The analytical results from the hydrogenation reactions of IMes-CO_2 have shown that IMes-CO_2 is generally unreactive at room temperature and 30 atm of H_2 pressure for up to 3 days. Moreover, the solvated adduct would slowly dissociate unless a background pressure of CO_2 was supplied. In Pd/C-catalyzed hydrogenation reactions, the C2-CO_2 bond of IMes-CO_2 is broken and the C2 is rehydrogenated, regenerating the imidazolium, as observed in the reappearance of the H2 peak position above 10 ppm in the ^{1}H-NMR spectrum. However, no further reduction occurred, as the H1 peak corresponding to the C=C double bond of the imidazole ring remained,

along with the aromatic and the IMes methyl peaks, and the spectroscopic signatures for CO_2 reduction products such as formate/formic acid, oxalate/oxalic acid, methanol, bicarbonate, and formaldehyde were not observed in their ^{13}C NMR results.

Nevertheless, the mesityl imidazolyl carbene demonstrated reversible uptake of CO_2 at ambient pressure and temperature, which could find application in a CO_2 adsorption cycle.

References

1. Davies. S. J.; Caldeira, K.; Mathews, H.D. *Science*. **2010**, *329*, 1330 – 1333.
2. Arrhenius, S. *Philosophical Magazine and Journal of Science*. **1896**, *41*, 237-276.
3. Cassia, R.; Nocioni, M.; Correa-Aragunde, N.; Lamattina, L. *Front. Plant Sci.* **2018**, *9*, 273.
4. Kiehl, J. T.; Trenberth, K. E. *Bulletin of the American Meteorological Society*. **1997**, *78*, 197-207.
5. Le Treut, H.; Somerville, R.; Cubasch, U.; Ding, Y.; Mauritzen, C.; Mokssit, A., Peterson, T.; Prather, M. *Historical Overview of Climate Change Science*. **2007**, 4.
6. Zhang, S.; Fan. Q.; Xia, R.; Meyer, T. J. *Acc. Chem. Res.* **2020**, *53*, 255-264.
7. Grondelle, R.V.; Boeker, E. *J. Phys. Chem.* **B2017**, *121*, 7229 -7234.
8. Berghout, N.; McCulloch, S. *International Energy Agency*. **2019**, Putting CO2 to use. Paris.
9. Ye, RP.; Ding, J.; Gong, W.; Morris, D.A.; Qin, Z.; Yujun, W.; Christopher, K.R.; Zhenghe, X.; Armistead, G.R.; Qiaohong, L.; Maohong, F.; Yuan-Gen, Y. *Nat. Commun*. **2019**, *10*, 1-15.
10. Randall, M.; Gerald, F. W. *Ind. Eng. Chem*. **1928**, *20*,1335-1340.
11. Muhammad, I.; Toma, N.G.; Oliver, C. K. *ChemSusChem.* **2011**, *4*, 300 – 316.
12. Anastas, P.; Eghbali, N. *Chem. Soc. Rev.* **2010**, *39*,301 -312.
13. Bai, S.; De-Smet, G.; Liao, Y.; Sun, R.; Zhou, C.; Beller, M.; Maes, B. U. W.; Sels, B.F. *Chem. Soc. Rev*. **2021**, *50*, 4259-4298.
14. Colin, F.; Sorcha, S.; Lesley, J.Y.; Jason, B.L. Chem. Commun. **2012**, *48*, 1392 -1399.

15. Li, C.; Negnevitsky, M.; Wang, X. *Energy Procedia*. **2019**, *160*, 324-331.

16. Ullmann's Encyclopedia of Industrial Chemistry.

17. Qu, R.; Junge, K.; Beller, M. *Chem. Rev.* **2023**, *123*, 1103-1165.

18. Sheng, Z.; Qun, F.; Rong, X.; Thomas, J. M. *Acc. Chem. Res*. **2020**, *53*, 1, 255.

19. Maryam, A.; Hossain, M. N.; Kraatz, H. B. *RSC Adv*. 2020, **10**, 38013.

20. Fairoosa, P.; Vishwas, G. C.; Kishore, N.; Rajenahally, V.J. *Catal. Sci. Technol*., 2**022**, *12*, 6623-6649.

21. Atsuki, Y.; Ryo, W.; Shigeki, K.; Yoshihito, K. Eur. *J. Inorg. Chem*. **2019**, 2375-2380.

22. Tominaga, K.; Sasaki, Y.; Kawai, M.; Watanabe, T.; Saito, M. J. *Chem. Soc., Chem. Commu.* **1993**, 629-631.

23. Schrock, R. R.; Osborn, J. A. *Chemical Communication*, **1970**, 567-568.

24. Wiedner, E. S.; Chambers, M. B.; Pitman, C. L. Bullock, R. M.; Miller, A. J. M.; Appel, A.M. *Chem. Rev*. **2016**, *116*, 8655-8692.

25. Ohkuma, T.; Ooka, H.; Hashiguchi, S.; Ikariya, T.; Noyori, R. *J. Am. Chem. Soc*. **1995**, *117*, 10417-10418.

26. Dub, P. A.; Ikariya, T. *ACS. Catal.* **2012**, *2*, 1718-1741.

27. Takao Ikariya. *Bull. Chem. Soc. Jpn*. **2011**, *84*,1, 1-16.

28. Milstein, D.; Gunanathan, C.; *Accounts of Chemical Research*. **2011**, *44*, 8, 588-602.

29. Deryn, E. F.; Eduardo, N. D. S. Coordination Chemistry Reviews. **2004**, *248*, 2365-2379.

30. Edward, S. R.; John, E. D.; Howard, J. H. *International Journal of Greenhouse Gas Control*. **2015**, *40*, 378-400.

31. Arduengo, A. J.; Rasika, D. H. V.; Harlow, R. L.; Kline, M. *J. Am. Chem. Soc.* **1992**, *114*, 5530-5534.

32. Arduengo, A. J.; Harlow, R. L.; Kline, M. *J. Am. Chem. Soc.* **1991**, *113*, 1, 361-363.

33. Arduengo, A. J.; Dixon, D. A. *J. Phys. Chem.* **1991**, *95*, 4180-4182.

34. Katritzky, A. R.; Ramsden, C. A.; Scriven, E. F.V. et al. *Elsevier*. **2008**, *1, 14. ed*. 1-13718.

35. Xi, N.; Huang, Q.; Liu, L. *Comprehensive heterocyclic Chemistry III*. **2008**, 143-364.

36. Verma, A.; Joshi, S.; Singh, D. *Journal of Chemistry*. **2013**, 12.

37. Santos, A. P.; Moreno, P. R. H. *Handbook of Natural Products*. **2013**, 6.

38. Gogineni, V.; Schinazi, R. F.; Hamann, M. T. *Chem Rev*. **2015**, *115(18)*, 9655-9706.

39. Zhong, J. *Nat. Prod. Rep.* **2016**, *33*, 1268-1317.

40. Bowdle, T.A.; Knutsen, L. J. S.; Williams, M. *Comprehensive medicinal Chemistry Elsevier*. **2007**, *2*, 351-367.

41. Voutchkova, M. A.; Feliz, M.; Clot, E.; Eisenstein, O.; Crabtree, R. H. *J. Am. Chem. Soc.* **2007,** *129, 42*, 12834-12846.

42. Connor, E. F.; Nyce, G. W.; Myers, M.; Mock, A.; Hedrick, J. L. *J. Am. Chem. Soc*. **2002**, *124*, *6*, 914–915.

43. Culkin, D. A.; Jeong, W.; Csihony, S.; Gomez, E. D.; Balsara, N. P.; Hedrick, J. L.; Waymouth, R. M. *Angew. Chem. Int. Ed*. **2007**, *46*, 2627-2630.

44. Duong, H. A.; Cross, M. J.; Louie, J. *Org Lett*. **2004**, *6*, *25*, 4679-4681.

45. Zhou, H.; Zhang, W.Z. et al. *J. Org. Chem*. **2008**, *73*, 8039 – 8044.

46. Tommasi, Immacolata.; Sorrentino, F. *Tetrahedron Letters*. **2005**, *46*, 2141-2145.

47. Ausdall, B. R. V.; Glass, J. L.; Wiggins, K. M.; Aarif, A. M, Louie, *J. Org. Chem.* **2009**, *74*, 7935-7942.

48. Liu, H.; Shi, L.; Zhang, Q.; Qi, P.; Zhao, Y.; Meng, Q.; Feng, X.; Wang, H.; Ye, J. *Chem. Commun*. **2021**, *57*, 1279-1294.

49. Tudose, A.; Demonceau, A.; Delaude, L. *J. Organomet. Chem*. **2006**, *691*, 5356-5365.

50. Solita Wilson, *Activation and Reduction of Carbon Dioxide Using Bis-Mesityl Imidazole Ylidene*, M. S. Thesis, Youngstown State University. **2019**, 26-36.

51. Nishimura, S. **2001**. *Handbook of Heterogeneous Catalytic Hydrogenation for Organic Synthesis.* United Kingdom, Wiley.

52. Zhenjun, M.; Haorui G.; Xufeng, L. *Catalysts.* **2021,** *11*, 1078.

53. Heck, R. F.; Nolley, J. P. *J. Org. Chem*., **1972**, *37*, 14.

54. Patti, A. Pedotti, S. *Tetrahedron*. **2010,** *66*, 5607-5611.

55. CHEMDraw Professional Application.

56. ACD NMR Predictor.

Appendix A

[1]H and [13]C NMR Spectra of Possible CO_2 Reduction Products.

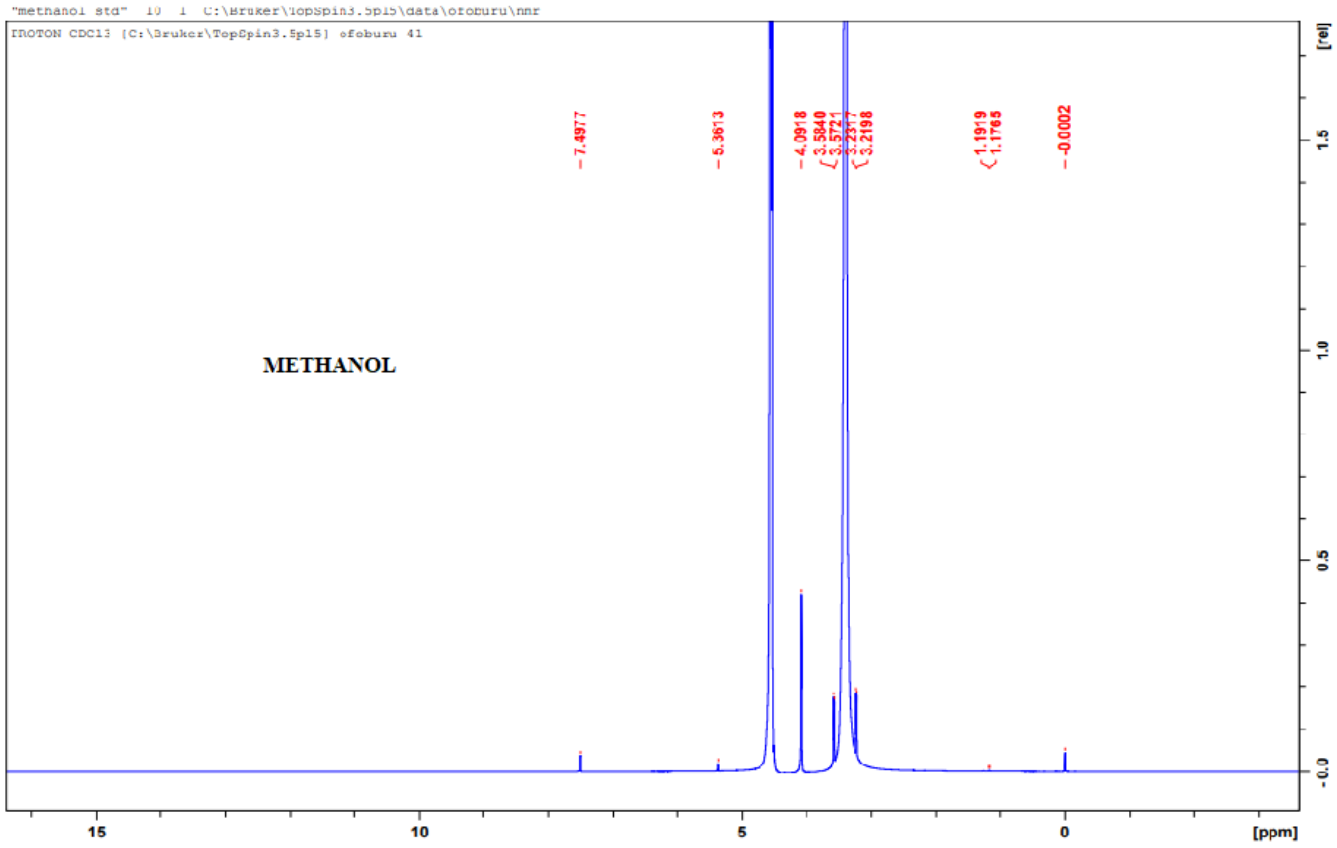

The [1]H NMR Spectrum of Methanol Standard

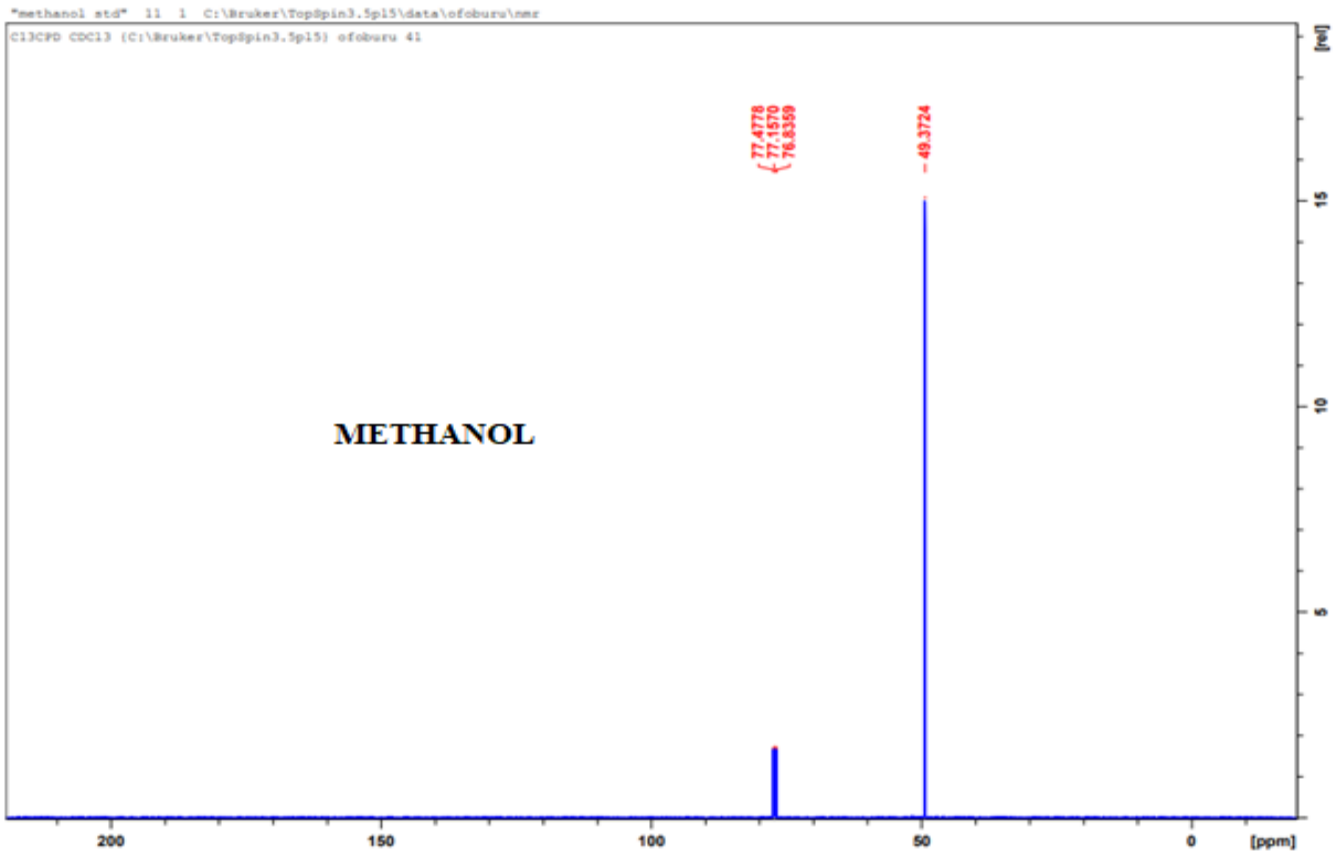

The ^{13}C NMR Spectrum of Methanol Standard

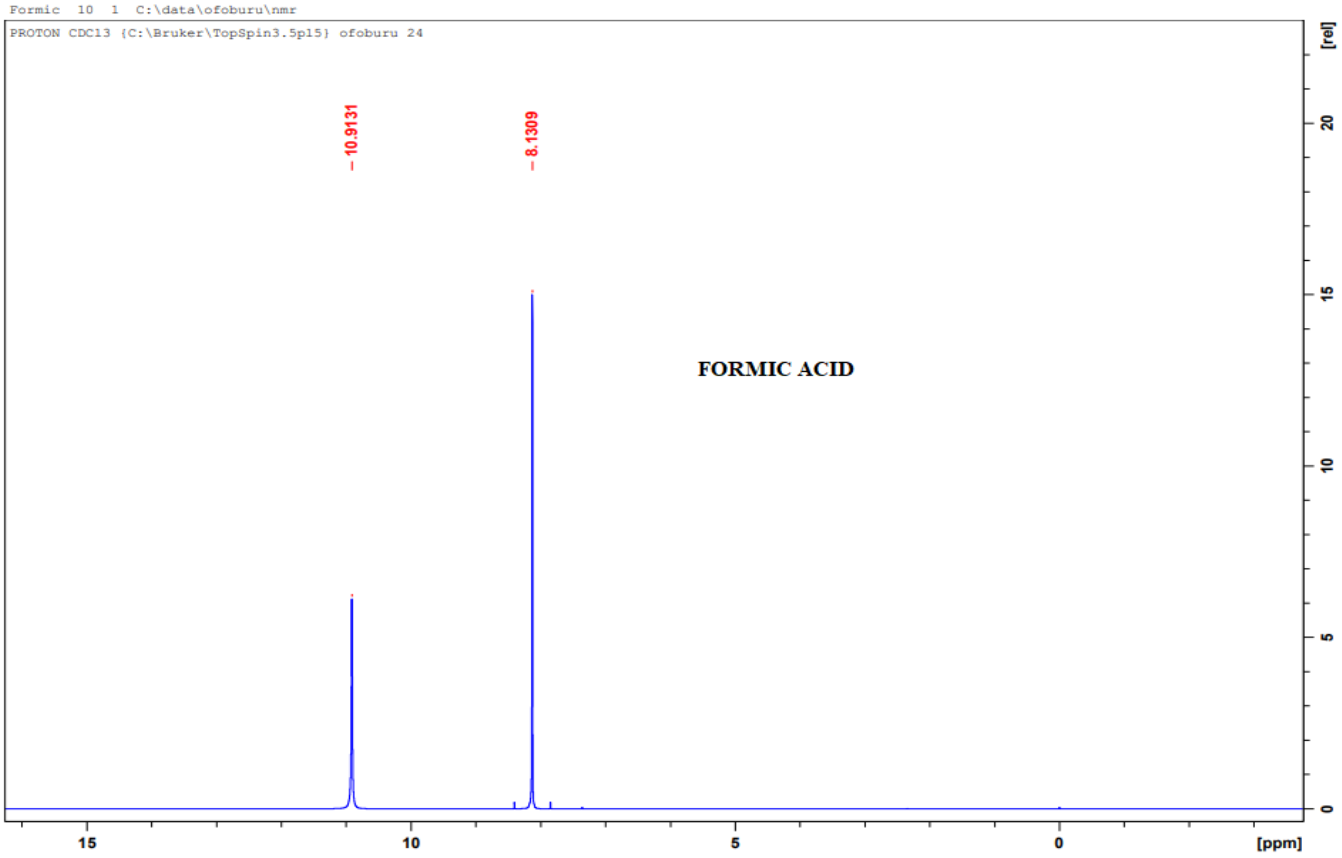

The ^{1}H NMR Spectrum of Formic acid Standard

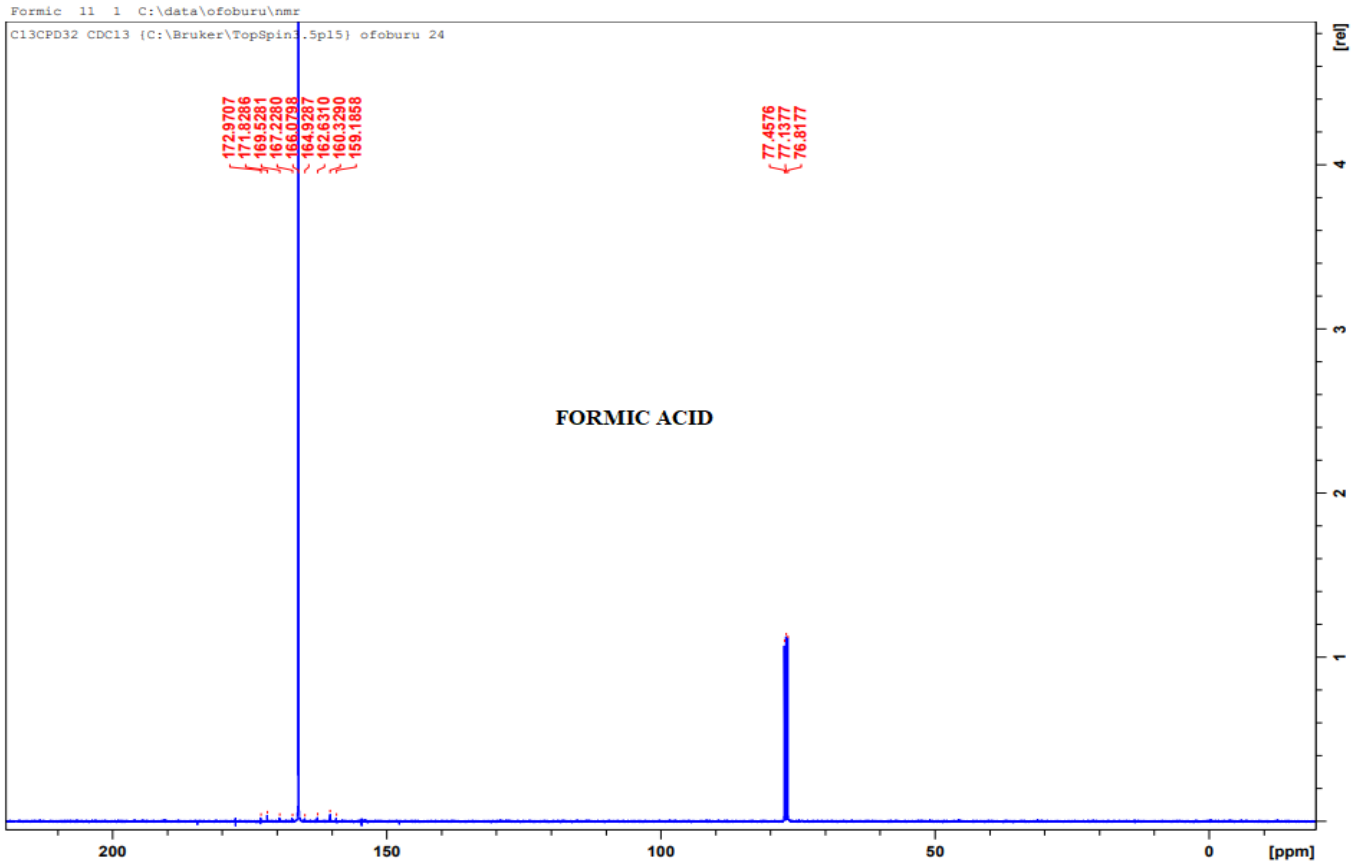

The ^{13}C NMR Spectrum of Formic acid Standard

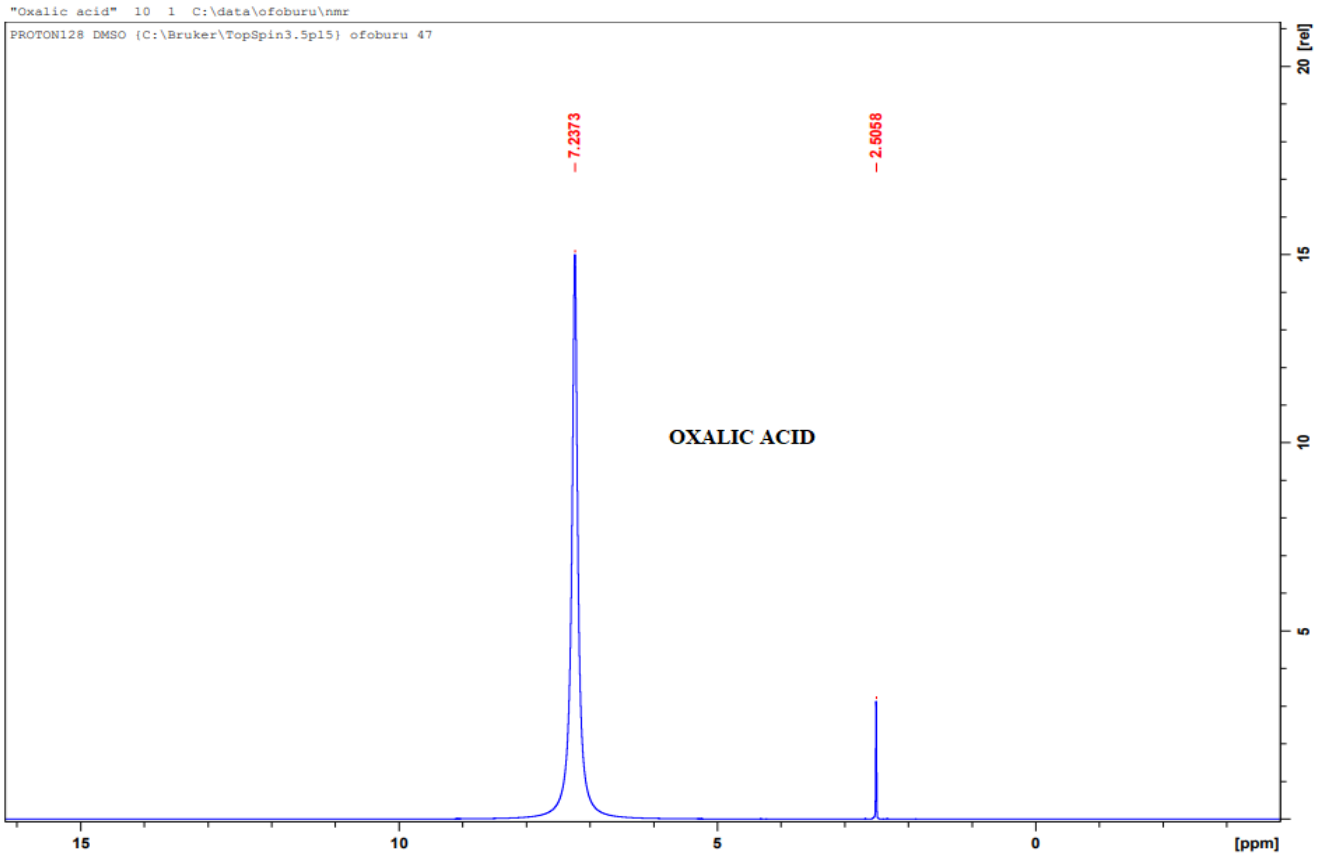

The ^{1}H NMR Spectrum of Oxalic acid Standard

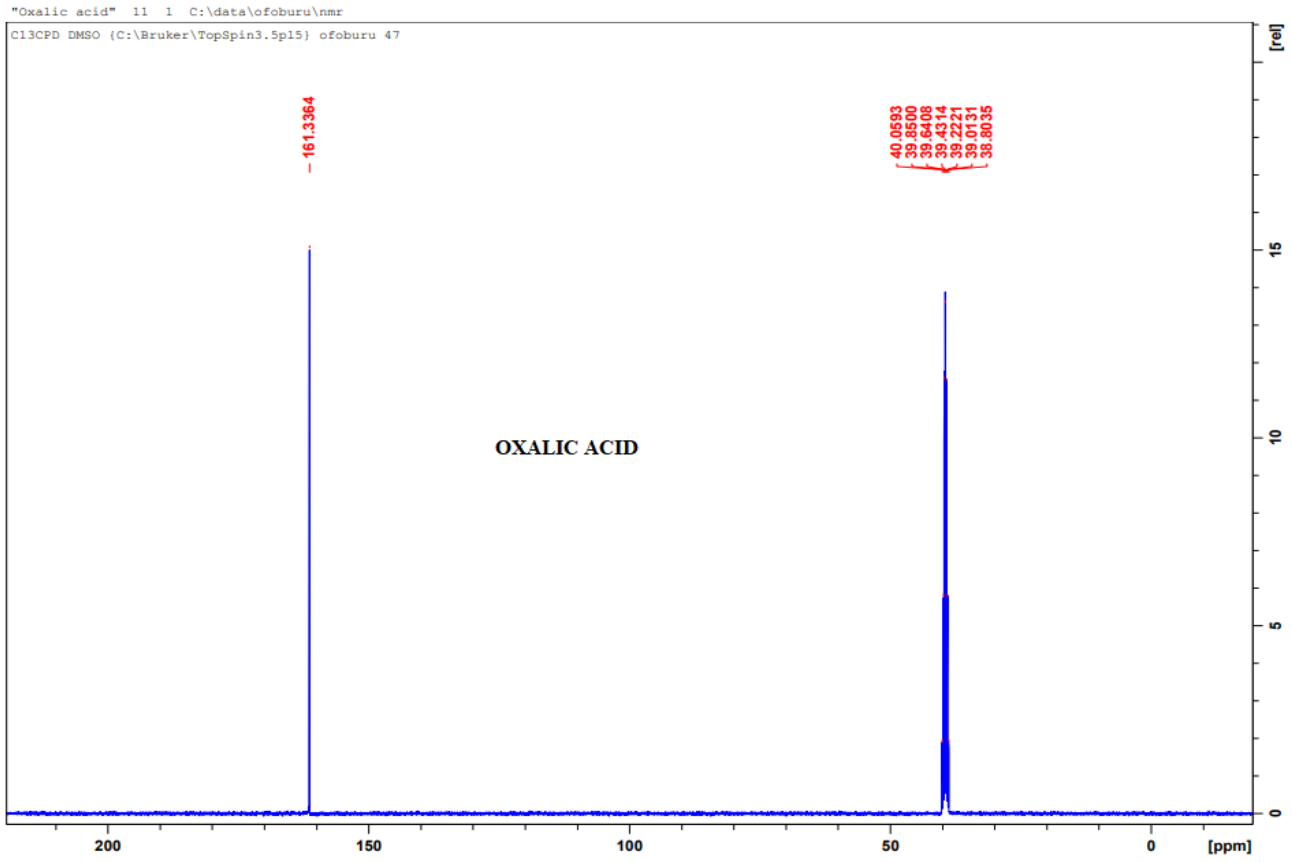

The ^{13}C NMR Spectrum of Oxalic acid Standard

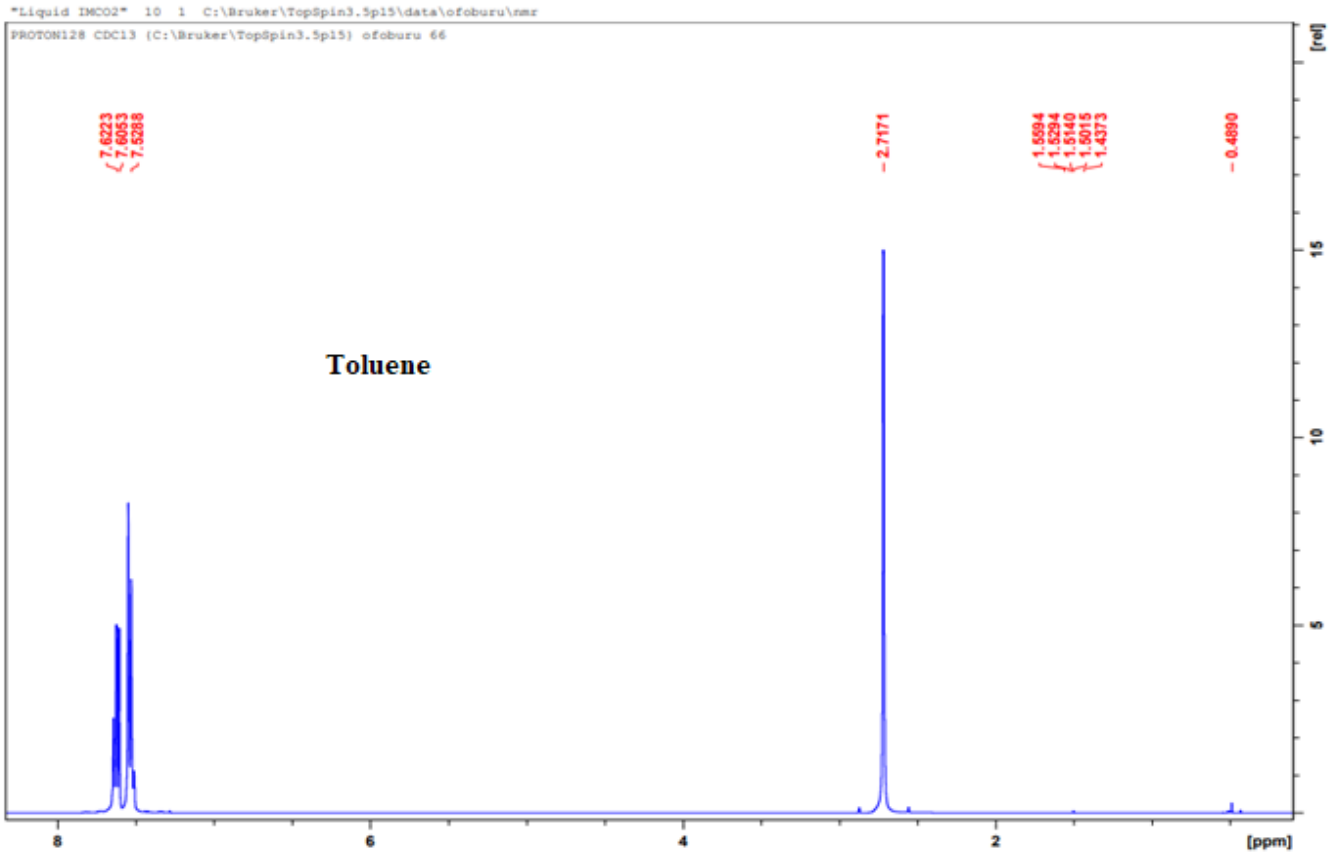

The ^{1}H NMR Spectrum of the Toluene Filtrate that Failed IMes- CO_2 Synthesis

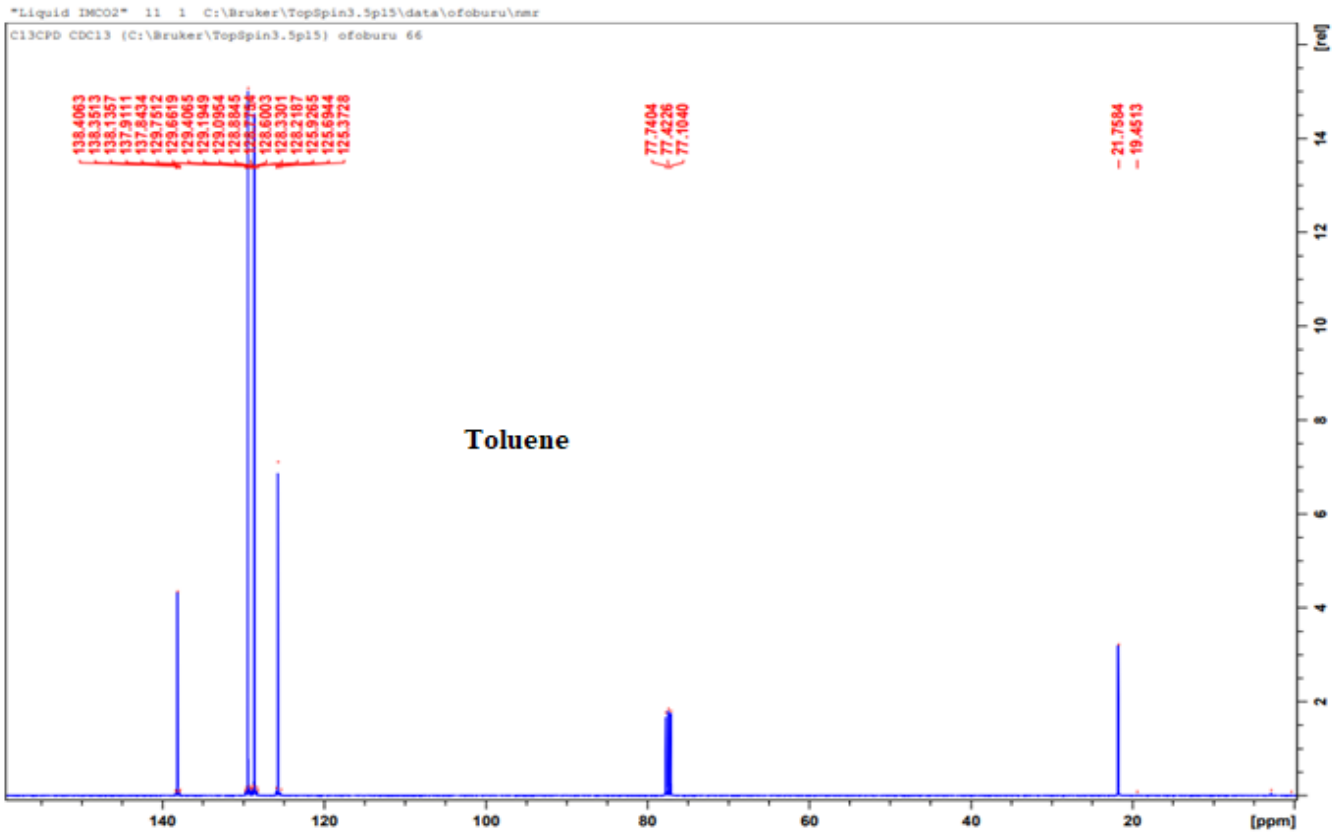

The ^{13}C NMR Spectrum of the Toluene Filtrate that Failed IMes- CO_2 Synthesis

Appendix B

COSY NMR, HSQC NMR and Extra NMR Spectra of Product of Synthesis.

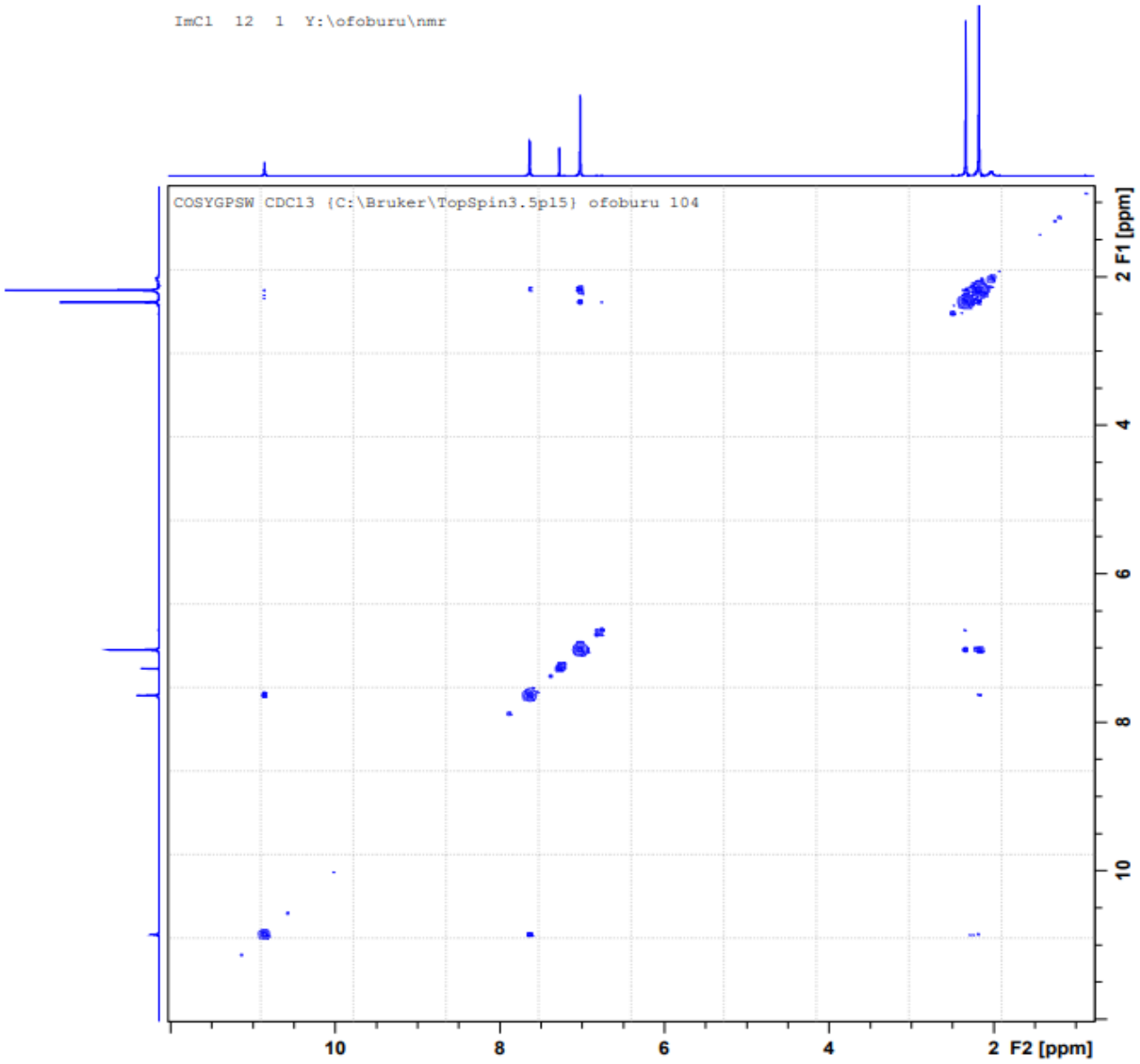

The COSY NMR Spectrum of 1,3-bis (2,4,6-trimethyl-phenyl) Imidazolium Chloride

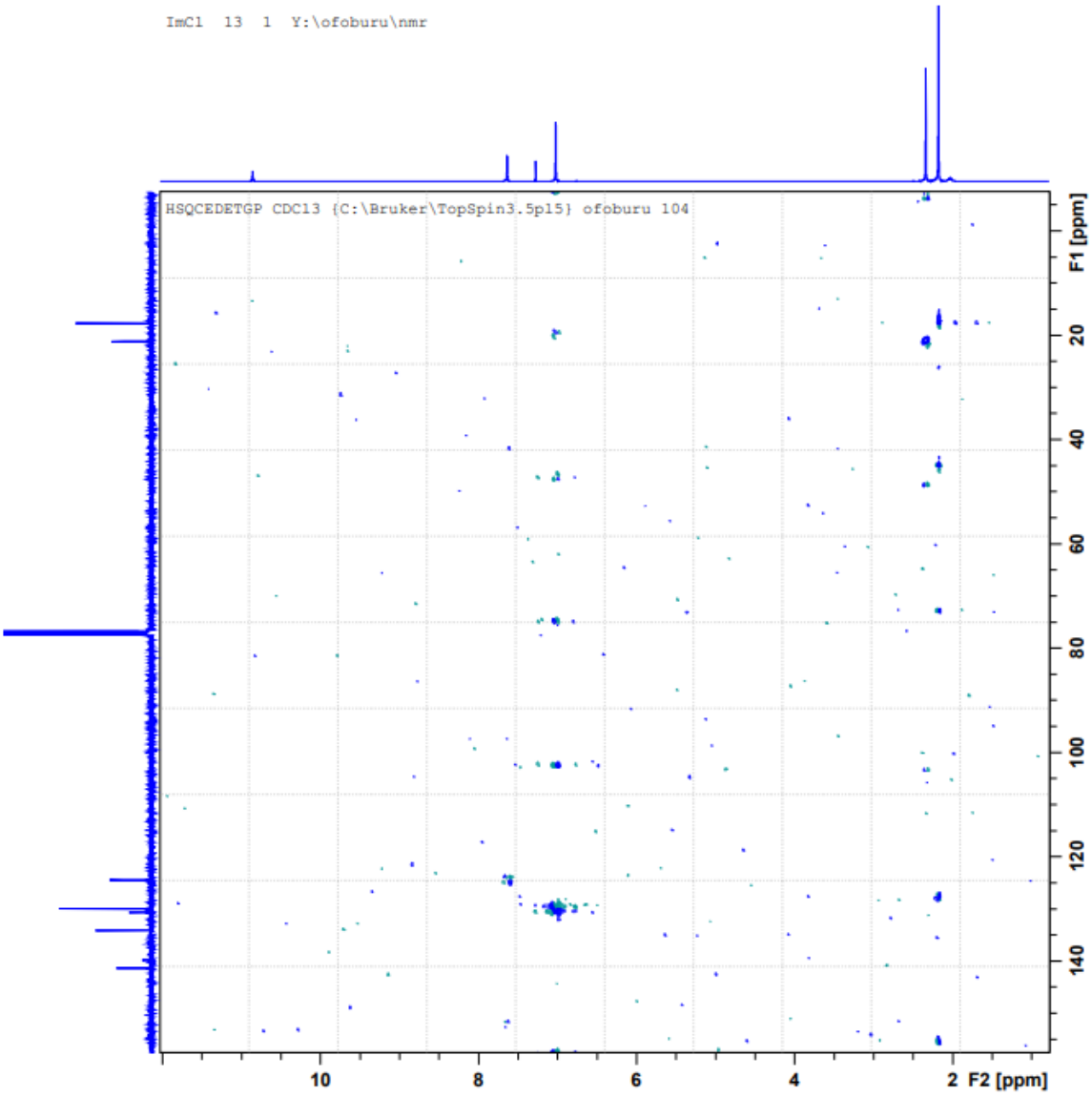

The HSQC NMR Spectrum of 1,3-bis (2,4,6-trimethyl-phenyl) Imidazolium Chloride

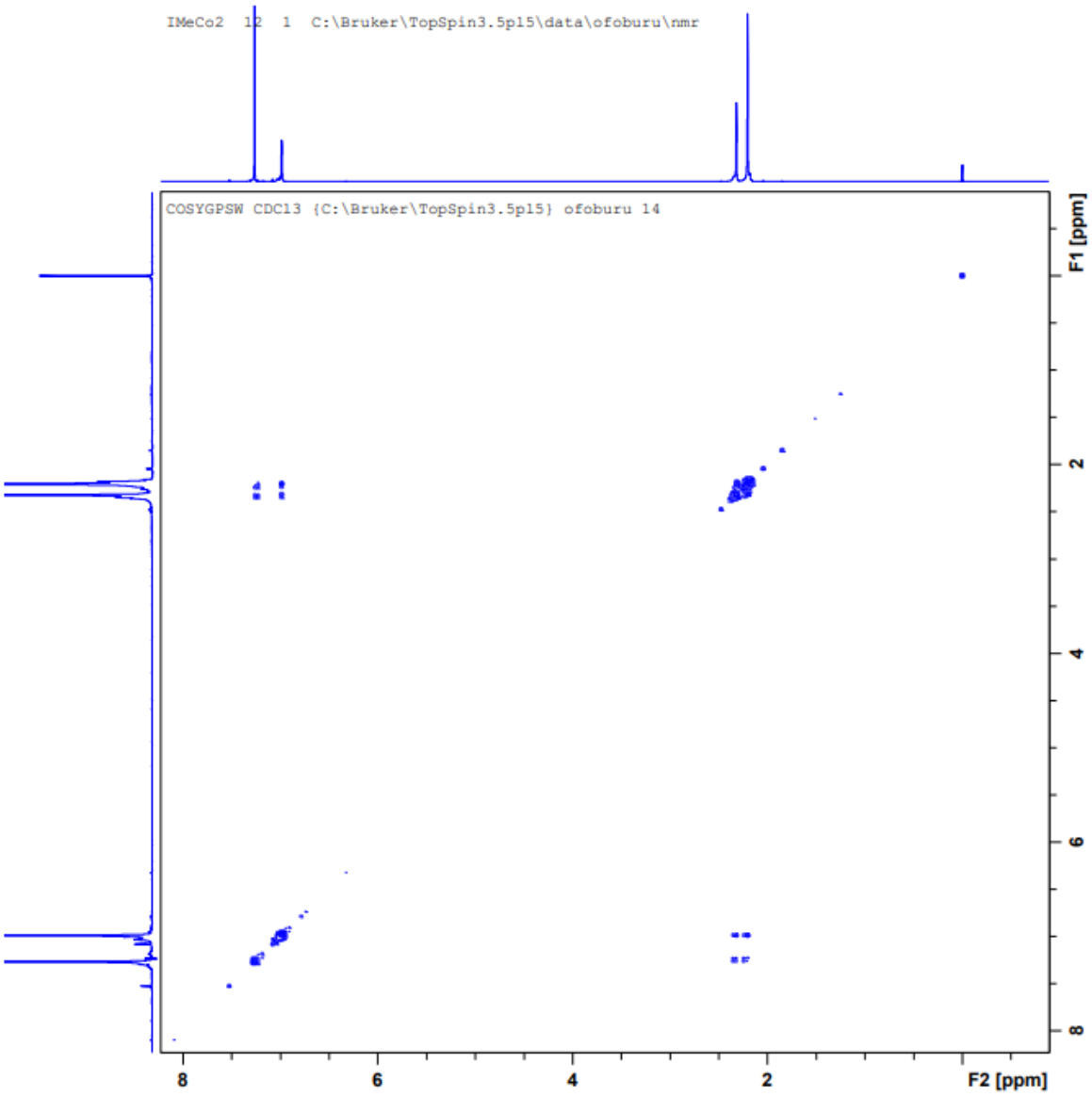

The COSY NMR Spectrum of 1,3-bis (2,4,6-trimethyl-phenyl) Imidazolium Carboxylate

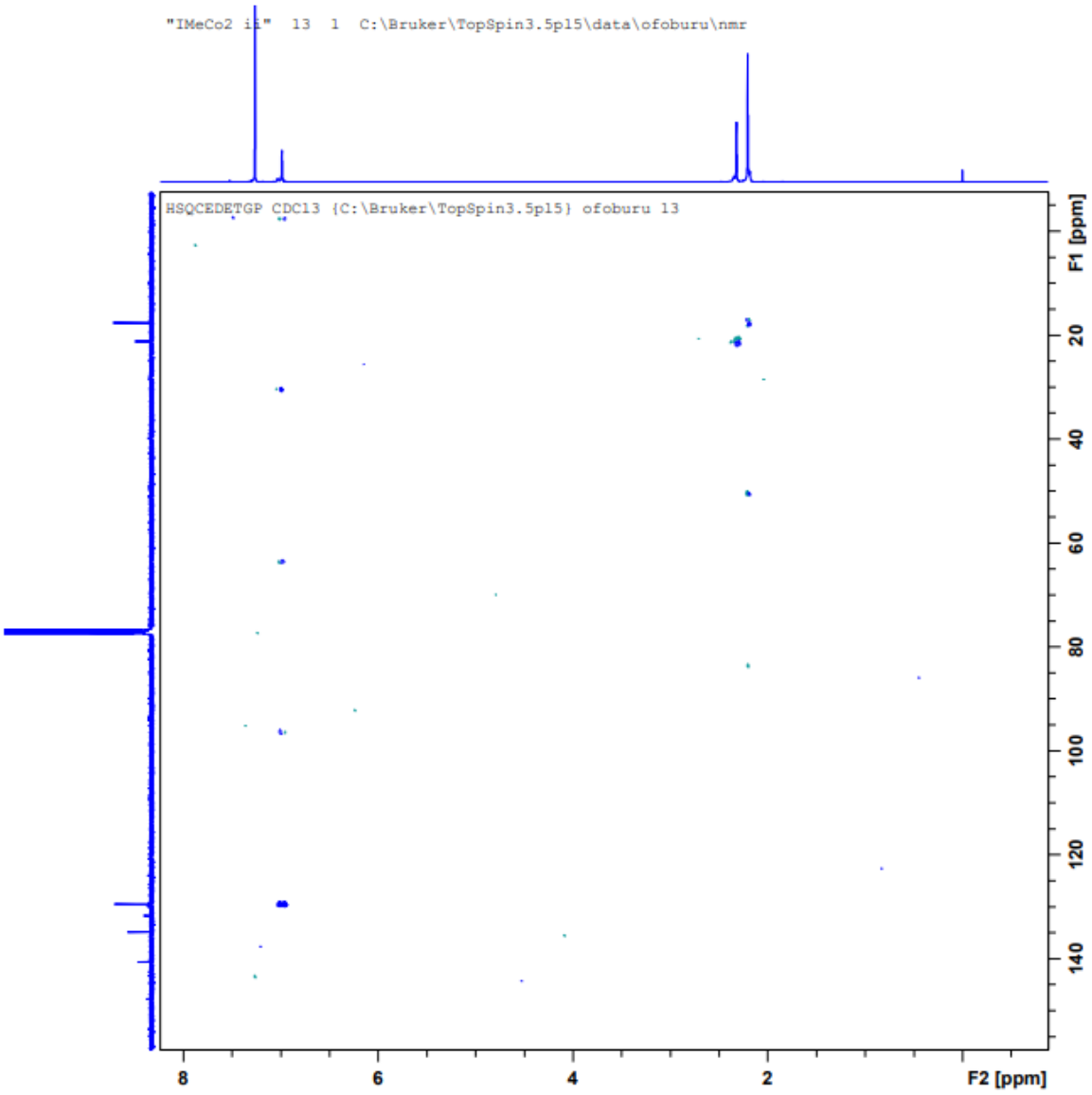

The HSQC NMR Spectrum of 1,3-bis (2,4,6-trimethyl-phenyl) Imidazolium Carboxylate

Appendix C

COSY NMR, HSQC NMR and Extra NMR Spectra of Hydrogenation Products

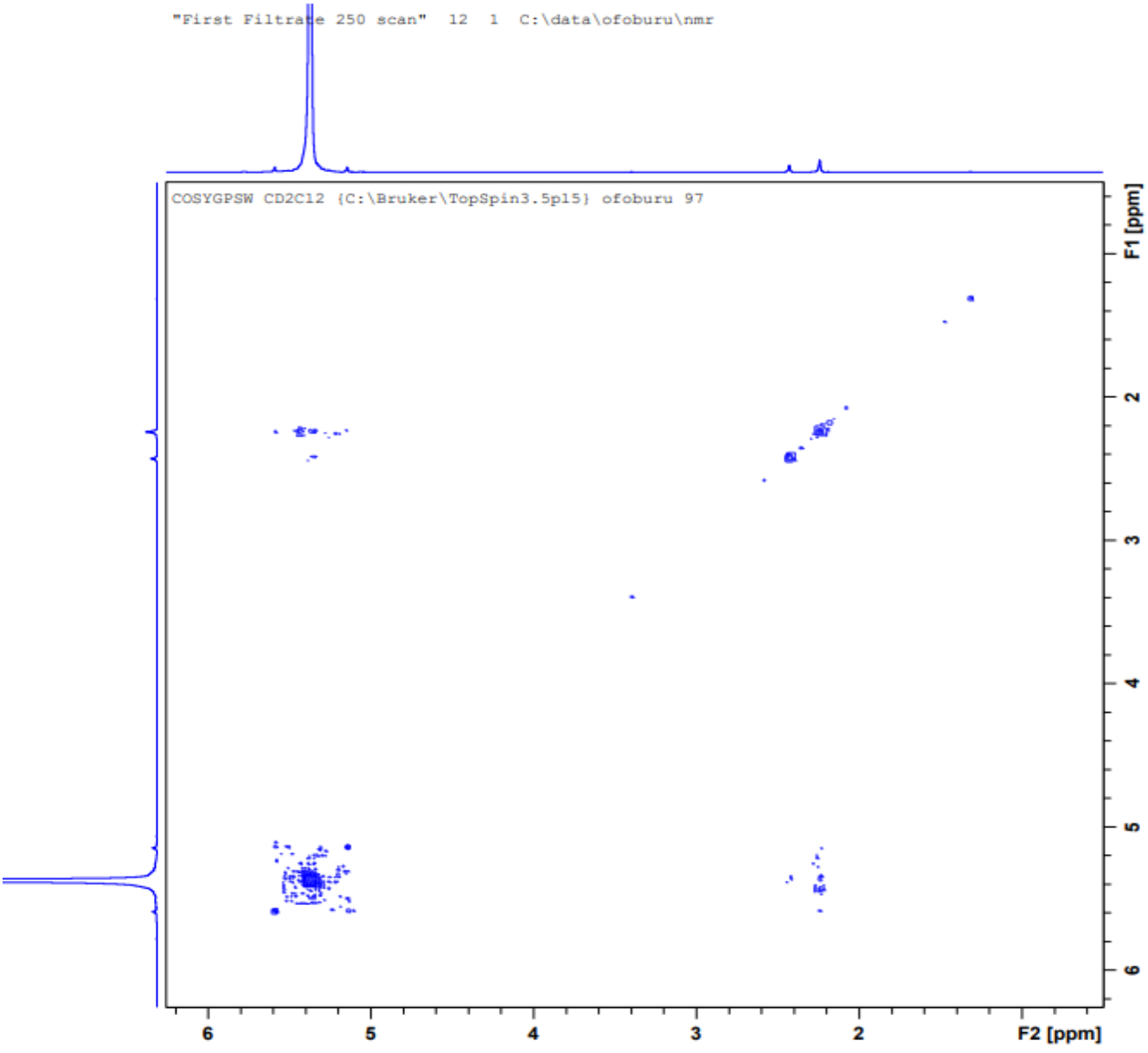

The COSY NMR Spectrum of the Product of IMes-CO_2 + H_2 at 25 Atm after 72 Hours

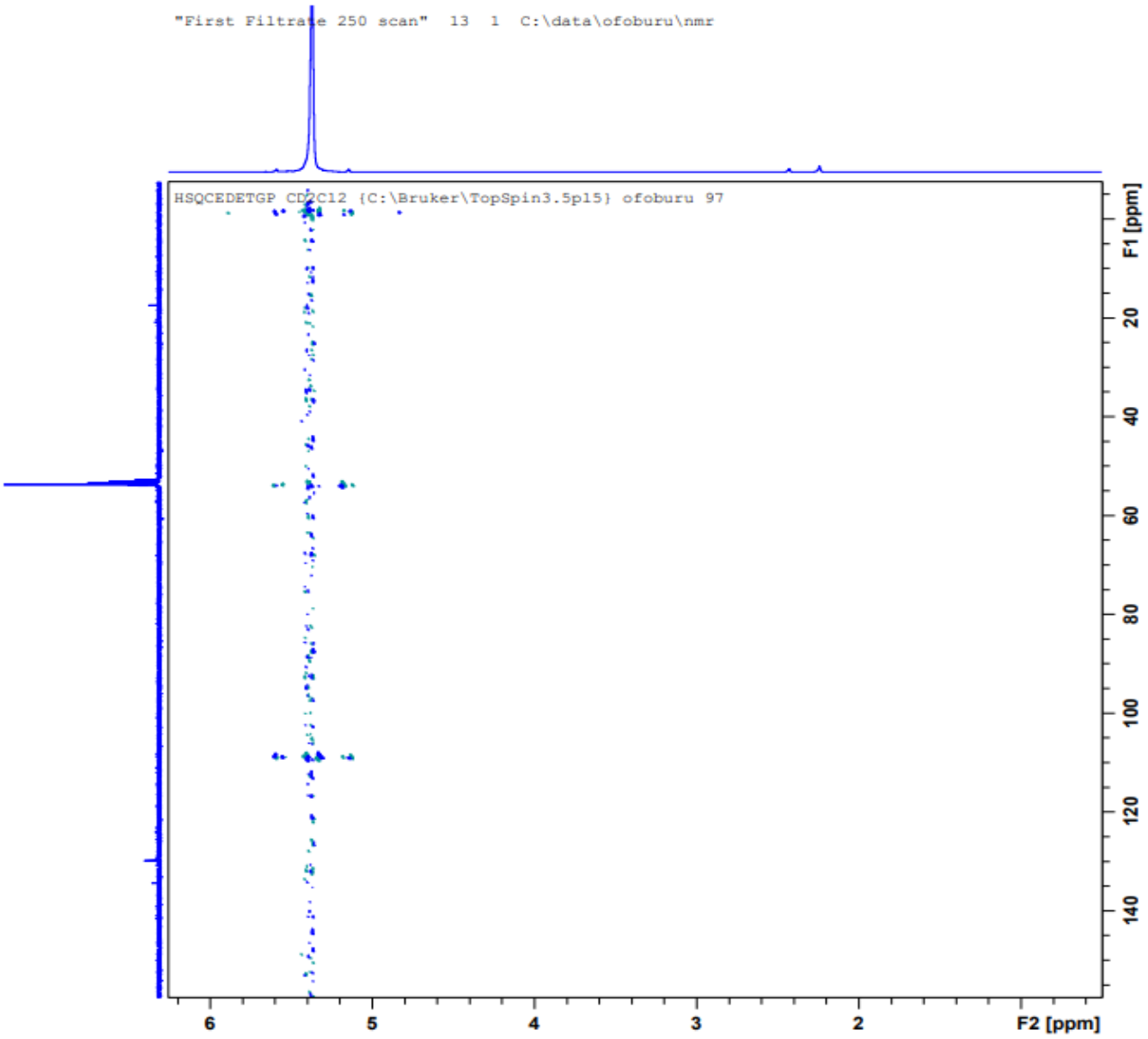

The HSQC NMR Spectrum of the Product of IMes-CO_2 + H_2 at 25 Atm after 72 Hours

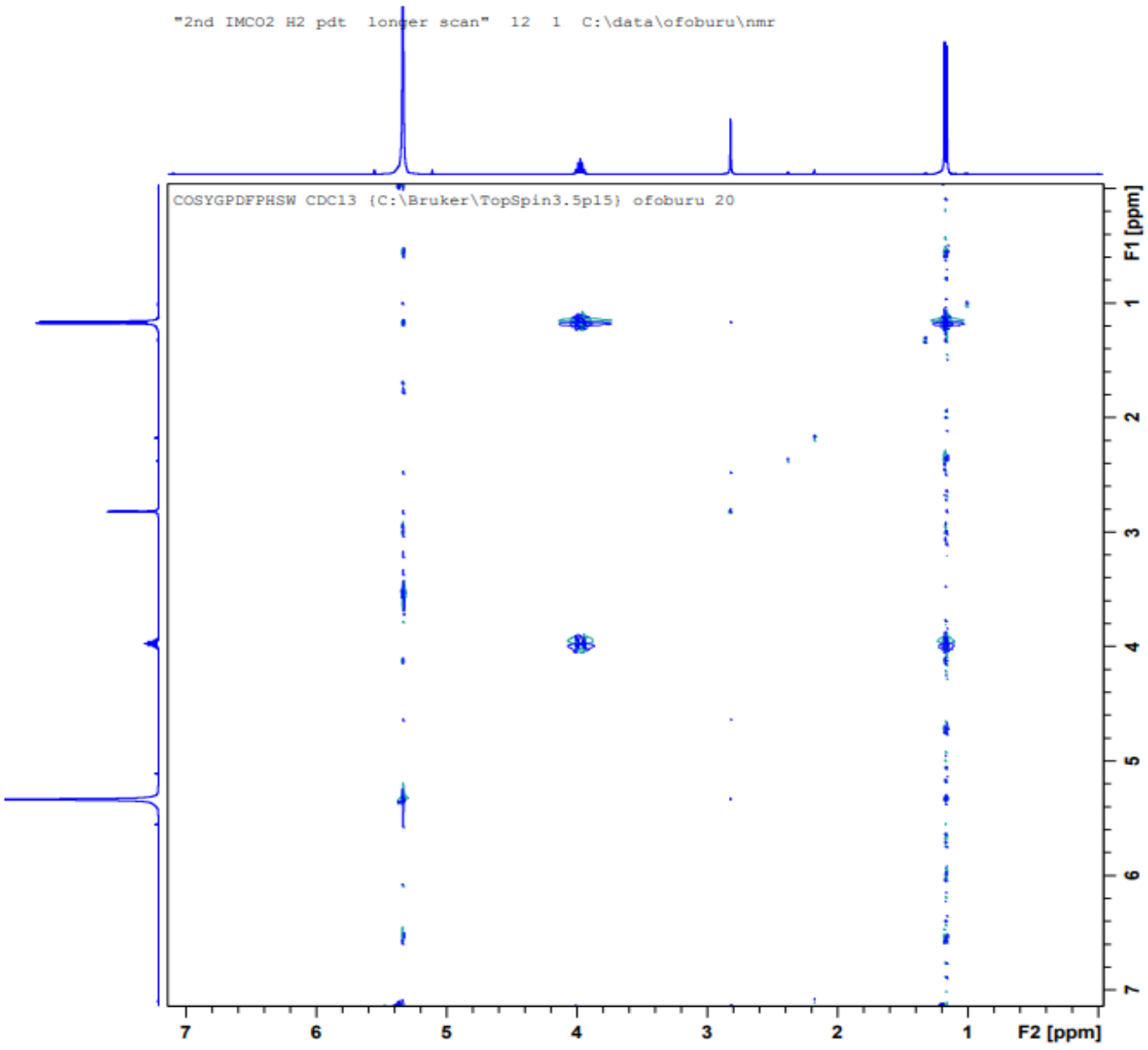

The COSY NMR Spectrum of Product of IMes-CO_2 + H_2 at 30 Atm after 72 Hours

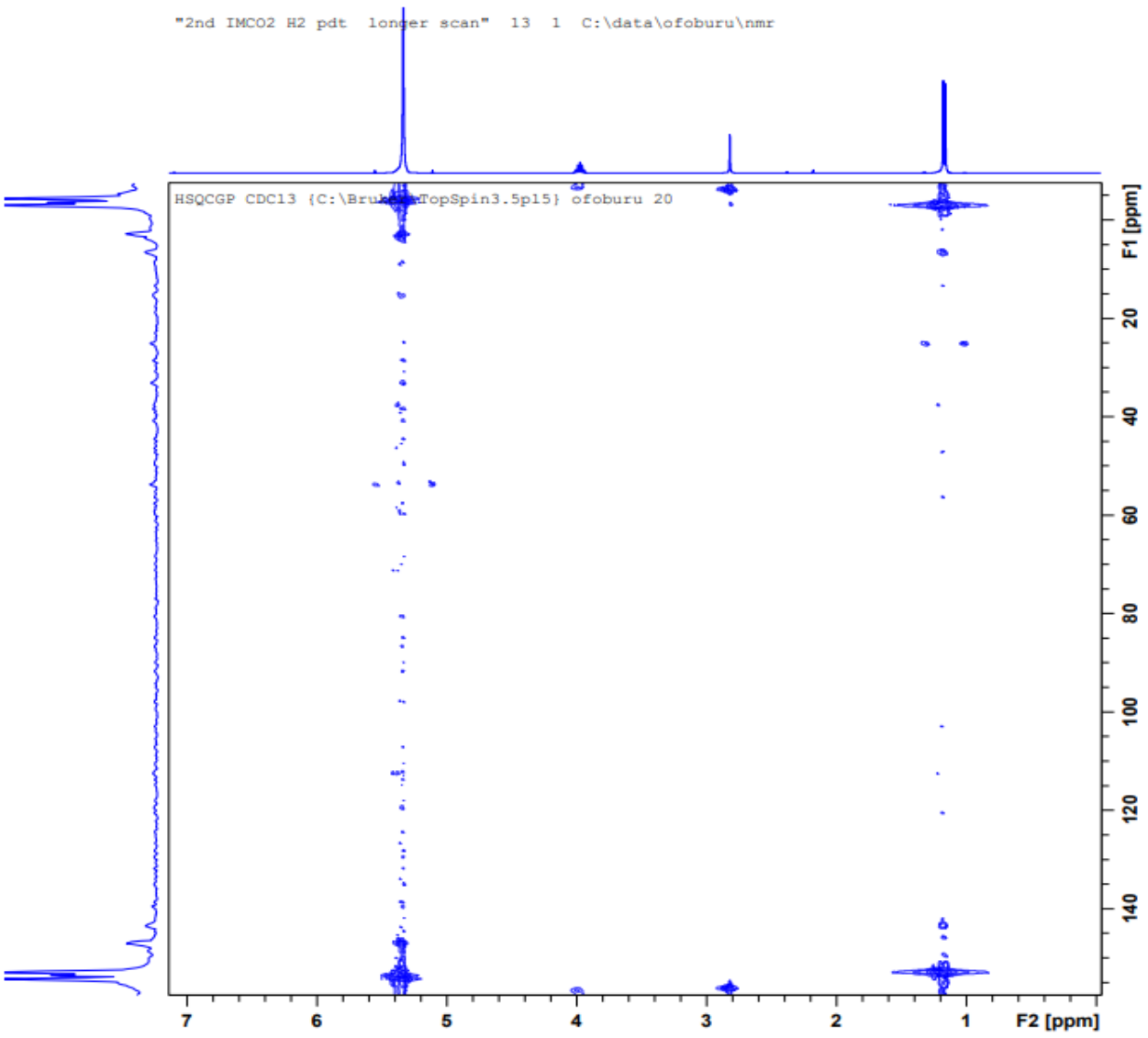

The HSQC NMR Spectrum of Product of IMes-CO_2 + H_2 at 30 Atm after 72 Hours

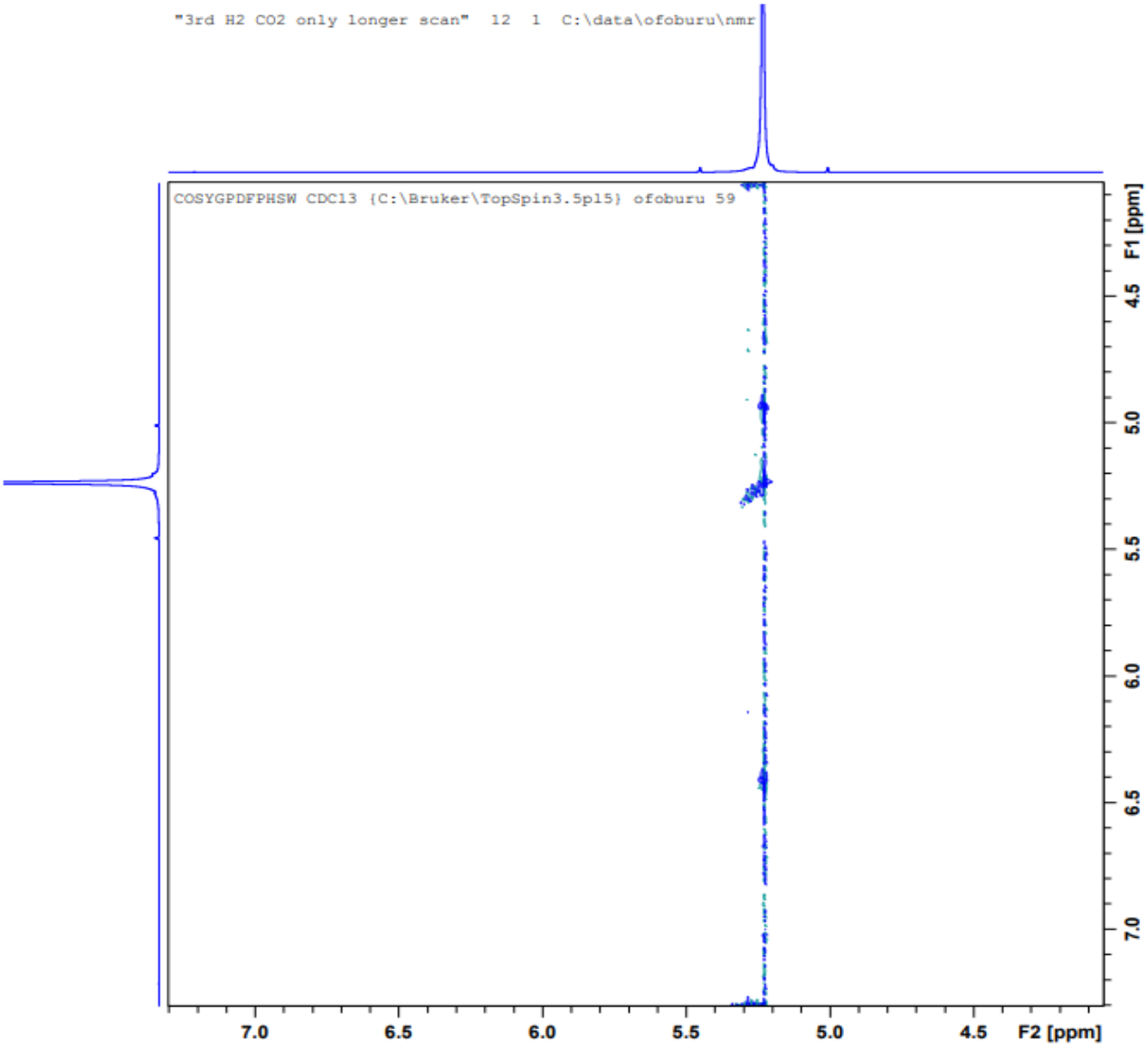

The COSY NMR Spectrum of Product of Uncatalyzed CO_2 + H_2 at 30 Atm after 72 Hours

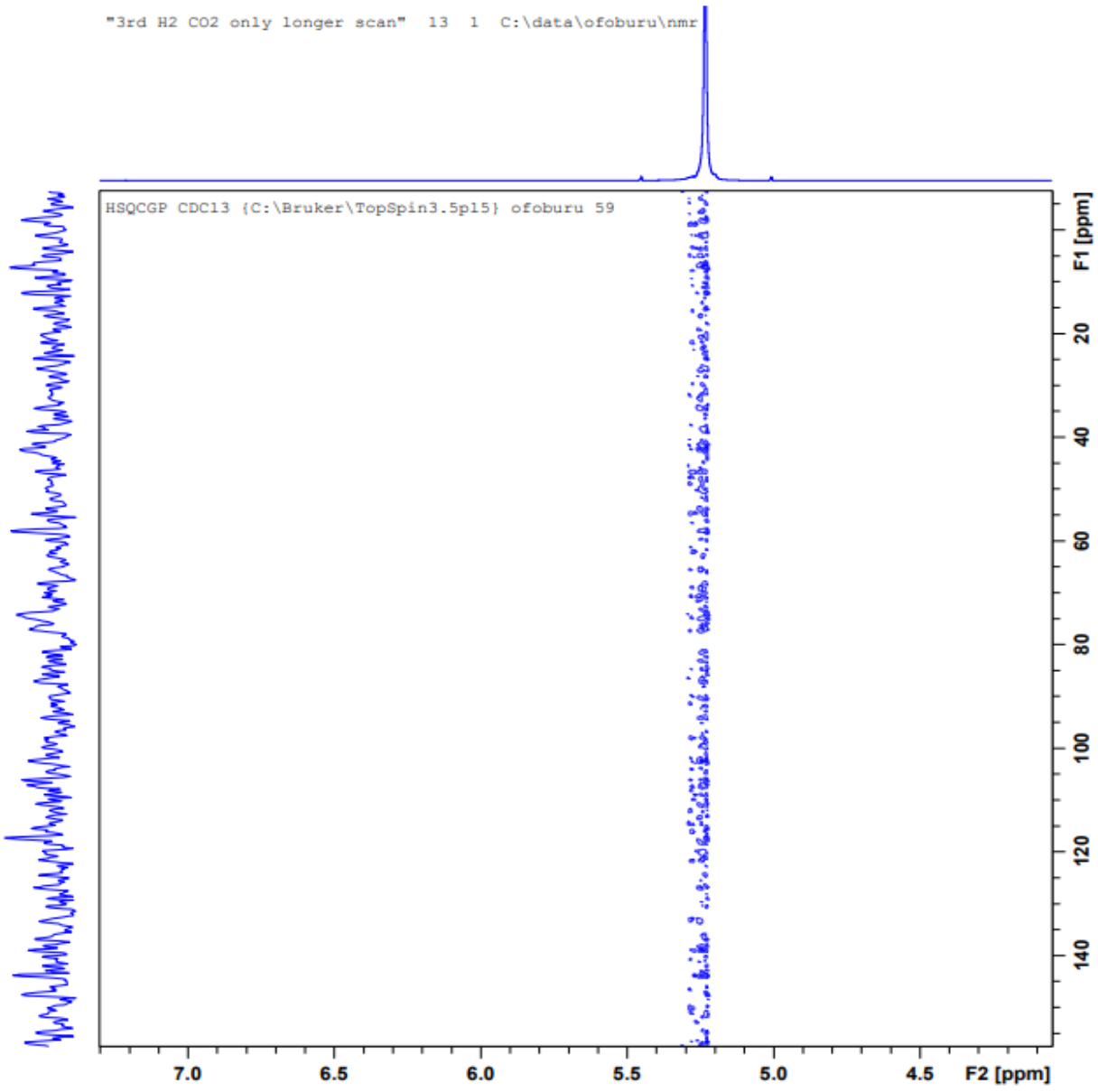

The HSQC NMR Spectrum of Product of CO_2 + H_2 at 30 Atm after 72 Hours

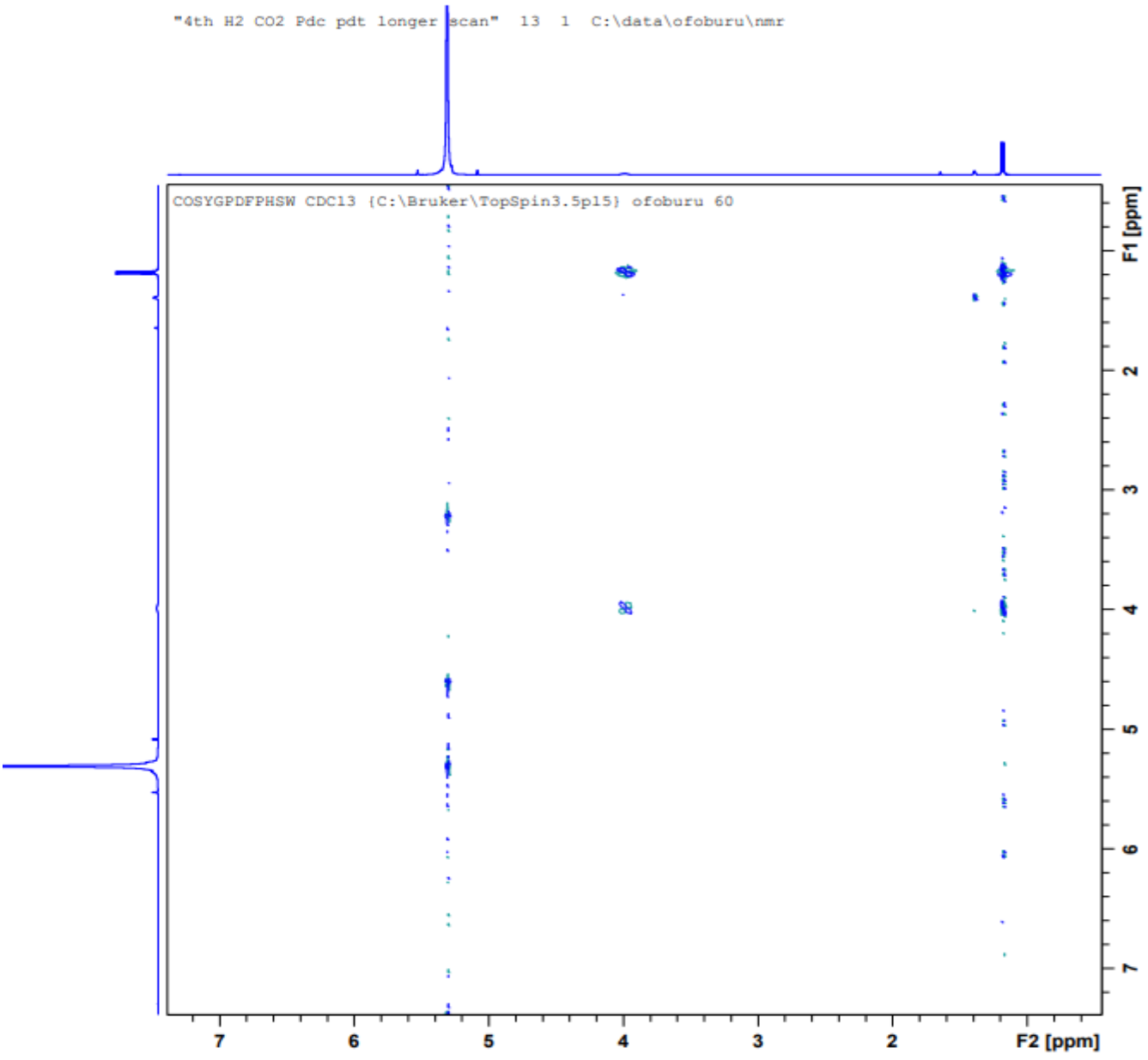

The COSY NMR Spectrum of Pd/C Catalyzed CO_2 + H_2 at 30 Atm after 24 Hours

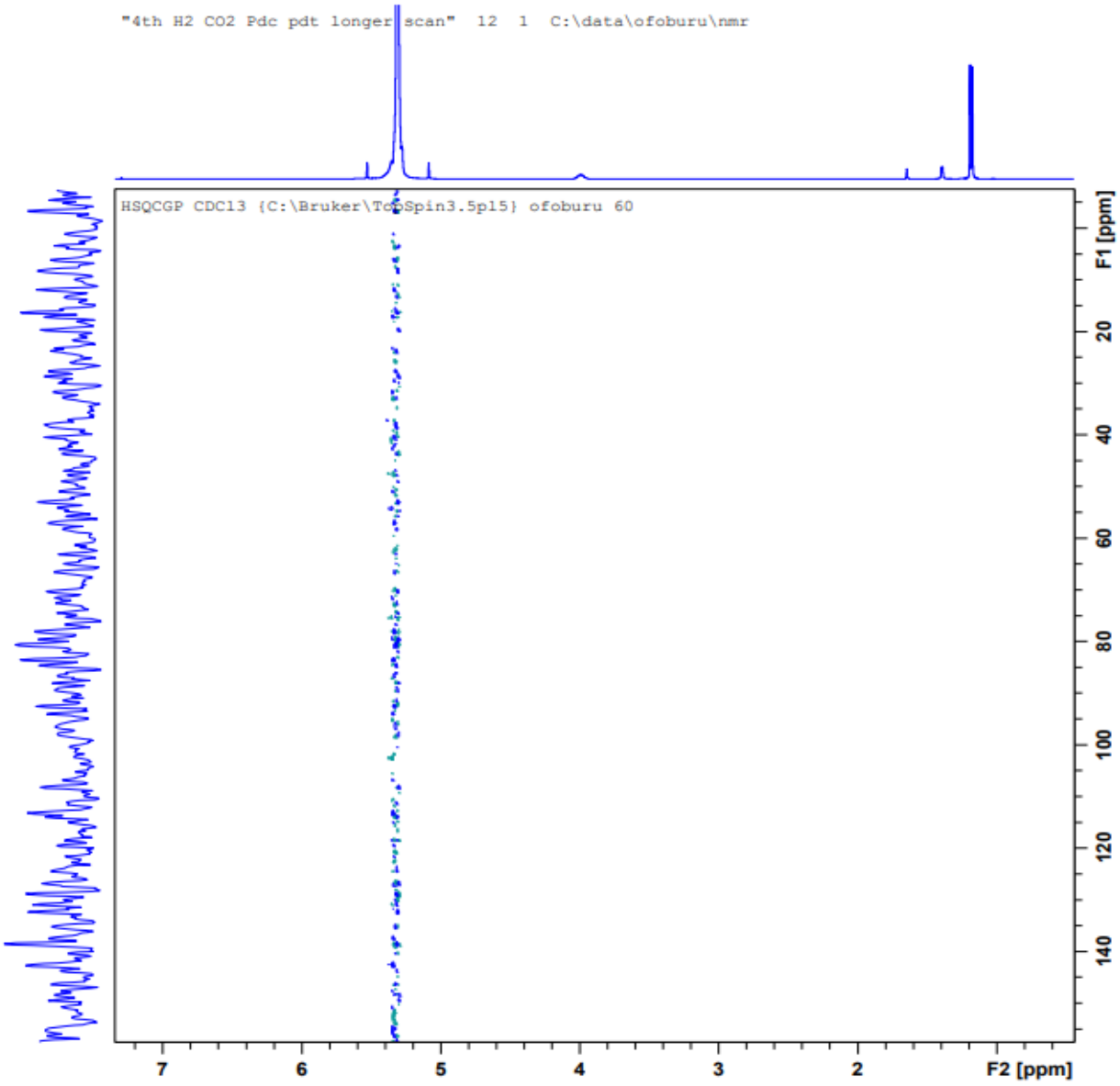

The HSQC NMR Spectrum of Pd/C Catalyzed CO_2 + H_2 at 30 Atm after 24 Hours

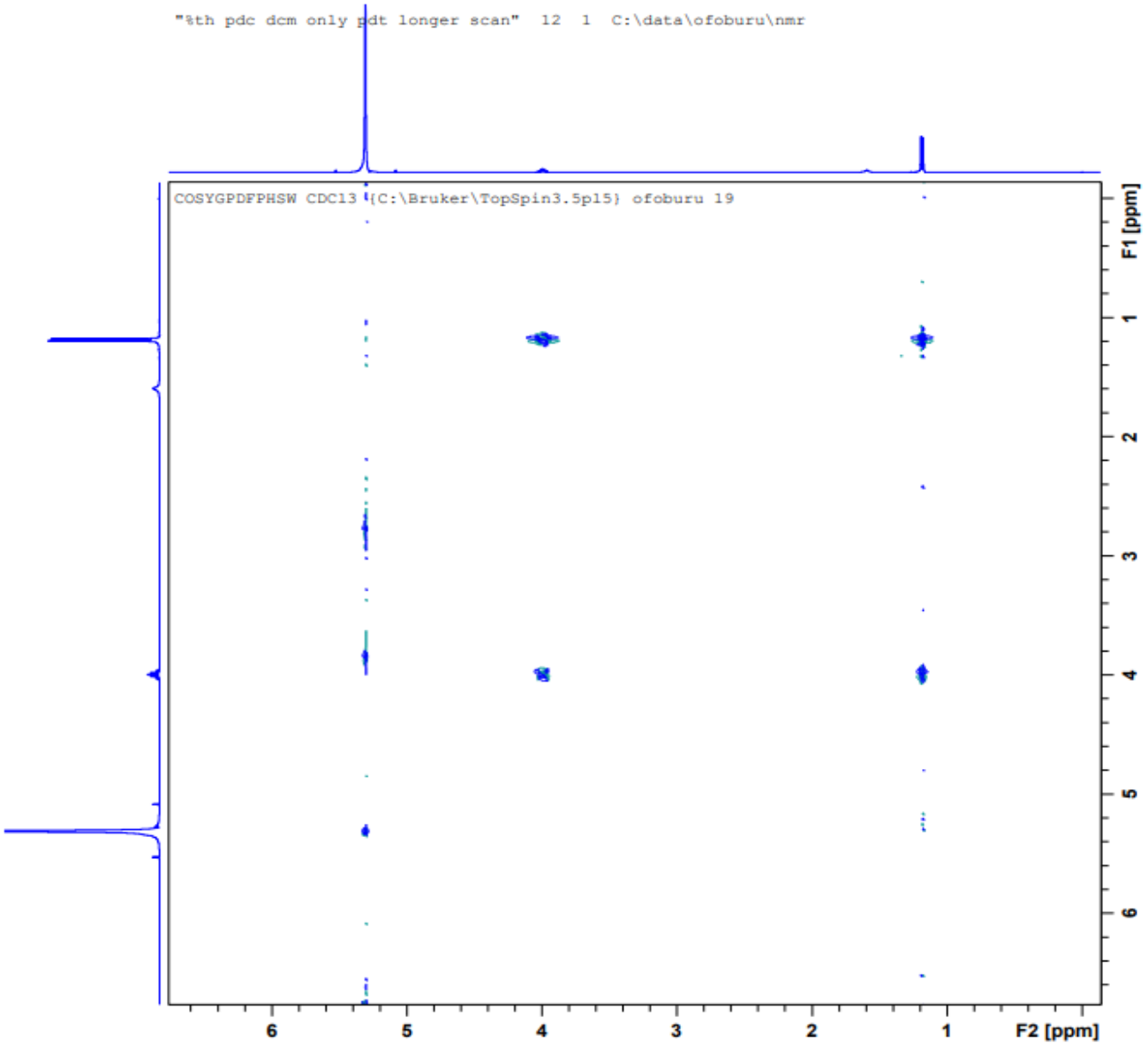

The COSY NMR Spectrum of Pd/C Catalyst Stirred in DCM under N_2 for 72 Hours

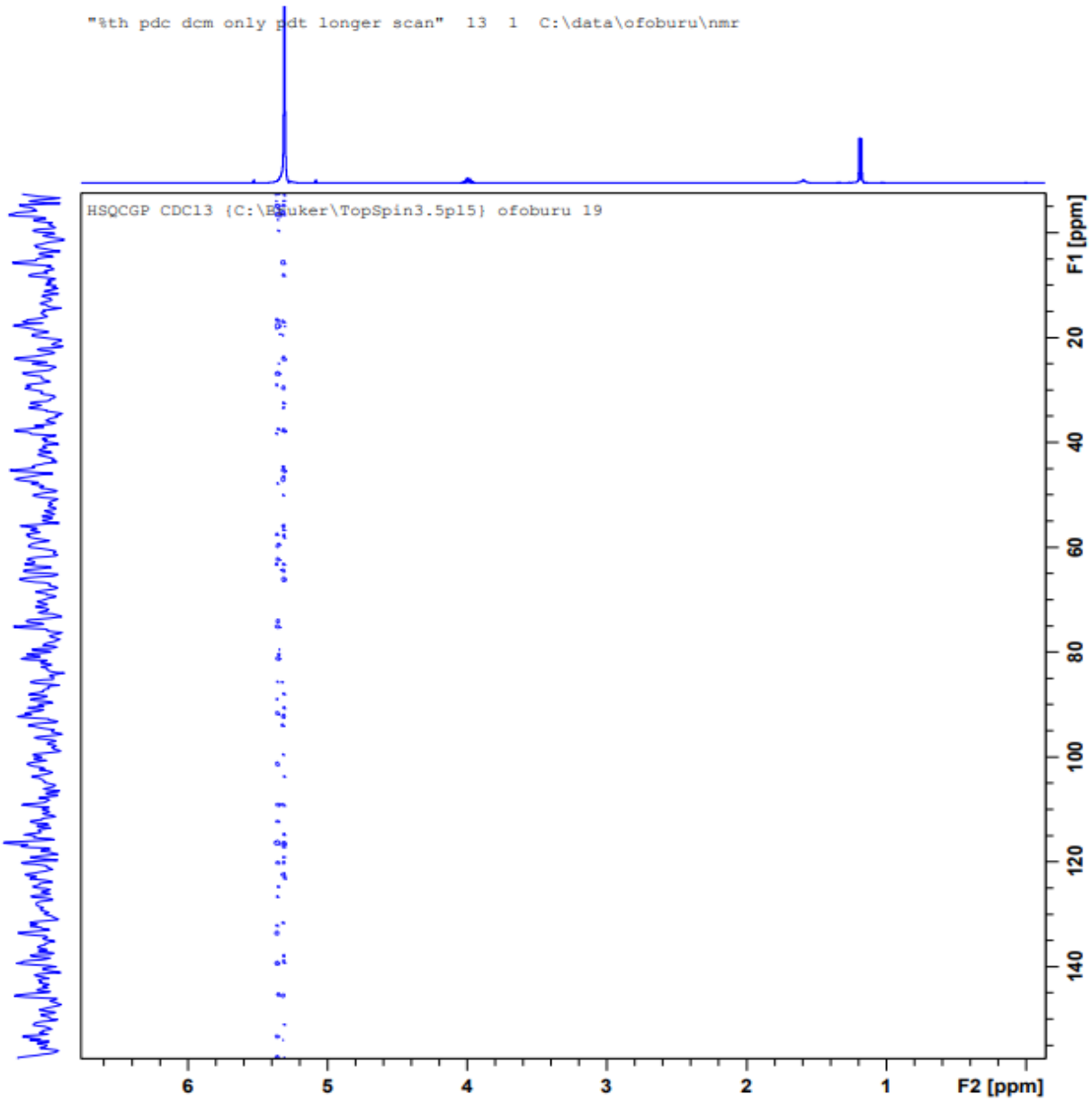

The HSQC NMR Spectrum of Pd/C Catalyst Stirred in DCM for 72 Hours under N_2

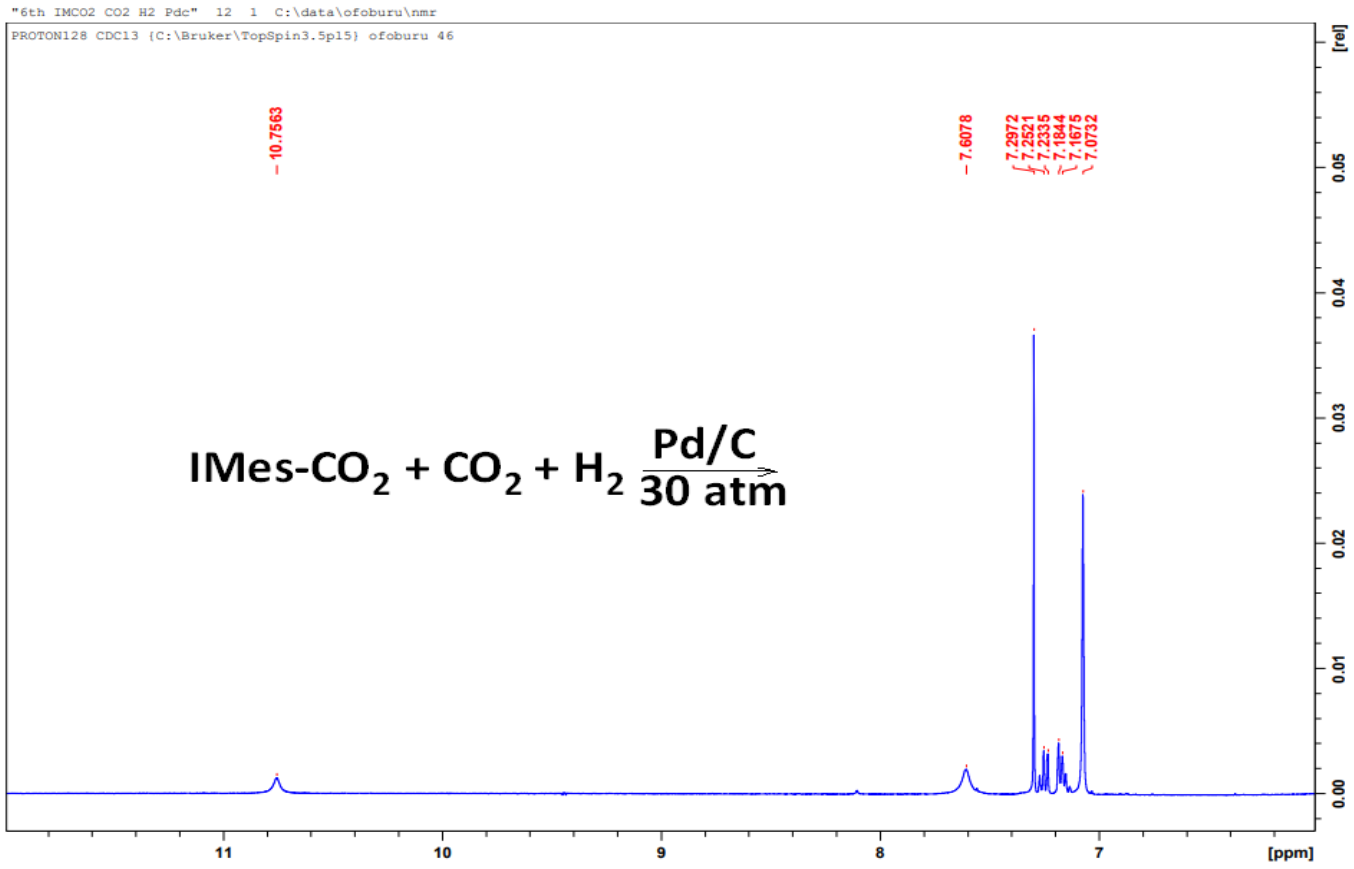

The Enlarged ^{1}H NMR Spectrum of Pd/C Catalyzed IMes-CO_2 + CO_2 + H_2 at 30 Atmospheres after 72 Hours

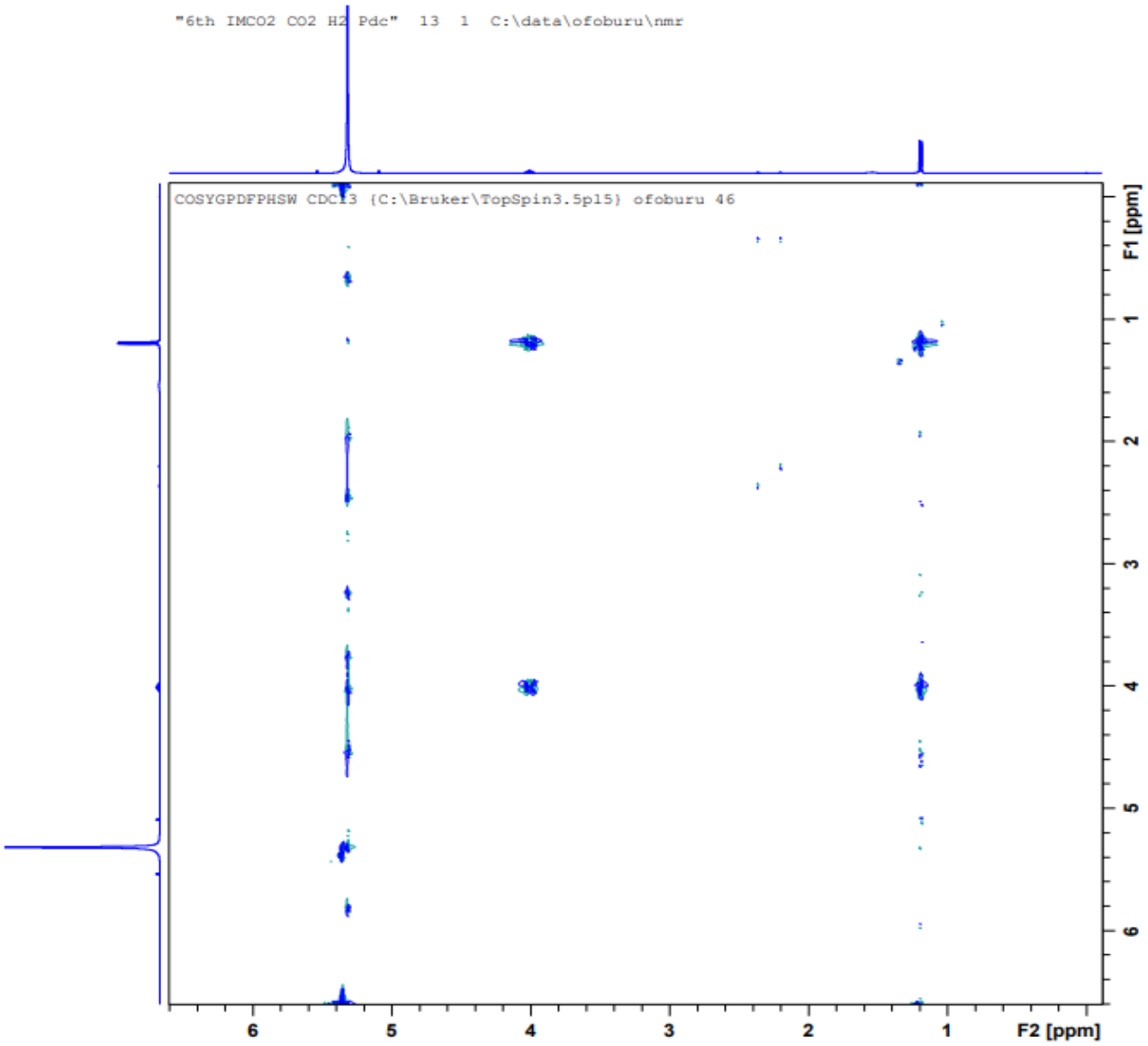

The COSY NMR Spectrum of Pd/C Catalyzed IMes-CO_2 + CO_2 + H_2 at 30 Atmospheres after 72 Hours

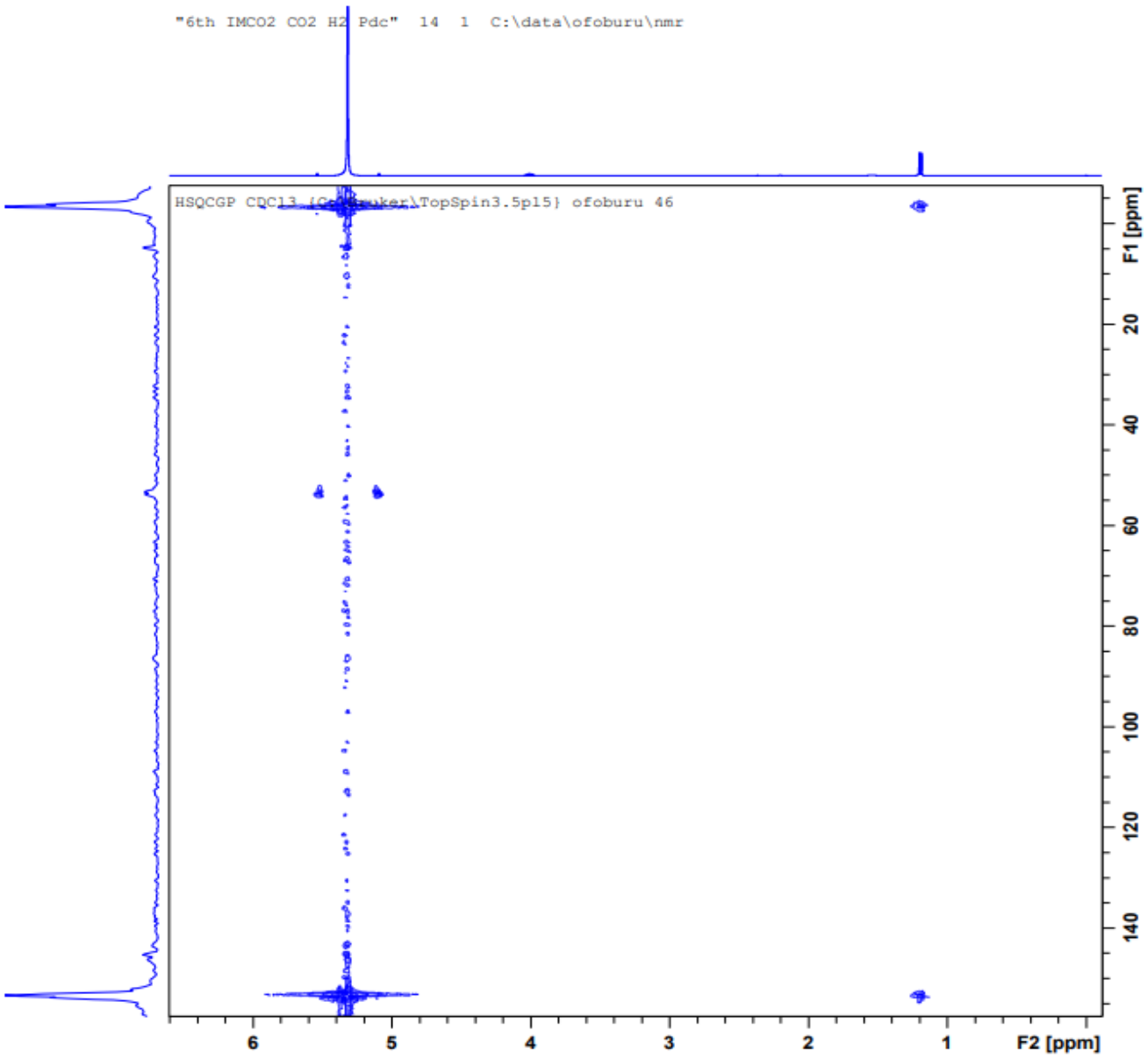

The HSQC NMR Spectrum of Pd/C Catalyzed IMes-CO_2 + CO_2 + H_2 at 30 Atmospheres after 72 Hours

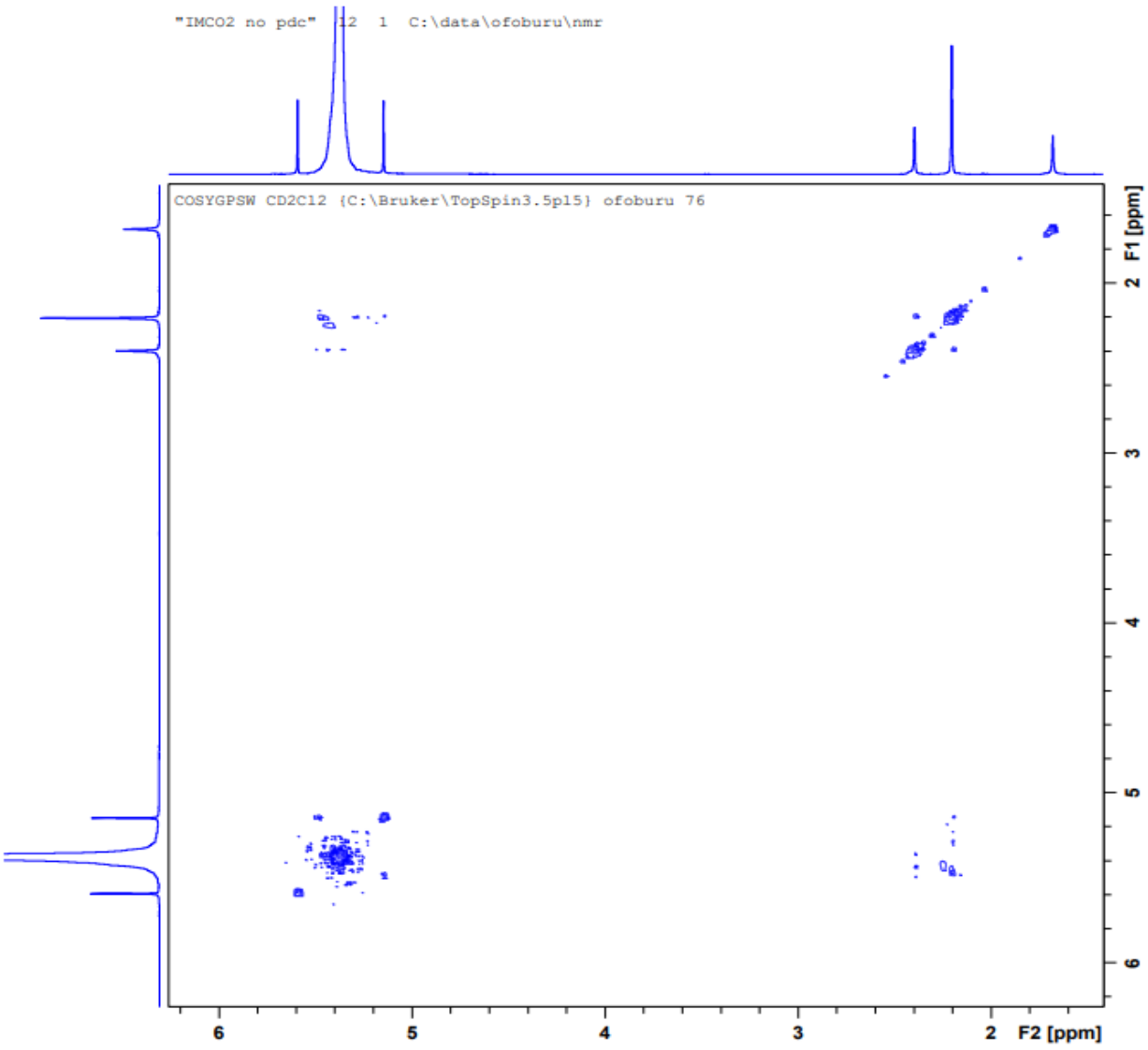

The COSY NMR Spectrum of Uncatalyzed IMes-CO_2 + CO_2 + H_2 at 30 Atmospheres after 72 Hours

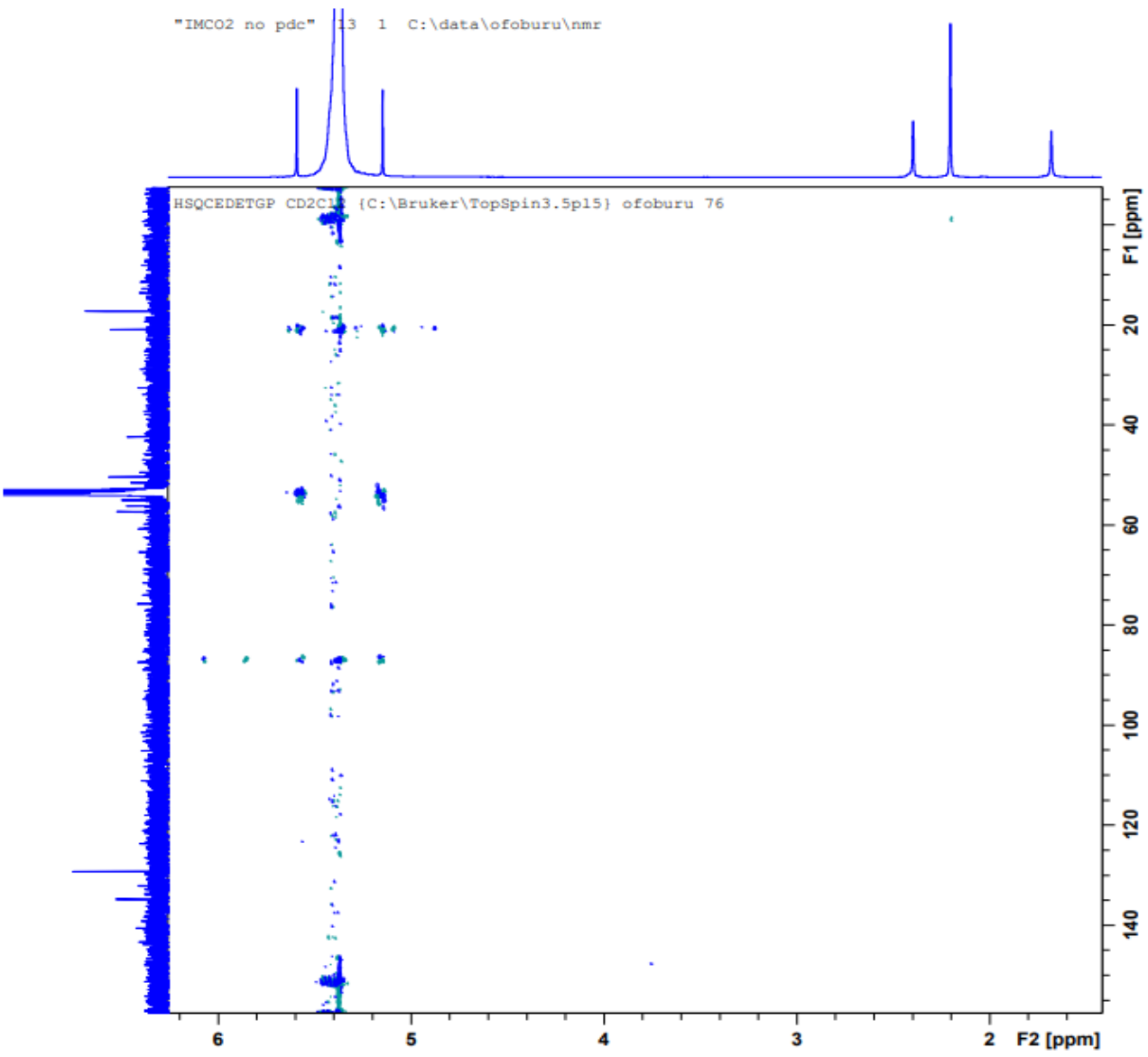

The HSQC78 NMR Spectrum of Uncatalyzed IMes-CO_2 + CO_2 + H_2 at 30 Atmospheres after 72 Hours

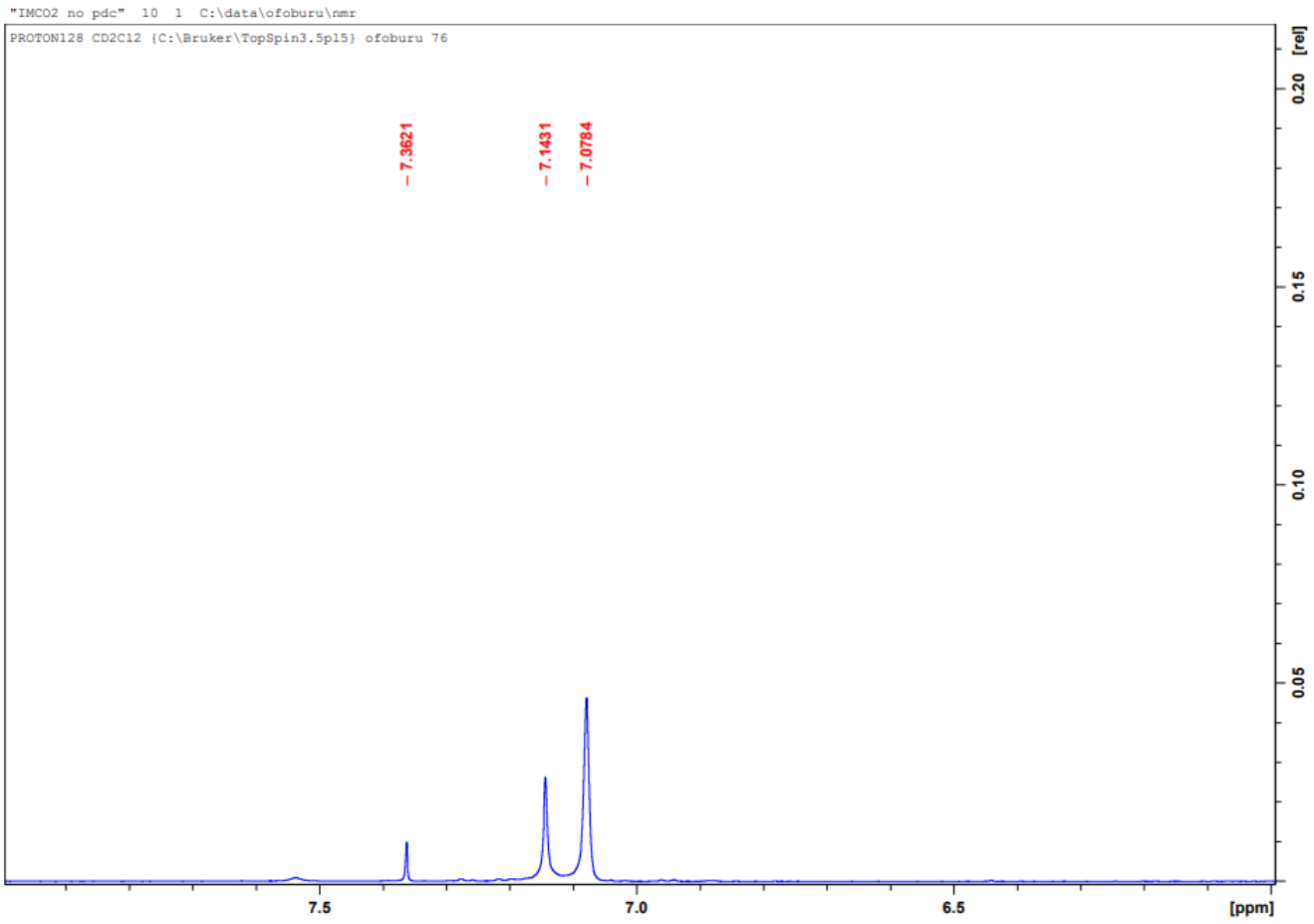

The Enlarged ^{1}H NMR Spectrum of Uncatalyzed IMes-CO_2 + CO_2 + H_2 at 30 atmospheres after 72 Hours

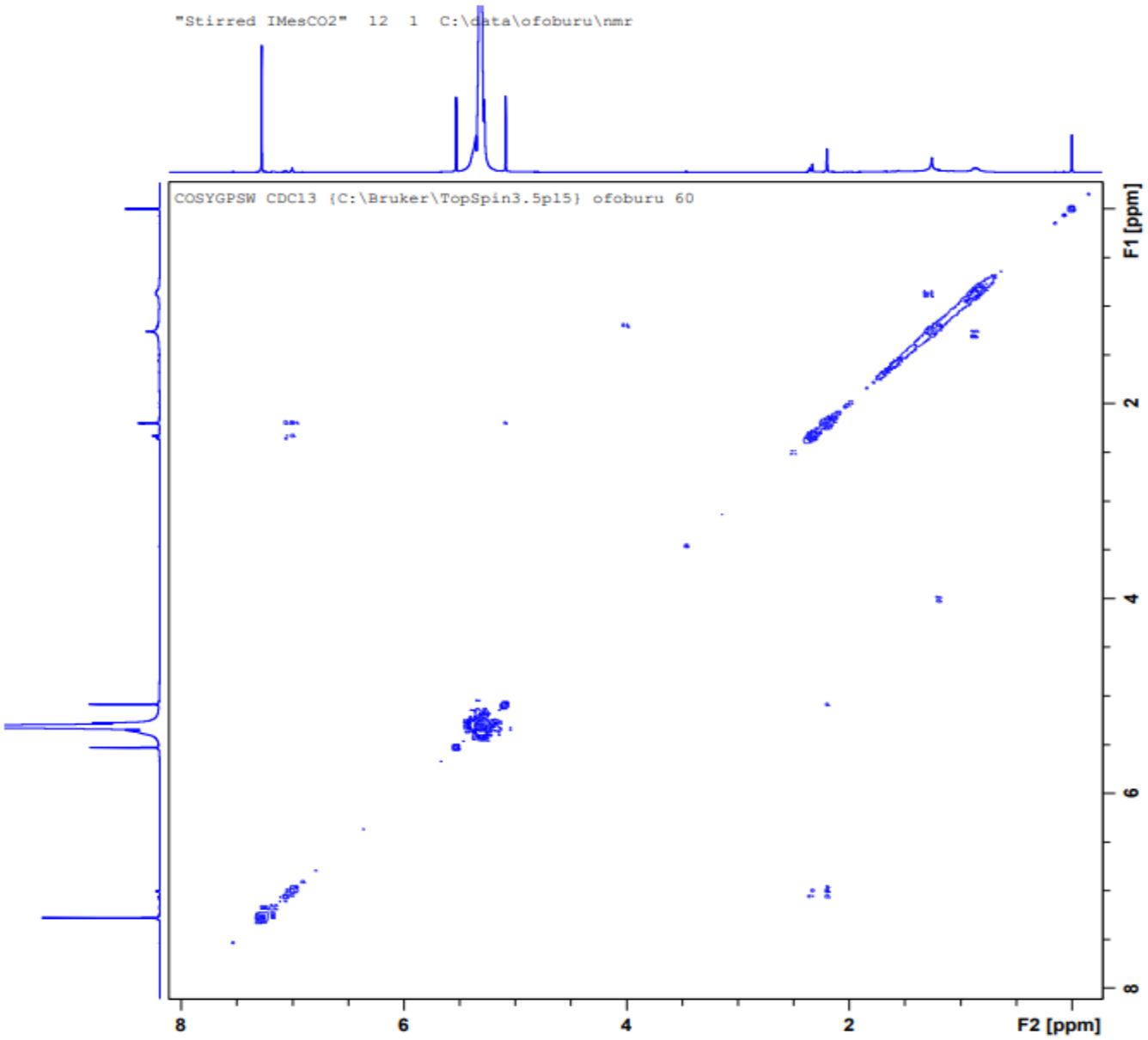

The COSY NMR Spectrum of IMes-CO_2 Stirred in DCM under N_2 for 72 Hours

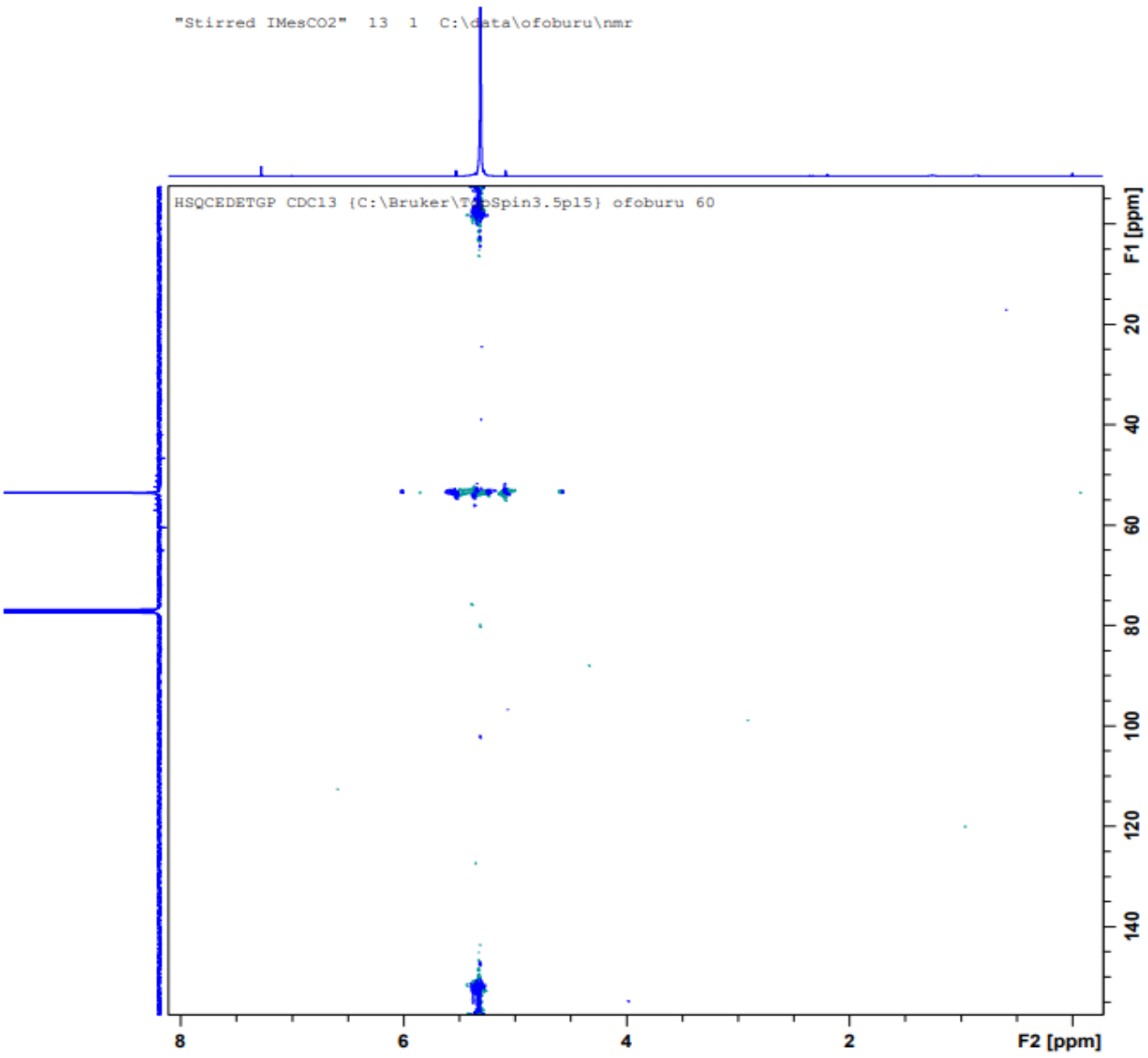

The HSQC NMR Spectrum of IMes-CO_2 Stirred in DCM under N_2 for 72 Hours

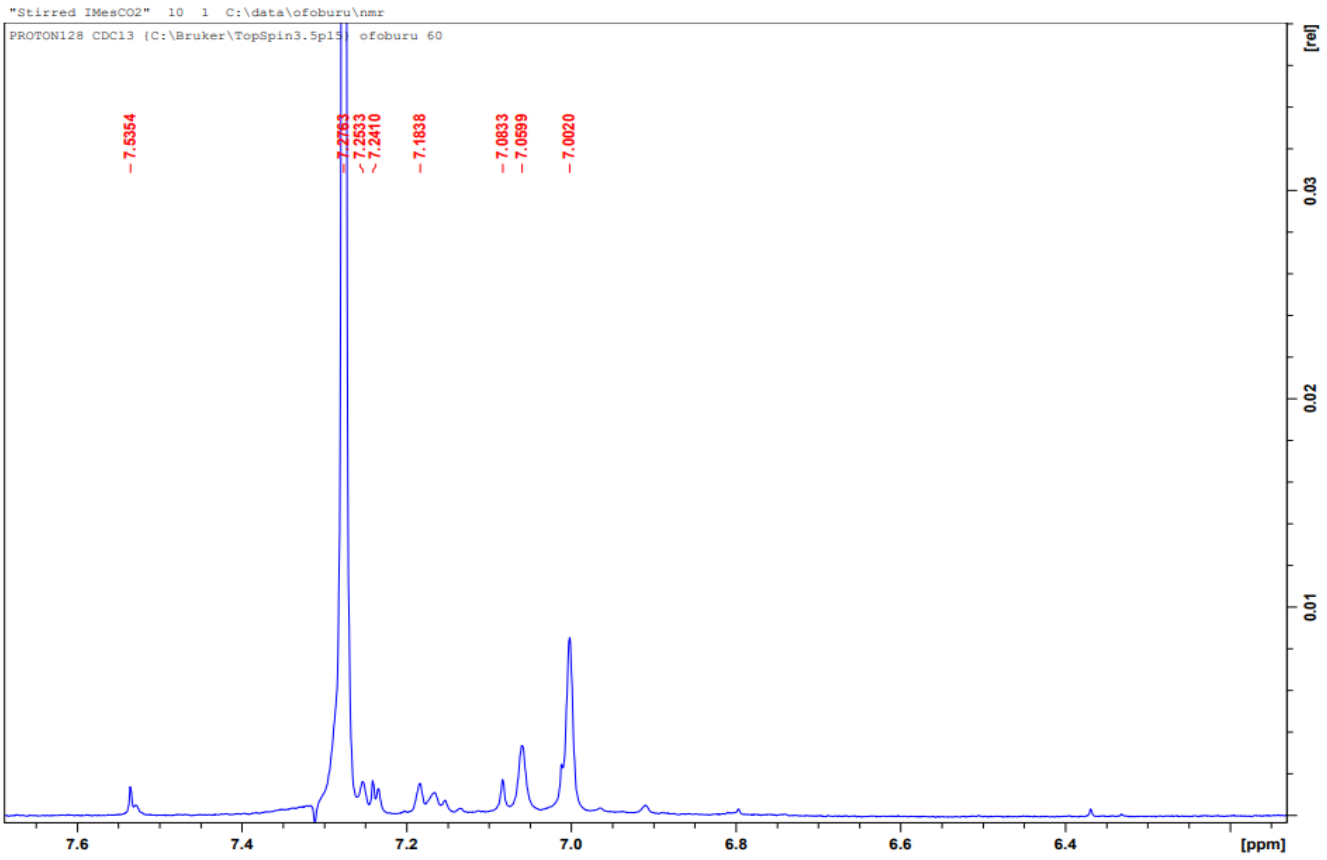

The Enlarged ^{1}H NMR Spectrum of IMes-CO_2 Stirred in DCM for 72 Hours under N_2